

ABSTRACT

GAJJAR, CHIRAG RAJESH. Improving the Hemostatic Property of Common Textile Fibers for Wound Dressings. (Under the direction of Marian McCord).

This project aims to characterize the relationship between fiber properties and the hemostatic behavior of common textile wound dressing materials. The ultimate goal is to improve the hemostatic property of the fibers. Fibers used in this study include cotton, rayon, polypropylene, polyester, nylon and fiberglass. Fiberglass is one of the most hemostatic agents which is believed to be due to its hydrophilicity and highly negative surface charge. Hence, the fibers are characterized using single fiber contact angle and zeta potential measurement in order to find the correlation between these properties and hemostasis, which is measured using a thrombin assay. The fibers are also treated with tetraethyl orthosilicate (TEOS) which imparts a glass-like surface to the fibers. TEOS treatment resulted in the decrease of contact angle and increase in thrombogenicity for all fibers except fiberglass.

In order to study the effect of specific functional end-groups on the process of coagulation, fiberglass was functionalized with surface carboxyl (-COOH), amine (-NH₂), hydroxyl (-OH), methyl (-CH₃) and amine (-NH₂) functional end-groups. There was no direct correlation between thrombogenicity and hydrophilicity or negativity of the zeta potential of a surface. The observations from this study contradict findings that indicate that a hydrophilic substrate with a highly negative surface charge provides superior hemostatic properties. We propose that a surface with a moderate contact angle, i.e. neither too hydrophilic nor too hydrophobic, and with a specific surface chemistry (with end-groups and surface charge similar to glass) would provide an ideal solution.

Improving the Hemostatic Property of Common Textile Fibers for Wound Dressings

by
Chirag Rajesh Gajjar

A thesis submitted to the Graduate Faculty of
North Carolina State University
in partial fulfillment of the
requirements for the degree of
Master of Science

Textile Chemistry

Raleigh, North Carolina

2011

APPROVED BY:

Dr. Russell Gorga

Dr. Samuel Hudson

Dr. Marian McCord
Chair of Advisory Committee

DEDICATION

To all those who 'never' believed in me... 😊

BIOGRAPHY

Chirag Rajesh Gajjar was born in Surat, India. He received his Bachelor of Engineer degree in Textile Processing in 2007 from South Gujarat University, India. After graduation, Chirag worked as Processing Engineer at Textile Research and Application Development Centre, a state of the art research and development centre of Aditya Birla Group. In 2008, Chirag joined Jay Krishna Dyeing and Printing Mills as a Shift Manager. While gaining industrial experience, Chirag received Post Graduate Diploma in Business Administration, with specialization in Marketing, from Symbiosis Centre for Distance Learning, Pune. In pursuit of higher education, Chirag joined College of Textiles at North Carolina State University in 2009. Upon completion of his Master Degree, Chirag plans to continue working in the field of bio-medical textiles.

ACKNOWLEDGMENTS

First and foremost, I want to thank my advisor Dr. Marian McCord for giving me the opportunity to work on this project and for her continuous guidance and inspiration. I also appreciate the time and effort of my committee members, Dr. Samuel Hudson and Dr. Russell Gorga.

I am thankful to Dr. Jeffry Owens at Air-force Research Laboratories for providing us the microwave-treated samples for the study and helping us with silane chemistry. Special thanks to Dr. Marin Hubbe, for sharing his expertise on zeta potential measurements and allowing me to work in his lab. I am also thankful to Dr. Susan Bernacki for allowing me to work in Tissue Engineering lab. I am thankful to Dr. Julie Willoughby for her guidance for contact angle measurements.

Many thanks to Fred Steve and Chuck Mooney at Analytical Instrument Facilities, NCSU for their guidance on XPS and SEM analytical techniques. I am thankful to Tabitha Rush who helped me to get acquainted with this project when I first started working on this project. I am thankful to Jim Snipes at Carolina Narrow Fabrics for providing the fiberglass samples and to NCRC for providing other fiber samples used in this study.

Last but not the least, I am indebted to my family and friends for all their support and encouragement!

TABLE OF CONTENTS

<i>List of Tables</i>	<i>vii</i>
<i>List of Figures</i>	<i>viii</i>
Chapter 1 Introduction	1
<i>1.1 Background</i>	<i>1</i>
<i>1.2 Importance of this research project</i>	<i>3</i>
Chapter 2 Literature Review	5
<i>2.1 Clotting of Blood</i>	<i>5</i>
<i>2.2 Influence of Foreign Surfaces on Hemostatic System and its Mechanism</i>	<i>18</i>
<i>2.3 Review of Existing Hemostatic Materials</i>	<i>24</i>
<i>2.4 Surface Modification of Fibers</i>	<i>33</i>
<i>2.5 Thrombin Assay</i>	<i>40</i>
<i>2.6 Zeta Potential</i>	<i>43</i>
<i>2.7 Contact Angle</i>	<i>47</i>
Chapter 3 Materials and Methods	49
<i>3.1 Material Preparation</i>	<i>49</i>
<i>3.2 Test Methods</i>	<i>50</i>
Chapter 4 Results and Discussion	54
<i>4.1 Results</i>	<i>54</i>
<i>4.1.1 XPS</i>	<i>54</i>
<i>4.1.2 SEM</i>	<i>59</i>
<i>4.1.3 Streaming Potential</i>	<i>64</i>

<i>4.1.4 Single Fiber Contact Angle</i>	69
<i>4.1.5 Thrombin Assay</i>	72
<i>4.1.6 SEM Images</i>	75
<i>4.2 Discussion</i>	82
Chapter 5 Future Work	91
References	92
Appendices	106

LIST OF TABLES

Table 1: Coagulation Factors	8
Table 2: Coagulation Factor Inhibitors	15
Table 3: XPS Analysis for Control and TEOS treated Yarns studied earlier	54
Table 4: XPS Analysis for TEOS treated Fibers used in this study.....	55
Table 5: XPS Analysis for Fiberglass with Specific End-Groups	55
Table 6: XPS Deconvolution Data for Fiberglass with Specific End-Groups.....	56
Table 7: EDS Analysis for Untreated and TEOS Treated Fibers	60
Table 8: EDS Analysis for Fiberglass with Specific End-Groups	62
Table 9: Single Fiber Contact Angle Measurements for Control and TEOS Fibers	69
Table 10: Contact Angle Measurements for Fiberglass with Specific End-Groups.....	71
Table 11: Chemical Composition of E-Glass	83

LIST OF FIGURES

Figure 1: Process Flow of Hemostasis.....	5
Figure 2: Platelet Response in Hemostasis	7
Figure 3: Coagulation Cascade	10
Figure 4: New Pathway for Coagulation Cascade	12
Figure 5: Stages of Hemostasis.....	16
Figure 6: Pathway of Hemostasis Summarized	17
Figure 7: Consensus Mechanism for Surface-mediated Contact Activation	20
Figure 8: Structure of TEOS	33
Figure 9: Formation of Silicon dioxide from TEOS.....	34
Figure 10: Deposition of TEOS on the material surface.....	34
Figure 11: Formation of Siloxane Bridges.....	35
Figure 12: Formation of Glass-Like Surface	35
Figure 13: Structure of Aspartic Acid.....	36
Figure 14: Structure of Glycidoxypropyltrimethoxysilane.....	36
Figure 15: Structure of Methyltriethoxysilane.....	37
Figure 16: Structure of N-[3-(Trimethoxysilyl)propyl]-ethylenediamine	37
Figure 17: Structure of Phosphatidylserine.....	38
Figure 18: Structure of Phosphatidylcholine	39
Figure 19: Typical Thrombin Generation Curve (Thrombogram)	41
Figure 20: Electric Double Layer at the Surface-Liquid Interface	44
Figure 21: Typical Plot of Zeta Potential Vs. pH	44

Figure 22: Streaming Potential Measurement across a Plug	46
Figure 23: Contact Angle of Liquid on a Solid Surface	47
Figure 24: Streaming Potential Jar.....	52
Figure 25: Deconvolution of Carbon Bonds for Untreated Fiberglass.....	57
Figure 26: Deconvolution of Carbon Bonds for Fiberglass treated with Aspartic Acid ...	57
Figure 27: Deconvolution of Carbon Bonds for Fiberglass treated with Glycidoxypropyl Trimethoxysilane	58
Figure 28: Deconvolution of Carbon Bonds for Fiberglass treated with Methyl Triethoxysilan	58
Figure 29: Graphical Representation of EDS Analysis for Untreated and TEOS Treated Fibers.....	61
Figure 30: Graphical Representation of EDS Analysis for Fiberglass with Specific End Groups.....	63
Figure 31: Zeta Potential values for Control Fibers.....	64
Figure 32: Zeta Potential values for TEOS Fibers.....	65
Figure 33: Zeta Potential values for Cotton.....	66
Figure 34: Zeta Potential values for Rayon	66
Figure 35: Zeta Potential values for PP	67
Figure 36: Zeta Potential values for PET.....	67
Figure 37: Zeta Potential values for Nylon.....	68
Figure 38: Zeta Potential values for Glass.....	68
Figure 39: Single Fiber Contact Angle Measurement for Control and TEOS Fibers.....	70
Figure 40: Contact Angle Measurement for Fiberglass with Specific End-Groups	71
Figure 41: Thrombin Assay for Control Fibers	72

Figure 42: Thrombin Assay Comparison for Control and TEOS Fibers	73
Figure 43: Thrombin Assay for Fiberglass with Specific End-Groups	74
Figure 44: SEM Image of Untreated Cotton and Cotton TEOS	75
Figure 45: SEM Image of Untreated Rayon and Rayon TEOS	76
Figure 46: SEM Image of Untreated Nylon and Nylon TEOS.....	76
Figure 47: SEM Image of Untreated PP and PP TEOS	77
Figure 48: SEM Image of Untreated PET and PET TEOS.....	77
Figure 49: SEM Image of Untreated Fiberglass and Fiberglass TEOS	78
Figure 50: SEM Image of Untreated Fiberglass and Glass Aspartic Acid	78
Figure 51: SEM Image of Untreated Fiberglass and Glass Glycidoxypopyl Trimethoxysilane	79
Figure 52: SEM Image of Untreated Fiberglass and Glass Methyl triethoxysilane	79
Figure 53: SEM Image of Untreated Fiberglass and Glass Diamine.....	80
Figure 54: SEM Image of Untreated Fiberglass and Glass Serine	80
Figure 55: SEM Image of Untreated Fiberglass and Glass Choline.....	81
Figure 56: Glass Surface.....	82
Figure 57: TEOS Coated Surface	82

CHAPTER 1: INTRODUCTION

1.1. Background

Hemorrhage or the uncontrolled bleeding from a wound is a major cause of casualties in most of the combat scenarios. KIA (Killed in Action – defined as being killed before reaching a treatment facility) accounts for approximately 20% of the combat casualties. Hemorrhage is the cause of death in 50% of the cases in this group. Even for DOW (Died of Wounds – where the injured survives long enough to be transported to a medical facility, but succumbs to death later on), hemorrhage is the leading cause of complications and death.[1] In the KIA group, the source of bleeding can be internal or external (suitable for application of dressings and/or tourniquets). Theoretically, the external sources can be controlled by compression but the reality is quite different. In the review of Vietnam War data, almost 40% of the soldiers that were KIA because of exsanguination had a source of hemorrhage that could have been controlled in the field.[1]

The WDMET (Wound Data and Munitions Effectiveness Team) study also suggests that exsanguination from the extremity wounds accounts for more than half of the potentially preventable deaths in combat.[2] A recent study on the causes of death during Iraqi operation showed that hemorrhage was the cause for 83% of deaths among potentially preventable casualties. Specifically, truncal or non-compressible hemorrhage was most common (46%), followed by “tourniquetable” hemorrhage (33%), and “non-tourniquetable but compressible” hemorrhage (21%).[3]

Traumatic injury claims 100,000 lives each year, making it the leading cause of death in United States for individuals aged 44 and under. In almost 50% cases, exsanguination is the cause of death.[4] A recent study on the causes of civilian accidental deaths in Australia showed that exsanguination (33%) and Central Nervous System (CNS) injury (33%) were the leading factors causing mortality followed by CNS + exsanguination (17%).[5]

During the surgery, continuous bleeding from minor capillaries or small venules can obscure the surgical field, prolong operation time, increase the risk of physiologic complications and expose the patient to risks associated with the blood transfusions. Risk of complications and ICU admission doubled in patients who received more than two units of blood due to intraoperative blood loss.[6] Postpartum hemorrhage, i.e. excessive bleeding following the birth of a baby is the leading cause of death related to pregnancy, especially in the developing countries. Most deaths resulting from postpartum hemorrhage are preventable.[7] A study shows that postpartum hemorrhage accounts for 3.9% of normal deliveries and 6.4% of cesarean delivery.[8]

These figures point out that uncontrolled hemorrhage is the single most prevalent cause of death during the pre-hospital period in both military combat and civilian trauma cases. This makes new methods and products for hemorrhage control a research priority for those who desire to avoid potentially survivable deaths in both combat and civilian scenarios. Again, during surgical procedures, effective hemostasis would result in fewer transfusions, better

visualization of surgical area and thereby reduced risk of accidental injury, reduced surgical time and decreased morbidity and mortality.[6]

1.2. Importance of this research project

Conventionally, compression using tourniquets and/or gauze has been the main line of action for the control of bleeding. These measures have not been quite effective. Tourniquets have been used since the time of Romans [9] to reduce bleeding by the means of external pressure which compresses the veins/capillaries and slows down the oozing of blood. However, the use of tourniquets is limited to certain parts of the body (such as limbs) excluding areas like head, neck, chest or abdomen. One of the earliest topical hemostatic agents was cotton, in the form of gauze pads, capable of absorbing approximately 250 ml of blood.[10] However, these pads are passive dressings, unable to initiate or accelerate blood clotting. In many cases, excessive blood loss puts the patients in hypovolemic shock when they are brought to the medical facility. In such cases, transfusion of isotonic saline is the primary life support. However, blood dilution limits the replacement with saline. Infusion with whole blood products is also a risky procedure even with the best of blood type matching and hence doctors will give blood transfusions only as a last resort and that too after many time consuming tests to match the patient's blood markers to the donor's. Plasma transfusion is considered safer than whole blood transfusion. It increases volume of the circulating blood and remains in circulation for a longer time. Plasma transfusion has several advantages over blood transfusion; however, plasma cannot take the place of whole blood.[11] Nothing would be a better life-saver than a material facilitating immediate enhancement of coagulation. If

one can modify the material to enhance the coagulation cascade and decrease the time to clot formation, the mortality and morbidity associated with accidental injuries can be decreased.

Over the time, the unmet need for an efficient topical hemostatic agent for early and effective control of hemorrhage has led to the development of various hemostatic agents based on different mechanisms and theories. When subjected to rigorous testing, many of these agents were found to be no better than regular dressings, while a few were very effective and some are even approved by Food and Drug Administration (FDA). Despite profuse research in the field of hemostasis and plethora of hemostatic agents, the search for the “ideal” hemostatic agent still exists. The ideal hemostatic agent is expected to be rapid and effective in control/cessation of bleeding, reliable and easy to manufacture and transport, easy to apply and have low complication rate.

Hemostatic agents that can initiate and/or accelerate the clotting mechanism through contact activation and/or actively contributing to the coagulation cascade are being sought. Recent products like HemCon® and Stasilon® have shown promising results.[4], [12] Based on this mechanism, we propose a new approach to the enhancement of hemostasis using modified textile materials commonly used for wound dressings. This research focuses on developing different material treatments and modifications and developing a standardized set of tests to determine the extent of the ability of the modified materials to enhance coagulation. The end goal is to develop a system that would accelerate the coagulation process and aid the process of hemostasis.

CHAPTER 2: LITERATURE REVIEW

2.1. Clotting of blood

Hemostasis is a physiological process initiated when damage occurs to the wall of a blood vessel, which culminates in the formation of a stable clot that prevents the further escape of blood from the vessel. It is a complex mechanism which involves a synchronized action of various plasma proteins, platelets, cells and signaling molecules.[13], [14]

Hemostasis occurs in three stages: vasoconstriction, platelet response and blood coagulation (Figure 1).[15]

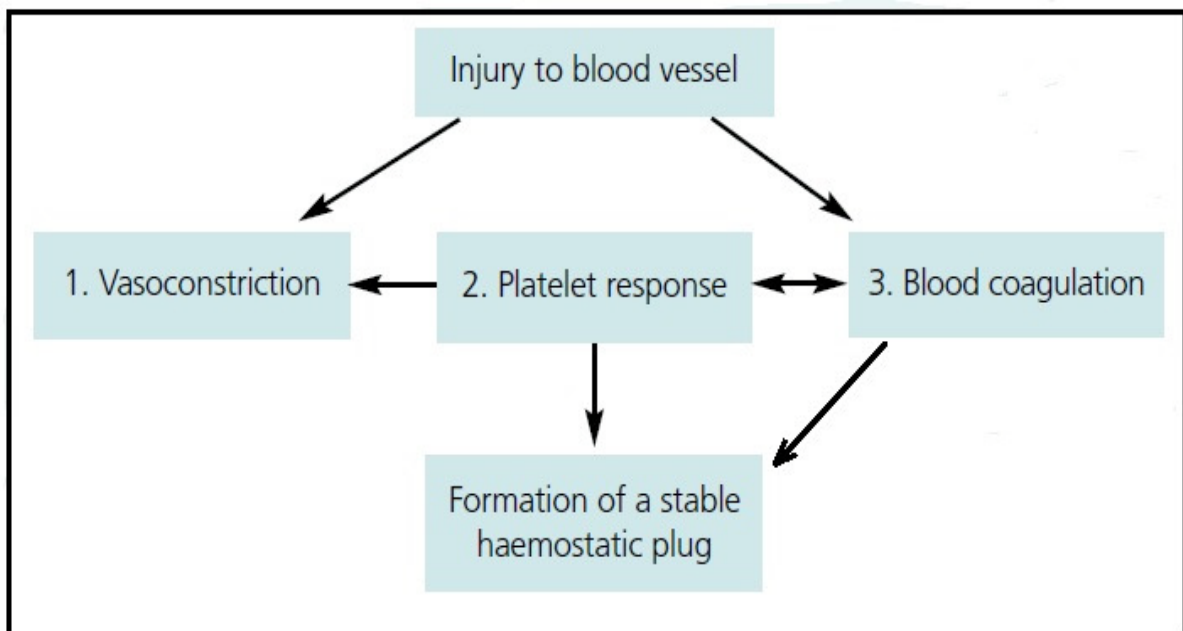


Figure 1: Process Flow of Hemostasis[15]

The entire process shown above is classified into two main phases: primary (i.e. cellular phase) and secondary (i.e. humoral phase).[16] Primary hemostasis begins immediately after vascular injury and endothelial disruption and is characterized by vasoconstriction, platelet adhesion and formation of a soft aggregate plug. The injury to the walls of the blood vessel triggers a reflex local contraction of vascular smooth muscle leading to vasoconstriction. This action compresses the blood vessel which slows down the blood flow and minimizes blood loss.[17]

The next step in primary hemostasis is Platelet Aggregation and Platelet Activation. Platelets, also known as thrombocytes, originate from stem cells in bone marrow. Their main functions are to adhere to damaged endothelium, store ADP and proteins, aggregate with other platelets and provide a surface for coagulation reaction. A damaged blood vessel exposes collagen, which binds the circulating von Willebrand factor at the site of injury. The von Willebrand factor in turn changes conformation at one end and binds to the glycoproteins on the surface of platelets, forming a platelet monolayer over the injured surface. This is followed by platelet activation which is signaled by changes in the shape of platelets from smooth discs to spiny spheres, and by release of various chemicals like adenosine diphosphate (ADP), Thromboxane A₂ and serotonin. Thromboxane A₂ and serotonin enhance further vasoconstriction, while Thromboxane A₂ and ADP activate neighboring platelets, enhancing platelet aggregation and leading to the formation of a loose platelet plug over the injured surface.[18] The platelet response in primary hemostasis is shown in Figure 2.[15] This

phase of hemostasis is short lived and the soft plug can easily be sheared from the injured surface.

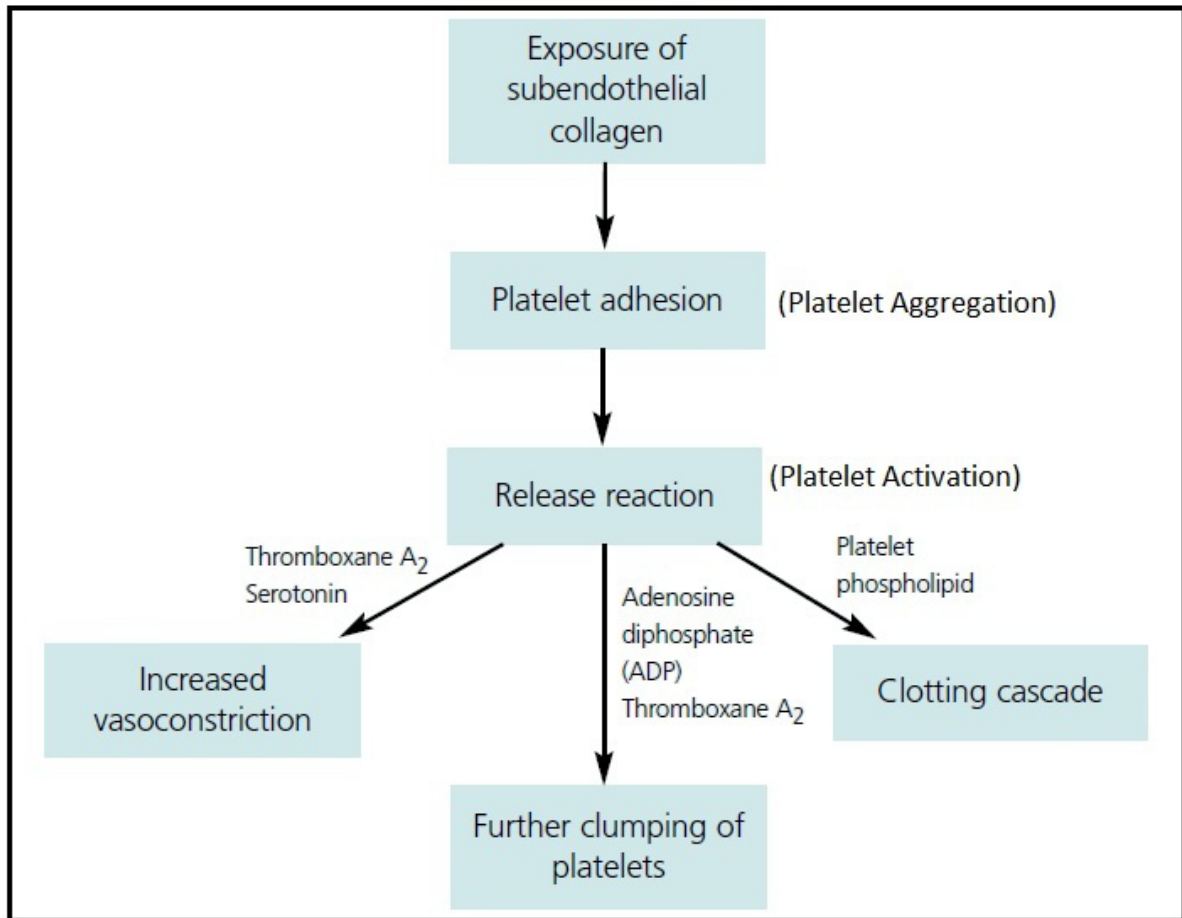


Figure 2: Platelet Response in Hemostasis[15]

The soft platelet plug is stabilized during secondary hemostasis to form a clot. This occurs through the coagulation cascade, which is a complex series of interdependent reactions involving several plasma proteins, calcium ions and platelets that lead to the conversion of fibrinogen to fibrin.[16] Platelets provide surfaces for the coagulation reactions to take place.

When activated, platelets expose a negatively charged phospholipid, ‘phosphatidylserine’, which causes the binding of coagulation factors at the site of injury, which would otherwise keep circulating in the blood. This allows all the coagulation factors to come close to one another and increases the efficiency of the reactions. Most coagulation reactions have four components i.e. ‘Quaternary Complex’. This includes enzymes (such as VIIa, XIa, Xa, IIa, protein C etc.), co-factors (such as V, VIII, tissue factor, protein S etc. which speed up the reactions by order of magnitude), calcium (that helps to bind protein to surface) and phospholipid surface (that has a negative charge and speeds up the reaction by bringing proteins closer). The enzymes are bound to the phospholipid surface by calcium. Co-factors activate enzymes which in turn activate other proenzymes and thus go on the complex coagulation cascade.[18] The coagulation factors, listed in Table 1[19], are produced by liver and circulate in an inactive form until the coagulation cascade is initiated.

Table 1: Coagulation Factors[19]

Name	Function
Fibrinogen (Factor I)	Adhesive protein that forms the fibrin clot
Prothrombin (Factor II)	Activated form is main enzyme of coagulation
Tissue factor (Factor III)	Lipoprotein initiator of extrinsic pathway
Calcium ions (Factor IV)	Metal cation necessary for coagulation reactions
Factor V (Labile factor)	Cofactor for activation of prothrombin to thrombin

Table 1 Continued	
Name	Function
Factor VII (Proconvertin)	With tissue factor, initiates extrinsic pathway
Factor VIII (Antihemophilic factor)	Cofactor for intrinsic activation of factor X
Factor IX (Christmas factor)	Activated form is enzyme for intrinsic activation of factor X
Factor X (Stuart-Prower factor)	Activated form is enzyme for final common pathway activation of prothrombin
Factor XI (Plasma thromboplastin antecedent)	Activated form is intrinsic activator of factor IX
Factor XII (Hageman factor)	Factor that nominally starts intrinsic pathway
Factor XIII (Fibrin stabilizing factor)	Transamidase that crosslinks fibrin clot
High molecular weight kininogen (Fitzgerald, Flaujeac, or William factor)	Cofactor
Prekallikrein (Fletcher factor)	Activated form that participates at beginning of intrinsic pathway

Until recently, the mechanism of coagulation cascade in vivo was thought to be similar to the in vitro mechanism that is seen in test-tubes in laboratories. The test-tube model of coagulation consists of extrinsic pathway, intrinsic pathway and a common pathway as shown in Figure 3.[6]

The second pathway, Contact Activation Pathway or intrinsic pathway, is started when the blood comes in contact with a foreign material (glass in case of test tubes). Within few seconds plasma proteins – factor XII, kininogen, prekallikrein, and factor XI start binding to the negatively charged surface of foreign material. A Vroman Layer is formed where there is a constant desorption and adsorption of proteins, resulting in those with weak binding affinity being replaced by those with strong binding affinity.[22][23] Factor XII is activated to factor XIIa in the Vroman Layer which marks the initiation of the Contact Activation Pathway. Activated factor XIIa converts factor XI to active factor XIa, which in turn activates factor IX to factor IXa. Factor IXa, along with factor VIII, activates factor X to factor Xa. This is the last step of intrinsic pathway which is same as that in extrinsic pathway.[24]

After activation of factor Xa through Tissue Factor Pathway and Contact Activation Pathway, the rest of the coagulation cascade proceeds through Common Pathway. This is considered to be the most important stage in the coagulation cascade since here prothrombin is converted to thrombin which acts on fibrinogen to form fibrin clot.[25] Factor Va, Xa and Ca^{++} combine to form the complex called prothrombinase. Prothrombinase acts on factor II (prothrombin) to convert it to factor IIa (thrombin). Thrombin then cleaves fibrinogen to form fibrin polymer which binds to the aggregating platelets and acts as glue to hold the clot together. Once this is achieved, hemorrhage is stopped and healing of the wound can commence.[14]

This new coagulation model has extrinsic and intrinsic pathways limbs, but the in vivo process of hemostasis is believed to be initiated only by the exposure of tissue factor (TF). Blood, under normal conditions, is never exposed to TF. Rupture of the blood vessel due to injury exposes blood to TF and this initiates the coagulation cascade (Initiation Phase). TF binds to factor VII to activate factor X to factor Xa, but this is rapidly shut down by an inhibitor produced by endothelial cells – tissue factor pathway inhibitor (TFPI). However, small amount of factor VII circulates in its active form factor VIIa. TF binds with factor VIIa to convert factor IX into IXa. Factor IXa along with cofactor VIIIa leads to further conversion of factor X to Xa. Thus, small amount of thrombin generated through extrinsic means from the initial activation feedback creates activated factors Va and VIIIa, which help to generate more thrombin. If conditions are right, the intrinsic mechanism causes further expansion of thrombin generation. It includes activation of factor XII to XIIa followed by the activation of factor XI to XIa by thrombin and factor XIIa, which ultimately leads to generation of more thrombin using factor IXa and VIIIa to activate factor X (Propagation Phase). The activation of factor X to factor Xa starts final pathway of clotting which is similar to the common pathway in the test-tube model. Factor Xa combines with factor Va along with Ca^{++} to form prothrombinase complex on the phospholipid surface. This complex facilitates the conversion of prothrombin to thrombin which in turn cleaves fibrinogen to form fibrin polymer that forms the clot.[19][18]

The clot thus formed is still not stable and will come apart if not covalently cross-linked. As discussed above, thrombin acts on fibrinogen and clips off fibrinopeptides to form fibrin

monomer. Fibrin monomers come close to each other to form loose fibrin polymer. Thrombin then activates factor XIII to XIIIa which stabilizes the clot by forming amide bonds between fibrin polymers (Stabilization Phase).

The final stage in the process of hemostasis is fibrinolysis (Termination Phase). When a clot is formed, there has to be some mechanism to limit the clot to the site of injury and ultimately to remove the clot when the injury has healed. Fibrinolysis is an important process to prevent thrombosis in an undesired place. The endothelial cells release antithrombin III and Tissue plasminogen activator (tPA). Antithrombin III inactivates factor IIa (thrombin) as well as factors Xa and IXa. tPA cleaves plasminogen to plasmin which in turn cleaves fibrin and stops the progression of clot. Any excess tPA that escapes in plasma is inactivated by plasminogen activator inhibitor (PAI-1). Any plasmin that escapes in the plasma is inactivated by α_2 antiplasmin. Thus, active fibrinolysis is confined to the thrombus only. Endothelial cells also release nitrous oxide and Prostaglandin I₂ (PGI₂) which inhibit platelet aggregation and induce vessel dilation, thus preventing the progression of clot. There are heparin like molecules – Thrombomodulin and Tissue Factor Pathway Inhibitor (TFPI), on the surface of the endothelial cells. TFPI inactivates factors VIIa and Xa. Thrombomodulin binds to factor IIa (thrombin) and activates protein C, which along with protein S inactivates factors Va and VIIIa. Thus, through the combined effects of various inhibitors and proteins (Table 2), the propagation of clot is ceased and unwanted coagulation is prevented.[18][26]

Table 2: Coagulation Factor Inhibitors

Name	Function
Tissue Factor Pathway Inhibitor (TFPI)	Inhibits TF-Factor VIIa complex
Protein C	Upon activation cleaves factors Va and VIIIa
Protein S	Cofactor for protein C
Antithrombin	Inhibits several serine proteases (coagulation cofactors); requires heparin as cofactor

Thus, hemostasis is a complex interaction of platelets and different coagulation factors along with endothelium with the goals of stopping the loss of blood at the site of injury and laying the groundwork for injury repair and healing. Figure 5[26] shows the stages of hemostasis described above, and Figure 6[19] summarizes the pathway of hemostasis.

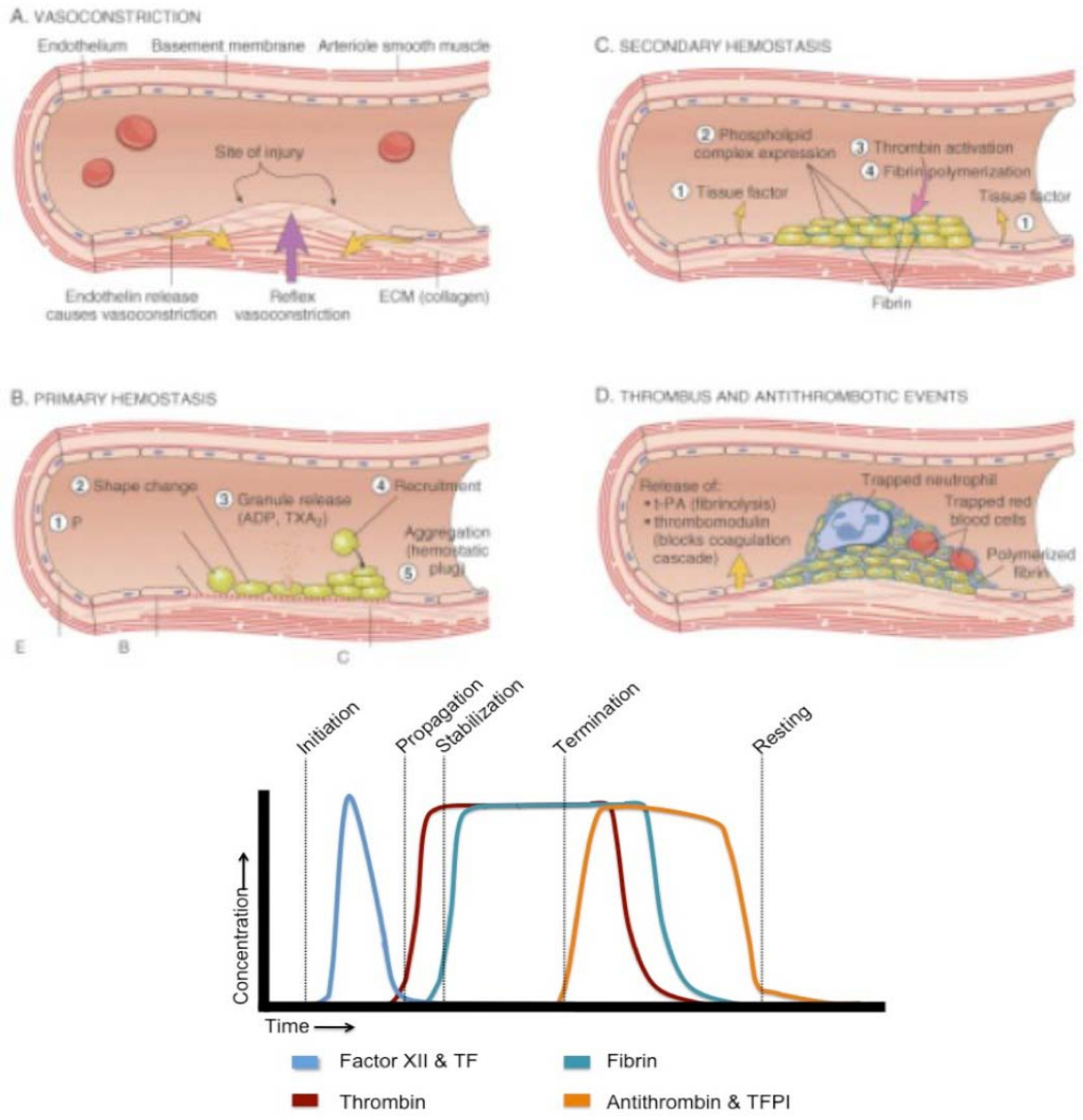


Figure 5: Stages of Hemostasis (adapted from [26])

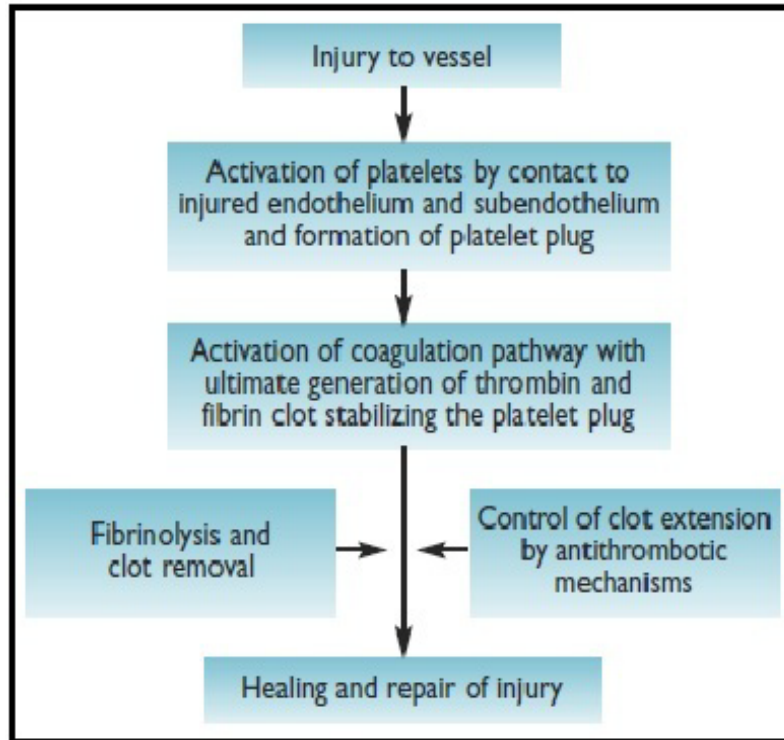


Figure 6: Pathway of Hemostasis Summarized[19]

2.2. Influence of Foreign Surfaces on Hemostatic System and its

Mechanism

Exposure of blood to various surfaces during in vitro testing and the subsequent clotting of blood led to the hypothesis of 'Contact Activation Mechanism' for clotting which was found to be different than the 'in vivo' mechanism involving 'Tissue Factor Activation'. It was observed long ago that the clotting of blood is markedly influenced by the nature of the surface with which it comes in contact. As early as 1886, Freund discovered that while the blood clotted rapidly in glass tubes, the coating of the tubes with Vaseline or paraffin markedly delayed the clotting time of blood.[25] Since then, researchers have toiled to understand the influence of surface characteristics on blood clotting. The 'Glass Effect' i.e. the rapid clotting of blood in contact with glass surface have been attributed to different properties like wettability, negative surface charge, chemical functionalities, charge density etc. through different studies. However, the exact reason for glass effect is yet not clear. This is an important aspect of research in the field of hemostasis. If this mechanism is understood, one can develop foreign materials as topical hemostasis with strong activation of hemostatic systems or one can develop foreign materials having benign interactions for long-term contact with blood.

Materials like Polyethylene terephthalate (PET) and Polytetra-fluoroethylene (PTFE) are being used for implantable medical devices due to their hydrophobic nature and neutral surface charge, which is believed to prevent platelet aggregation and clot formation.[28] This observation points to some general relationships, e.g., hydrophobic neutral materials tend not

to activate hemostasis while hydrophilic materials with negative surface charge lead to rapid, stable clot formation.[28][29] Surface negativity has been correlated with rapid coagulation onset and higher clot strength.[29]

However, this relationship is not uniform across the array of materials. As described later in this section, even the hydrophobic materials have been shown to be coagulants. Not all the negatively charged surfaces are thrombogenic and even some positively charged surfaces show hemostatic properties. Heparin is one well-studied example of a negatively charged surface with antithrombotic properties. On the other hand, chitosan is a positively charged oligosaccharide that is found to be a procoagulant.[29] Thus, the exact requisite for a material to be hemostatic and the mechanism of foreign surface induced hemostasis is yet not understood completely. Lack of understanding of the relationship between material science and hematology has resulted in a trial and error approach for the development of topical hemostatic systems.

A three-step mechanism has been hypothesized for the response of blood components to foreign surfaces: initial selective adsorption of plasma proteins to the foreign surface which is related to material's surface structure and chemical properties; conformational distortion of the adsorbed proteins; functional response (activation) of hemostatic system.[30] The initiation, amplification and propagation of surface-mediated coagulation involve four proteins that exist in plasma in the zymogen form – factor XII (Hageman factor), factor XI, prekallikrein (PK) and high molecular weight kininogen (HMWK).[31] Surface-dependent

activation of FXII to FXIIa, also known as autoactivation, is the initiating step. The traditional consensus theory of contact activation (Figure 7) proposes that FXII binds to a surface having negatively-charged functional groups through domains rich in positively charged lysine residues. The binding supposedly induces conformational change in FXII, leading to formation of active FXIIa through autoactivation. The binding followed by the conformational changes renders FXII much more susceptible to proteolytic cleavage and activation by kallikrein. It has been shown that surface-bound FXII is 500 times more susceptible to activation by kallikrein than soluble FXII in blood.[32] Thus, surfaces do play an important role. FXIIa formed at the surface, in turn, cleaves PK-HMWK complex bound to the surface to form kallikrein. This mutual activation of PK and FXIIa at the surface is called reciprocal amplification. FXIIa can also hydrolyze FXII through autohydrolysis, which is known as self-amplification. FXIIa also activates FXI-HMWK complex bound at the surface to form FXIa, leading to the propagation of coagulation cascade.[33]

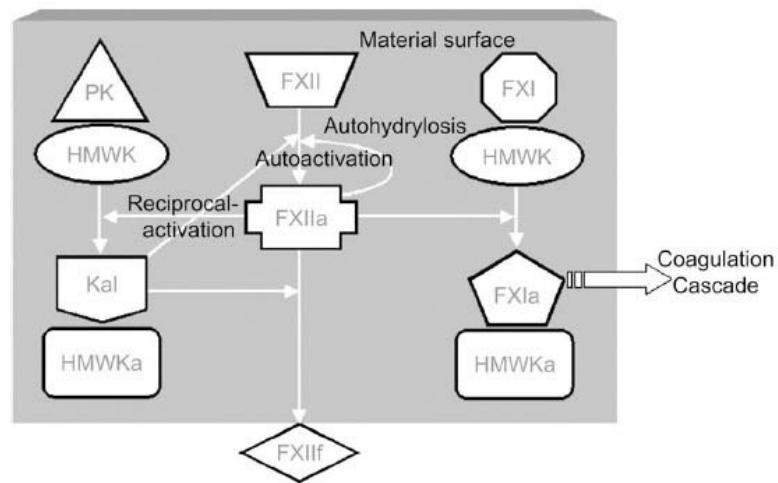


Figure 7: Consensus Mechanism for Surface-mediated Contact Activation[33]

The observation that blood clots rapidly in glass tubes (hydrophilic and anionic) but slowly in plastic tubes (relatively hydrophobic) led to the perceived relationship between contact activation and anionic-hydrophilic surface, hence to the mechanism described above. The idea was corroborated by the fact that other negatively charged surfaces like kaolin, ellagic acid, dextran sulfate, sulfatides, celite etc. showed similar results.[34] Some studies[35] also showed that the contact activating materials were characterized by high wettability and high negative zeta potential. This resulted in the idea of chemical-specificity i.e., there exists some sort of chemically-specific binding between FXII and anionic surfaces, which catalyzes the coagulation process.[33]

However, Zhuo et al. showed that autoactivation of FXII to FXIIa in 'neat-buffer solution' (a solution devoid of all proteins other than FXII and activation products therefrom) occurs with equal efficiency (in terms of rate and FXIIa yield) at both anionic hydrophilic (clean glass) and neutral hydrophobic (silanized glass) surfaces, thereby challenging surface-energy dependent catalytic potential effect of surfaces such as glass.[36] On the other hand, FXII activation in whole plasma occurs at significantly greater efficiency at hydrophilic surfaces. This indicates a strong interaction of other plasma proteins with the surfaces that governs the surface mediated activation of FXII. Vogler and Siedlecki have proposed 'adsorption-dilution effect', for the difference in the activation behavior of hydrophilic and hydrophobic surfaces.[33] For hydrophilic surfaces, strong hydrogen bonding to water resists the protein adsorption on the surface while the hydrophobic surfaces are equally attractive to all the plasma proteins (some of which are in much larger proportion as compared to FXII). The

resulting 'competitive-protein adsorption' at hydrophobic surfaces greatly minimizes chances of FXII contact with the surface, it being relatively dilute. In contrast, since the proteins do not adsorb to hydrophilic surfaces, no adsorption competition occurs and FXII has fair chances of contact with the surface, thereby being activated to FXIIa and leading to rapid coagulation. Thus, it is actually a relative diminution of surface-mediated FXII activation on hydrophobic surfaces that leads to the speculation that FXII activation has an apparent specificity for anionic-hydrophilic surfaces. This theory even answers the observation that plasma eventually clots in the hydrophobic tubes. Despite the adsorption competition with other proteins, FXII sooner or later comes in contact with the hydrophobic surface and gets activated to FXIIa and propagates the coagulation cascade.[33][37]

In another study, Sperling et al. showed that contact activation and platelet adhesion together have a strong synergistic effect on surface-mediated coagulation. They showed that platelet adhesion was maximum for 100% -CH₃ surface and contact activation was maximum for 100% -COOH surface while, the thrombin formation (measured as the thrombin peak time) was fastest at surface composed of -COOH/-CH₃ (83/17). It is believed that contact activation forms traces of thrombin, initiating the coagulation, and the adherent activated platelets provide binding sites for propagation of coagulation. Positive interactions between these two processes thus produce synergistic effect boosting the coagulation process.[38]

Zinc ions are thought to play a physiological relevant role in contact activation. Various studies have shown that Zn⁺² is an important cofactor in FXII activation.[34] Thus, the

presence of zinc particles on the surface may also aid the coagulation process. Ostomel et al. found that basic oxides with an isoelectric point above the pH of blood are anticoagulants while acidic oxides with an isoelectric point below the pH of blood are procoagulants. Through a study comparing different metal oxides, they suggested that the time for clotting increases with the increasing isoelectric point (Isoelectric point is the pH where the Zeta Potential (ζ) is zero).[29] Bioactive glass is another substrate which is of interest for wound healing due to its mesoporous morphology, biocompatible composition, high calcium content and easily modified functionality.[29] Griep et al. studied the contact activation from a thermodynamic standpoint. They showed that the contact activation is a general surface phenomenon rather than biological reaction of certain functional groups and that the rate of activation of FXII to FXIIa is temperature dependent. At temperatures below their thermal transition temperatures, i.e. the temperature at which there is a decrease in the activation rate, all surfaces would be equally effective in stimulating the activation of FXII. A surface with low-temperature thermal transition would be a poor topical hemostatic agent.[39]

From the above discussion, it can be seen that there has been a multidimensional approach to understand the mechanism of surface mediated contact-activation in order to find the ideal implantable biocompatible surface or ideal topical hemostatic agent, both of which aim at the opposite end of spectrum of the surface coagulation phenomenon. However, the exact mechanism is still unclear. Our study focuses on the approach of surface modification in order to determine the ideal surface chemistry that would enhance the surface induced coagulation and act as topical hemostatic agent.

2.3. Review of Existing Hemostatic Materials

Hemostatic materials can save lives in military and civilian trauma as well as during surgical procedures. From the tourniquets in earlier days to the recent advanced topical hemostatic agents, there has been a great progress in this field. The mechanism, advantages and disadvantages of some of the well-known commercial hemostatic agents have been discussed in this section.

The hemostatic agents have been derived from various sources, each having their own different mechanism, advantages and disadvantages. These hemostatic agents are plant (cellulose)-based, gelatin-based, collagen-based, fibrin-based, thrombin-based, chitin/chitosan-based or mineral-based. Topical hemostatic agents that are available today can be classified, based on their mechanism, as Physical Agents, Absorbable Agents, Biologic Agents, Synthetic Agents and Hemostatic Dressings. Most of these hemostatic agents can also be grouped as Active Hemostatic Agents or Passive Hemostatic Agents.[6] Active agents are those which contribute to the mechanism of coagulation cascade in a biologically active manner. These agents perform biological activity and directly participate in the process of coagulation to induce clot at the site of bleeding. Thrombin-based hemostatic agents are Active Hemostatic Agents. Passive Hemostatic Agents are those which act passively through contact activation and promotion of platelet aggregation. Their basic mechanism is to provide a physical structure around which platelets can aggregate so a clot can form. Cellulose and Collagen based agents are Passive Hemostatic Agents.

In the early days, when the mechanism of hemostasis was not fully understood, 'Bone wax' was used to stop the blood flow from damaged vessels during the surgery. Bone wax (a product obtained by softening the natural wax produced in the bee hive of honey bees) was introduced in 1886 and its mechanism was based on tamponade of blood vessels. However, it had problems related to allergy, infection and interference with the healing process.[40] With the increased understanding of hemostasis, more and more approaches were sought after and 'absorbable agents' like plant-based and gelatin-based hemostatic agents were introduced in 1942 and 1945 respectively. The mechanism by which these 'absorbable agents' induce hemostasis is that they absorb the fluid from the blood, resulting in the increased concentration of clotting factors and platelets at the wound site. They also swell and physically seal the wound.

Plant-based hemostatic agents include oxidized cellulose (OC) and oxidized regenerated cellulose (ORC). The latter is produced by decomposing the wood pulp and then regenerating the cellulose fibers. Oxidation converts the hydroxyl groups into carboxylic acid, which causes denaturation of blood proteins initiating hemostasis. A number of mechanisms are thought to contribute to their hemostatic action, including fluid absorption and subsequent hemoconcentration of blood, swelling, surface interaction with proteins and platelets and acidic pH.[40] The low pH also imparts bacteriostatic properties. Moreover, these materials are biodegradable (OC 3-4 weeks and ORC 1-2 weeks).[41] Some well-known products in this category are Surgicel® (Ethicon, Inc.), BloodStop® (Life Science Plus) and TraumaDex™ (Medafor, Inc). Surgicel® was approved by the Food and Drug

Administration (FDA) in 1960.[42][43][44] TraumaDex is a microporous polysaccharide hemosphere available in the powder form.[45] The disadvantage with these materials is that they cannot be used in combination with other agents (e.g. thrombin based) due to the low pH. Moreover, the swelling might pose the risk of spinal cord compression. Although biodegradable, it is advised to remove these materials using irrigation as soon as hemostasis is achieved since they may lead to complications like foreign body reactions, fibrous encapsulation and migration away from wound site.[46]

Gelatin-based materials were introduced a few years after the oxidized cellulose materials. The gelatin sponge consists of purified pork or bovine skin. Its mechanism for hemostasis is attributed to its ability to absorb 45 times its weight, expanding up to 200% of its initial volume. It is also believed to induce surface activation via the intrinsic pathway. Unlike oxidized cellulose, the pH of the gelatin sponge is neutral, hence, it can be used in combination with other agents such as thrombin.[47] Well-known products include Gelfoam® (Pharmacia and Upjohn) and Surgifoam™ (Ethicon, Inc.). Due to excessive swelling, the risk of nerve compression is the biggest disadvantage. In addition, these being derived from animals, there is a risk of antigenicity.[46]

Collagen-based hemostatic materials were introduced in 1970. Collagen is a tissue-derived biomaterial (derived from bovine corium) having good cell compatibility in terms of adhesion, growth and migration.[48] Collagen-based agents have microfibrillar structure consisting of collagen molecules with hydrochloric acid non-covalently bound to some of the

available amino groups. The hemostatic properties of Microfibrillar Collagen (MFC) rely on the promotion of platelet aggregation. MFC provides large surface area which, when in contact with blood, allows platelets to adhere to its fibrils and activate them. Platelet activation is followed by platelet aggregation and thrombus formation.[41] Hemostatic properties are also improved by the strong adhesion of MFC to injured surfaces. MFC does not swell significantly and is absorbed within 6-8 weeks.[46] Commonly used MFC hemostatic agents are Avitene® (Davol, Inc.), Helistat® (Integra) and Instat® (Ethicon, Inc.), which are available both in microfibrillar form (short slender fibers) and sponge form.[49] CoStasis® (Cohesion Technologies) is also a promising product. Adverse effects of MFC hemostatic agents are infrequent but include fibrous encapsulation, allergic reactions and interference with the healing process. As with oxidized cellulose, it is advised to remove MFC after hemostasis is achieved, since it may bind to nerves causing pain or numbness. Moreover, since MFC may pass through filters of blood scavenging systems, blood contaminated with MFC should not be returned to the patient.[41]

Fibrin-based hemostatic agents were first reported in 1909 but did not receive FDA approval until 1998.[50] Fibrin sealants are biological adhesives derived from blood. These products consist of high concentrations of fibrinogen, thrombin and additional components like calcium and factor XIII, all of which work to mimic the final stages of the blood coagulation cascade. Although these components are naturally present in the blood, fibrin sealants provide the clotting factors in much higher concentration, leading to more rapid clot formation.[51][45] Inactivated fibrinogen (plasma derived) and thrombin (mostly human) are

packaged in a dual barrel syringe that allows both the components to flow at equal rates and combine at the wound site to mimic the final stages of clotting process. The mechanical strength of fibrin sealant is determined by the concentration of fibrinogen while the relative thrombin concentration determines the rapidity of clot formation. Sealants with high fibrinogen concentration produce stronger but more slowly forming clots while those with high thrombin concentration form rapid but less strong clot.[46] Products based on this mechanism are Tisseel™ (Baxter), Hemaseel™ (Haemacure) (both approved by FDA in 1998), Artiss™ (Baxter) and Evicel® (Ethicon) (previously known as Crosseal™ and approved by FDA in 2003).[52] Though very effective, these liquid fibrin sealants have certain limitations which restrict their use for trauma applications. Both the components of fibrin sealants need to be kept frozen. Hydrating the lyophilized products, prior to use, requires warming and prolonged agitation, which is time consuming. Moreover, they cannot be used for high volume venous or high pressure arterial hemorrhages. In order to overcome these limitations, American Red Cross developed the Dry Fibrin Sealant Dressing (DFSD) which is a lyophilized, immobilized version of fibrin glue. It contains active thrombin and fibrinogen along with calcium on a glycan backing. On wetting with blood, it rapidly forms fibrin and clots the wound.[53][54] DFSD has a reduced risk of viral transmission, is stable at room temperature and requires no mixing of components. However, it is slow to manufacture, it is very expensive (about \$1000 per dressing) and it is yet not approved by the FDA for clinical use.[1] A similar approach is presented by TachoComb® (Nycomed), in which freeze-dried collagen is doped with fibrinogen and thrombin, but the concentrations are lower than in DFSD, and the product is intended only for use in surgery.

Thrombin-based hemostatic agents, like fibrin-based agents are active hemostatic agents and directly participate in the coagulation cascade. Thrombin is the important factor in the coagulation cascade which promotes and modulates coagulation. Production of thrombin is the final step of coagulation process which is required to cleave fibrinogen to fibrin and provide a hemostatic lattice for platelet aggregation and thrombus formation. Until recently, the only source of pure thrombin was bovine plasma (Thrombin-JMI®, King Pharmaceuticals, Inc.). Though effective, bovine thrombin is prone to induce robust immune response on human exposure.[46][55] Hence, researchers developed thrombin from human plasma which received FDA approval in 2007 (Evithrom®, Omrix Biopharmaceuticals). Although relatively safe, human thrombin possesses theoretical risks of viral transmission and it has the limitation of finite availability. In response, Recombinant Human Thrombin (rh Thrombin) was developed (Recothrom®, Zymogenetics Inc.). rh Thrombin an amino acid sequence that is identical to human thrombin, is made from a genetically modified Chinese hamster ovary cell line. It was approved by the FDA in 2008.[47] Stand-alone thrombin can be cumbersome for topical application unless sprayed into mist or used with another carrier like gauze/pad or used as a solution in combination with fibrinogen or gelatin to create a glue. Gauze/pad type thrombin dressings available are: Thrombi-Gel® (Vascular Solutions), D-Stat Dry® (Vascular Solutions) and Thrombi-Pad™ (King Pharmaceuticals). Thrombin-based products used in combination with fibrin are the fibrin sealants discussed earlier. Another combination sealant product is FloSeal™ (Baxter), which differs from fibrin sealants in that it depends on the patient's own blood for fibrinogen. FloSeal is a combination of gelatin-based matrix from bovine collagen containing microgranules, cross-linked with

glutaraldehyde and human thrombin solution. Upon contact with blood the gelatin particles swell and induce a tamponade-like effect while thrombin directly participates in the coagulation cascade resulting into faster clotting.[56][57]

Poly-n-acetyl glucosamine (P-NAG) based hemostatic dressings are interesting because they are effective, have no side effects and are stable without special storage requirements. Poly-n-acetylglucosamine (chitin) is a polysaccharide biopolymer produced naturally by algae through fermentation. It is also obtained from crustacean shells. Its deacetylated form, chitosan (poly-d-glucosamine), has been shown to be more effective than chitin in controlling severe hemorrhage.[45][58] The exact mechanism of action is still unclear but chitin and chitosan dressings are thought to be working by inducing vasoconstriction and rapidly mobilizing and adhering to red blood cells, platelets and clotting factors.[59][60] Moreover, chitosan also absorbs some fluid at the wound site thereby increasing the concentration of clotting factors and forming gel-like matrix over the wound.[61] These dressings have also shown antibacterial properties. HemCon® (HemCon Medical Technologies, Inc.) is a well-known chitosan dressing which received the FDA approval in 2002. It costs about \$100 per dressing. A prominent FDA approved chitin dressing is Rapid Deployment Hemostat – RDH (Marine Polymer Technologies) which costs \$300 per dressing.[46] In one of the studies, it is shown that polymeric fiber material based on poly-n-acetyl glucosamine is more effective than chitin or chitosan, since the later two have a heterogeneous structure and are complexed with minerals and proteins. Moreover, the β -structure (parallel orientation) of the fibers was found to be more effective than the α -

structure (antiparallel orientation).[62] In another study, the hemostatic and antibacterial properties of chitosan dressings have been shown to be improved by the addition of polyphosphate polymers and silver nanoparticles respectively.[63] One limiting factor is that all forms of chitin or chitosan bandages are not equally effective and the effectiveness varies from batch to batch.[1]

BioHemostatTM (Hemodyne) is a polymeric hemostatic dressing. It consists of a liquid absorbing core made of microporous hydrogel-forming polyacrylamide which is attached to a traditional bandage made of ethylene-vinyl acetate co-polymer. When applied to the wound, it absorbs the fluid and expands to occlude the wound creating backpressure to stop bleeding. The material is said to be able to absorb 1400 times its weight.[64]

A mineral Zeolite hemostatic agent QuikClot® (Z-Medica) was approved by FDA in 2002.[65] Zeolite is an inert mineral product composed of oxides of silicon, aluminum, sodium and magnesium and small amount of quartz. It acts as molecular sieve and absorbs fluid at the site of injury thereby increasing the local concentration of clotting factors.[1] It is stable, easy to use and costs only \$10 per packet. However, a serious issue with this product is that the reaction being exothermic, high temperature is generated at the wound site which could result in burns and tissue damage. Although the risk of tissue damage is far outweighed by the increased chance of survival when QuikClot® is used to treat an otherwise uncontrollable exsanguinating hemorrhage, the product may have unacceptable risk:benefit ratio if used for minimal, nonlethal wounds. Another issue is that QuikClot® is ineffective

for high-pressure arterial bleeding. It has been reported that the powder is carried away from the wound due to high pressure bleeding, rendering the product ineffective.[45] To deal with these problems, the manufacturers started using prehydrated zeolite so that it absorbs water less exothermically and mineral zeolite is now enclosed in a gauze mesh pouch so that it can be applied at the wound site without the powder being washed away. However, with these changes, the change in the efficacy of the product is a matter of investigation.[46][66] Z-Medica also launched QuikClot® eX™ for over-the-counter use. It consists of kaolin as the hemostatic agent which works by activating factor XII and initiating contact activation pathway.[67][68] A recent development is a product called WoundStat™ (Trauma Cure). It consists of a smectite mineral and a superabsorbent polyacrylic polymer that can absorb 200 times its weight. An alternative to zeolite based QuikClot® is currently under investigation which is based on aluminophosphate.[41]

Another recent development in the field of hemostatic dressing is Stasilon® (Entegriion). It consists of a woven fabric with continuous filament texturized E-glass as warp and bamboo-rayon and glass filament as weft. The fiberglass contributes to the hemostatic mechanism through contact activation of the coagulation cascade and bamboo rayon helps through fluid absorption and binding of red blood cells.[4][69]

Thus, there are number of approaches for hemostatic dressings each with its own mechanism, advantages and disadvantages. Depending on the type and severity of the injury, one may be better suited than another. Despite such a development in the field of topical hemostasis, the search of the ideal hemostatic dressing still continues.

2.4. Surface Modification of Fibers

Surface chemistry plays a major role in determining the hemostatic properties of a substrate. Moreover, glass has been found to be one of the most potent hemostatic materials. Hence, it is logical that if a glass-like surface is replicated on other materials, their hemostatic properties could be improved. In order to test this idea, we treated different fibers with a material that imparts silicon dioxide (glass-like surface) on the substrate. It has also been noted in the literature that different functional groups such as carboxyl (-COOH), methyl (-CH₃), hydroxyl (-OH) etc. might be helpful in improving the coagulation process through different mechanisms like platelet activation, platelet adherence or fibrinogen adsorption.[70][71][72][38] Hence, to determine the effect of various functional groups, we treated fiberglass with different chemicals having specific functional end-groups. The chemicals used for surface modification are described below.

2.4.1. Tetraethyl orthosilicate (TEOS)

TEOS is tetra-ethyl-ortho-silicate (also known as tetra-ethoxy-silane) having the structure as shown in Figure 8.

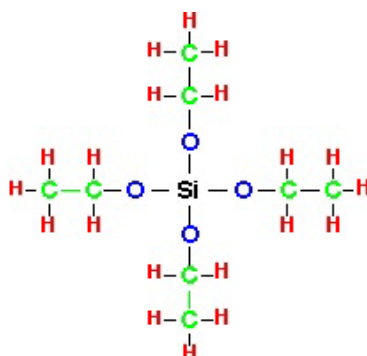


Figure 8: Structure of TEOS

TEOS hydrolyzes into silicon dioxide and ethanol in presence of atmospheric moisture and hence imparts silicon dioxide (glass-like surface) to the material.[73] Formation of silicon dioxide requires removal of ethane groups and two oxygen atoms (Figure 9).

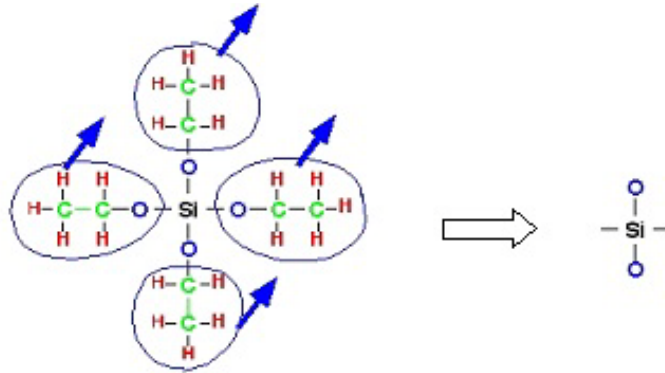


Figure 9: Formation of Silicon dioxide from TEOS[73]

Silicon dioxide is bound to the surface of the material through silanol groups (Si-OH) and the additional TEOS is deposited through siloxane bond (Si-O-Si) with the removal of ethane (Figure 10).

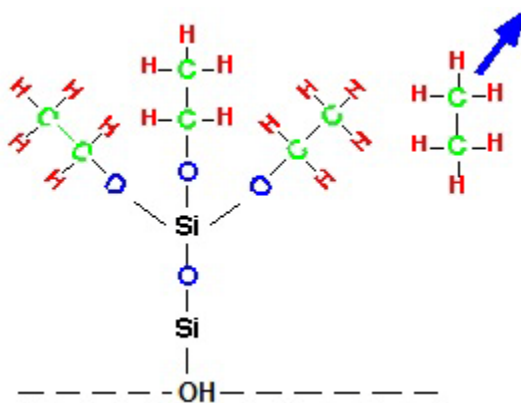


Figure 10: Deposition of TEOS on the material surface[73]

The alkyl-covered surface prevents further deposition of TEOS. Hence, the deposition is limited by the removal of alkyl groups. However, the alkyl groups readily react with water (or moisture) to form silanols (Si-OH). The neighboring silanols then react with each other to eliminate ethanol and form stable siloxane bridges (-Si-O-Si-) (Figure 11).

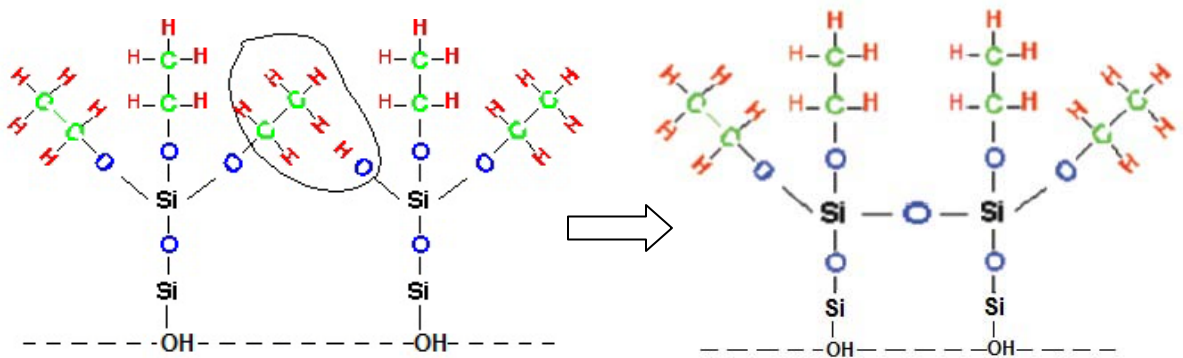


Figure 11: Formation of Siloxane Bridges[73]

Finally, in presence of water (moisture), ethanol is released and a reactive silanol (-Si-OH) group is formed on the surface (Figure 12).

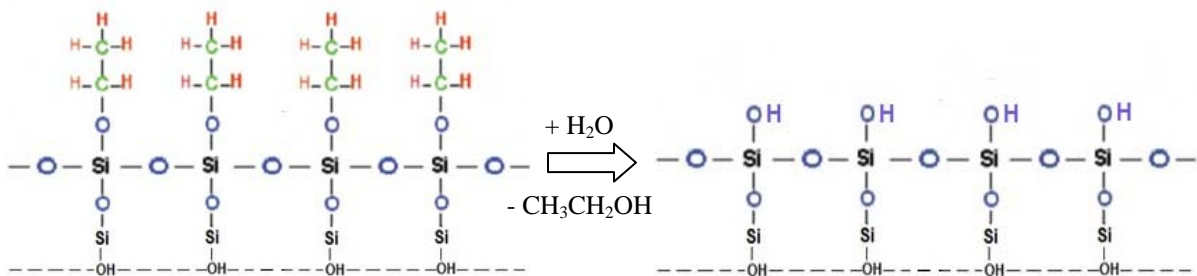


Figure 12: Formation of Glass-Like Surface

Thus, the TEOS coated material surface has a surface charge and exposed functional groups similar to glass. TEOS molecules can also be further functionalized to impart specific end-groups on the substrate and tailor the surface properties of the material.[74][75]

2.4.2. Aspartic Acid

Aspartic acid is an amino acid with the structure shown in Figure 13. Based on the type of catalyst (acid or base), it can give carboxyl (-COOH) or amine (-NH₂) end-groups.

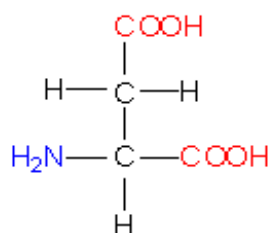


Figure 13: Structure of Aspartic Acid

2.4.3. Glycidoxypropyltrimethoxysilane

Glycidoxypropyltrimethoxysilane is an organosilane with the structure shown in Figure 14. The epoxide ring is susceptible to hydrolysis and it gives two hydroxyl groups (-OH) per molecule.

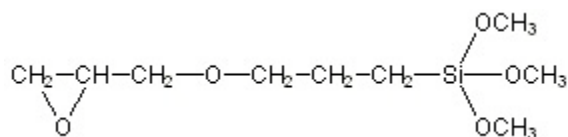


Figure 14: Structure of Glycidoxypropyltrimethoxysilane

2.4.4. Methyltriethoxysilane

Methyltriethoxysilane is also an organosilane with the structure shown in Figure 15.

It gives methyl (-CH₃) end-groups on the surface.

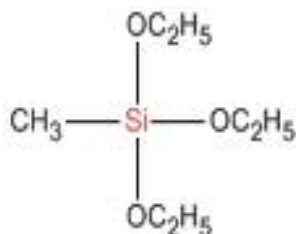


Figure 15: Structure of Methyltriethoxysilane

2.4.5. N-[3-(Trimethoxysilyl)propyl]-ethylenediamine

N-[3-(Trimethoxysilyl)propyl]-ethylenediamine is an organosilane as shown in Figure 16. It would give amine (-NH₂) end-groups on the surface of the material.

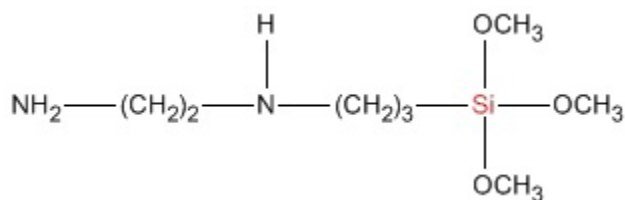


Figure 16: Structure of N-[3-(Trimethoxysilyl)propyl]-ethylenediamine

2.4.6. Phosphatidylserine

Phosphatidylserine is an anionic phospholipid with three ionizable groups i.e. the phosphate moiety, the amino group and the carboxyl group (Figure 17). The negatively

charged phosphatidylserine is believed to facilitate the assembly of tenase and prothrombinase complexes and enhance the rate of coagulation. Under normal conditions, phosphatidylserine is present in the inner-layer of plasma cell membrane. During platelet activation, it is exposed to the activated factors of tenase and prothrombinase complexes, which have affinity for negatively charged phospholipid surface. It is also believed that phosphatidylserine binds to the discrete regulatory sites on factors Xa and Va and allosterically alter their proteolytic and cofactor activities. Thus, phosphatidylserine is thought to play an important role in blood coagulation.[76][21]

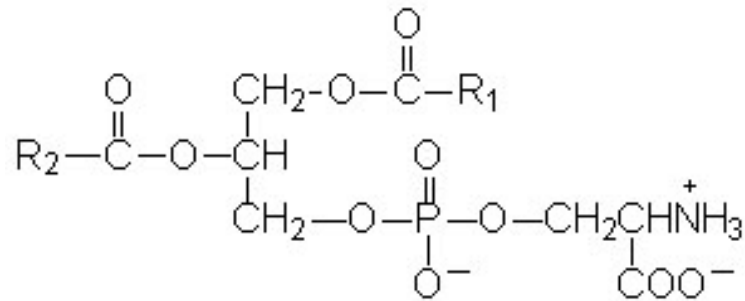


Figure 17: Structure of Phosphatidylserine

2.4.7. Phosphatidylcholine

Phosphatidylcholine is also a phospholipid (Figure 18) and a major constituent of cell membranes. It is found in the outer-layer of cell membrane. It is believed that phosphatidylcholine inhibits the activity of blood coagulation regulatory system i.e. anticoagulation system (protein C and protein S) and thus facilitates coagulation.[77]

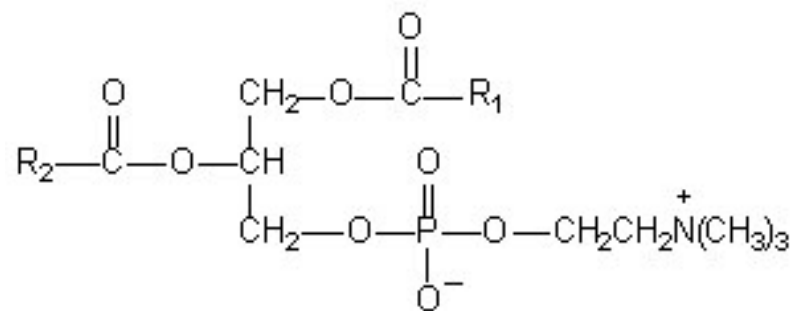


Figure 18: Structure of Phosphatidylcholine

2.5. Thrombin Assay

Various clinical tests have been proposed to measure/predict the coagulation properties of blood, mainly to aid the treatment for patients with hypocoagulability or hypercoagulability. Generally accepted standardized methods include Prothrombin Time (PT) and Activated Partial Thrombin Time (APTT). PT measures the time taken for clot formation via tissue factor dependent stimulation of extrinsic pathway and APTT measures contact stimulation of the intrinsic pathway. However, these methods use clot formation as their endpoint and do not assess the whole coagulation system.[78][79] Thrombin plays an important role in hemostasis through its multiple functions. The trace amount of thrombin formed during initiation phase (after the exposure of tissue factor to the blood) helps in overcoming the inhibitory effect of TFPI (Tissue Factor Pathway Inhibitor) by activating platelets and other coagulation factors (XI, V and VIII) to generate more thrombin (amplification phase). The additional thrombin generated, catalyzes the conversion of fibrinogen to fibrin that helps to stabilize the platelet plug and to form the clot. Thus, it is the capacity to generate thrombin, and the enzymatic work that thrombin does, that determines blood coagulability. Therefore, the measurement of thrombin generation is a reliable indicator of the rate and extent of coagulation in a true sense. Most of the thrombin (> 95%) is generated after initial formation of fibrin and hence the tests like PT and APTT, whose end points are the formation of fibrin, do not give true measure of thrombin potential. This led to the development of dedicated Thrombin Generation Assays.[80][81][82]

There has been a great development in the Thrombin Assays over the time from laborious sub-sampling technique to the use of chromogenic substrate to the recently developed Thrombin Assays that use fluorogenic substrate and Calibrated Automated Thrombogram (CAT). The Fluorogenic Thrombin Assay uses a fluorogenic substrate, Z-Gly-Gly-Arg-AMC. Upon splitting by thrombin, it releases fluorescent AMC (7-amino-4-methylcoumarin), which is measured by 390 nm excitation and 460 nm emission filters in a fluorometer. The fluorescence intensity can thus be used to determine the amount of thrombin generated. Using a calibration factor, the fluorescence intensity (RFU – Relative Fluorescence Unit) can be converted to thrombin activity (nM – nano Molar). If a first order derivative is then plotted, it gives ‘lag time’, ‘peak thrombin generation’, ‘time to peak thrombin generation’ and ‘Endogenous Thrombin Potential (ETP)’ as shown in figure 19.[83][84][85][86]

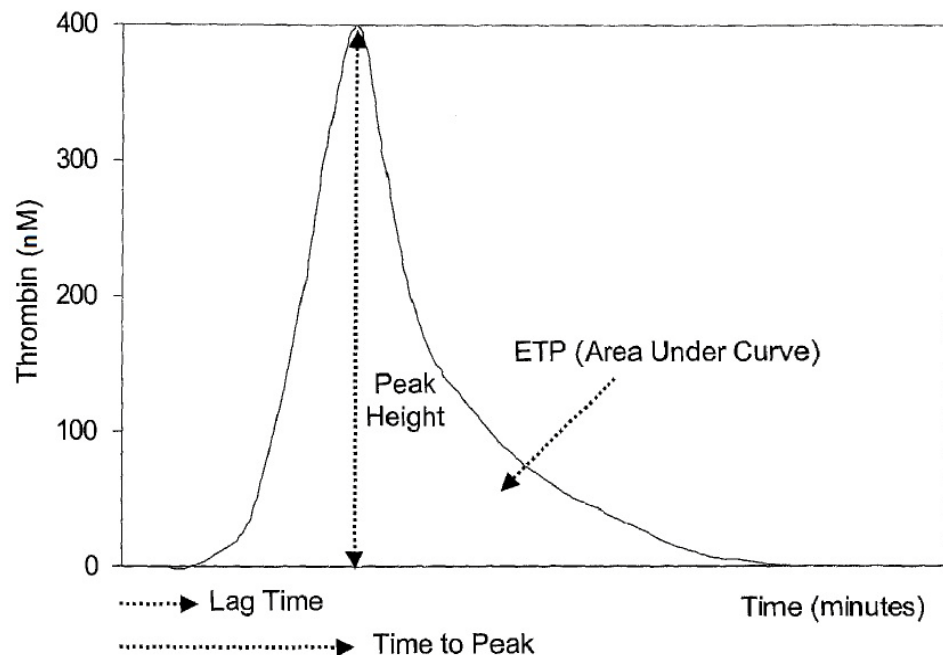


Figure 19: Typical Thrombin Generation Curve (Thrombogram)[86]

The curve gives information about the time to initial thrombin formation i.e. 'lag time', which is the initiation phase. The rapid burst of thrombin generation that occurs during amplification and propagation stage is given by 'maximum rate of thrombin generation' and the thrombin concentration reaches to maximum, given by 'peak thrombin generation'. 'Time to peak thrombin generation' is the measure of initiation, amplification and propagation phases together. After this, the thrombin generation slows down due to inhibition and the curve returns to baseline. The area under the curve is called 'Endogenous Thrombin Potential' (ETP) which is defined as work potential of thrombin or the capacity of plasma to generate thrombin over time.[87] Thus, the thrombogram reflects the action of the total clotting mechanism.

The Fluorogenic Thrombin Assay is probably the most accurate in-vitro representation of in-vivo clotting process. It provides the tool to study the clotting process and the interaction of clotting factors in a better way since even the slightest changes in the coagulation factors will affect the thrombin-generation capacity. There are reports suggesting that this technique would work for whole blood as well [88], while some doubt this and believe more work needs to be done.[89] Despite all the developments, there remains a major issue with respect to the standardization of thrombin generation assays. Comparison and analysis of studies in literature is difficult due to the use of different samples, substrates, reagents and methods.

2.6. Zeta Potential

'Electrokinetics' is the study of electric potential caused by the tangential fluid motion adjacent to a charged surface. Electrokinetic measurements give surface charge characteristics of the material. Electrokinetic measurements are also helpful for monitoring and control of certain chemical modifications of fibers.[90][91] Electrokinetic properties of fibers are influenced by surface chemical composition, surface polarity, microstructure, fiber porosity, fiber orientation, packing density and swelling behavior of the fibers. When the surface of a material is in contact with a polar medium (such as water), a surface charge is developed which is governed by association/dissociation of surface chemical groups, adsorption of ionic species and/or dissolution of ions from the material into the solution. In order to balance the surface charge, a thin layer of oppositely charged counter-ions is formed in the liquid at the interface. These two layers of opposite charge constitute the Debye Layer or Electric Double Layer (EDL), which generates electrokinetic properties.[92][93] EDL, as the name suggests, consists of two layers. The layer of counter-ions closest to the surface is called Stern Layer, which is immobile. The outer region where the ions are less firmly bounded is called Diffuse Layer. Within the Diffuse Layer there exists a boundary, known as hydrodynamic shear or slipping plane, separating the counter-ions from the bulk of the solution. The potential that exists at this shear plane is called Zeta Potential (ζ), which is the basis for electrokinetic measurements (Figure 20).[94][95]

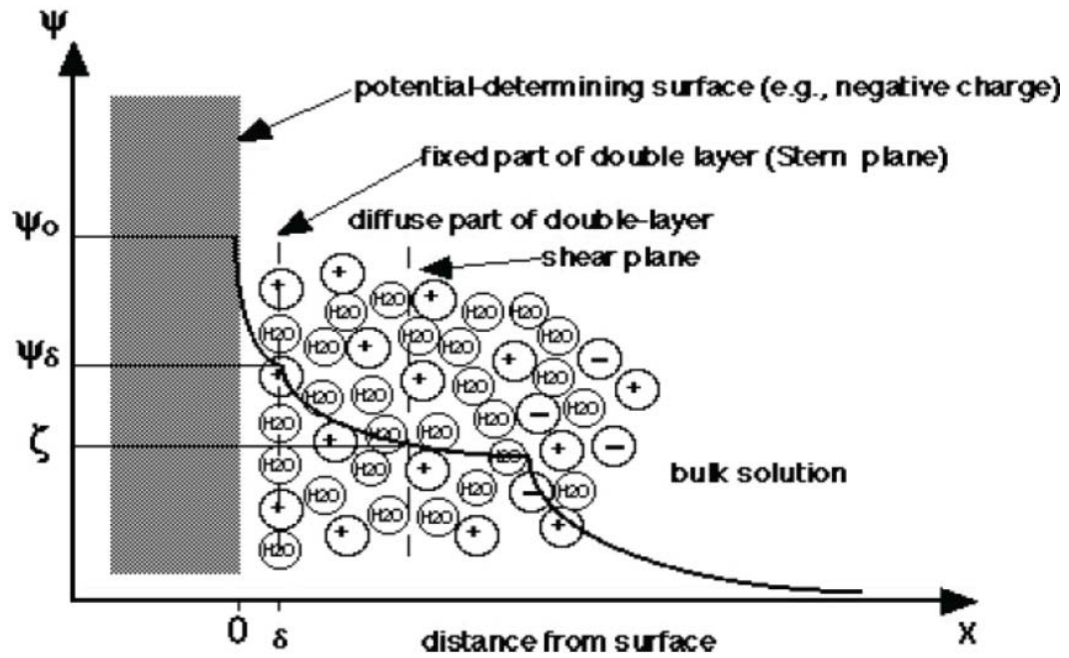


Figure 20: Electric Double Layer at the Surface-Liquid Interface

Zeta potential for a surface is influenced by impurities, additives and finishes on the material. It is also a function of pH, counter-ion concentration, counter-ion valency and ionic strength of the electrolyte solution. A typical plot of zeta potential versus pH is shown in Figure 21.

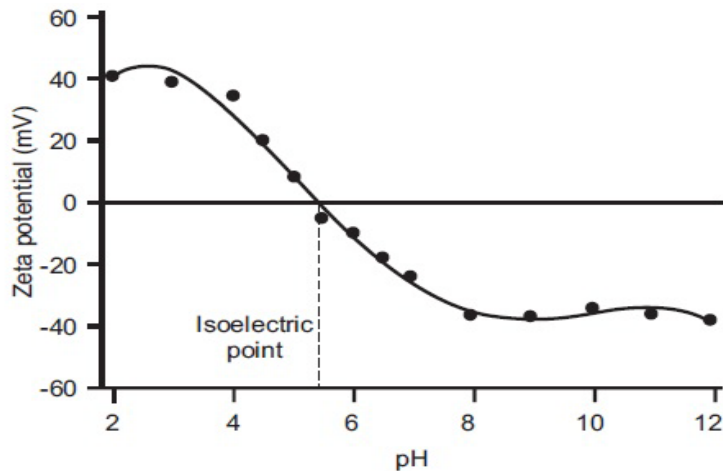


Figure 21: Typical Plot of Zeta Potential Vs. pH

The point where the plot passes through zero zeta potential is called the isoelectric point which is also an important consideration. For a material to have rapid coagulation through contact activation, not only the higher negative zeta potential but also the lower isoelectric point is believed to be favorable. It has been shown that the clotting time increases with the increasing isoelectric point.[29]

Different techniques have been developed to measure zeta potential of the surface. The basic principle in all the methods involves relative motion of the liquid or solid surface in contact with each other. This causes a flow of counter-ions adjacent to the surface, resulting in an electrical potential. Some of the commonly used techniques to measure zeta potential include electrophoresis (the movement of charged particles relative to the surrounding liquid under the influence of an applied electric field), electro-osmosis (the movement of a liquid relative to the stationary charged particle under the influence of an applied electric field), streaming potential (electric potential generated when a liquid is forced to flow past a stationary charged surface), sedimentation potential (electric potential generated when charged particles move relative to a stationary liquid) and recently developed electronic sonic amplitude (ESA) technique. The streaming potential technique is suitable for the fiber materials used in our study.[96][97]

Streaming potential is the potential difference at zero electric current, caused by the flow of liquid under a pressure gradient through a capillary or a plug. The streaming potential test measures the electrical potential difference between the two ends of the plug or capillary

which is filled with fibers. Electrolyte solution is pumped through the plug which causes movement of counter-ions adjacent to the charged surface. The flow of ions gives rise to electrical potential (Figure 22).[98][99]

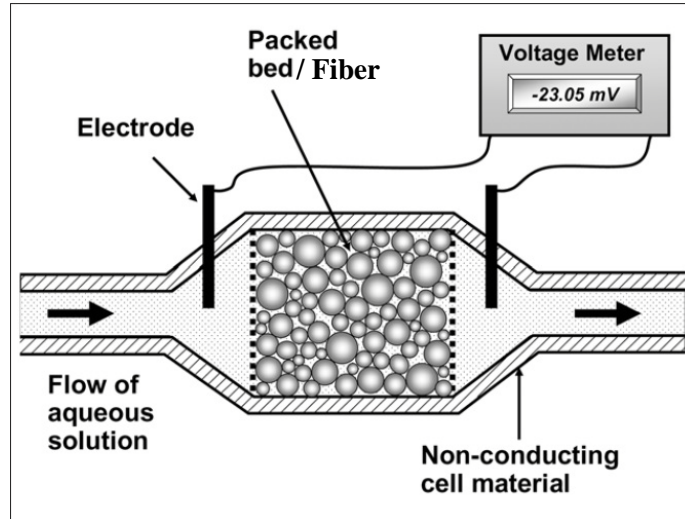


Figure 22: Streaming Potential Measurement across a Plug

The voltage resulting due to pressure differential across the sample is compared to the baseline potential measured in the absence of applied pressure. Streaming potential values are converted to the more fundamental quantity, zeta potential, using the Helmholtz-Smoluchowski equation (Eq. 1).[100]

$$\zeta = \frac{\eta \lambda V}{\epsilon_0 D \Delta P} \quad (\text{Eq. 1})$$

Where, ζ is the zeta potential (millivolt), η is the viscosity of electrolyte solution, λ is the conductivity of the solution, V is the streaming potential (mv), ϵ_0 is the permittivity of free

space, D is the dielectric constant of the liquid and ΔP is the applied pressure gradient across the sample (Pa).

Zeta potential measurement has the ability to quantify the relationship between the surface charge and the hemostatic ability of the material since it has been shown that coagulation properties of the material correlate with their surface charge and hydrophilicity. Thus, zeta potential measurements can help in understanding the coagulatory effects and predicting the hemo-compatibility or thrombogenicity of the material.

2.7. Contact Angle

Contact angle (θ) is the quantitative measure of wetting of a surface by a liquid. Depending on the contact angle, a surface can be classified as hydrophilic (water loving/wettable) or hydrophobic (water repelling/non-wettable). The contact angle is the angle where a liquid-vapor interface meets a solid surface (Figure 23).

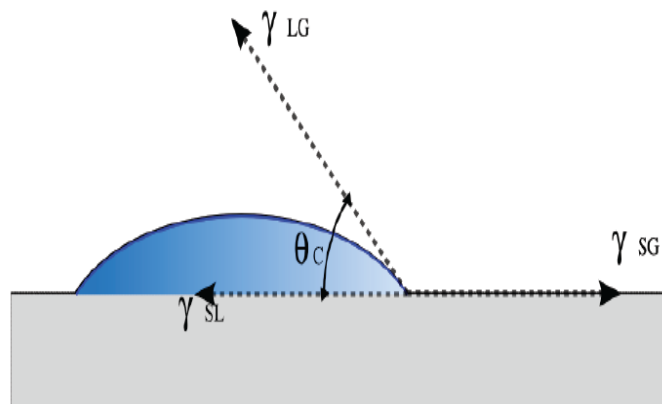


Figure 23: Contact Angle of Liquid on a Solid Surface

If the angle is less than 90° , the surface is considered wettable (hydrophilic) and if it is greater than 90° , the surface is considered non-wettable (hydrophobic). Parameters including surface energy of the material and surface tension of the liquid determine the cohesive (attraction between the liquid molecules) and the adhesive (attraction between liquid molecules and solid molecules) forces of the system. If the adhesive force dominates the cohesive force, the surface is hydrophilic and the liquid spreads easily on the surface giving low values for contact angle. However, if the cohesion is greater than adhesion, the material is hydrophobic and the liquid forms the sphere-like shape to reduce the surface contact and gives high contact angle values.

Blood is primarily composed of water, hence the hydrophilicity or hydrophobicity of a material is expected to affect its hemostatic properties. As discussed earlier, hydrophilic materials show better hemostatic properties. They enhance the surface-binding of platelets and other co-factors and promote rapid contact activation of the coagulation cascade.

CHAPTER 3: Materials and Methods

3.1. Material Preparation

In this research, the control fibers (untreated fibers) are compared with TEOS treated counter-parts as well as other TEOS treated samples for their hemostatic efficacy. The fibers used in this study include heat cleaned E-glass fibers (generously donated by Carolina Narrow Fabrics), cotton fibers, rayon fibers, polyester fibers, nylon fibers and polypropylene fibers (all donated by Nonwovens Cooperative Research Center at NCSU). The counts of the fibers used are: cotton 2 denier, rayon 2.8 denier, nylon 9 denier, polyester 6 denier and polypropylene 1.8 denier. Prior to the TEOS treatment, the samples were washed with non-ionic detergent in hot water and rinsed with DI water to remove any surface impurities or processing additives. The samples were then treated with TEOS (CAS: 78-10-4, Sigma-Aldrich). (See appendix A for detailed procedure).

In addition to TEOS treated samples, we also studied fiberglass samples treated with aspartic acid (CAS: 1783-96-6, Sigma Aldrich) using acid catalyst, aspartic acid using base catalyst, glycidoxypropyltrimethoxysilane (CAS: 2530-83-8, Sigma Aldrich), methyltriethoxysilane (CAS: 2031-67-6, Sigma Aldrich) and N-[3-(Trimethoxysilyl)propyl]-ethylenediamine (CAS: 1760-24-3, Sigma Aldrich) which impart carboxyl (-COOH), amine (-NH₂), hydroxyl (-OH), methyl (-CH₃) and amine (-NH₂) functional end-groups respectively on the fiber surface. Fiberglass was also treated with phosphatidylserine and phosphatidylcholine which

are present in endothelial cells and are believed to affect the coagulation process. All these treatments were carried out using the same procedure as TEOS treatment.

3.2. Test Methods

3.2.1. Thrombin Assay

Corning® 96-well plates (Cat. No. 3790) are prepped using a blocking reagent prior to the thrombin assay (Appendix A). This isolates the plate and prevents the contact activation of the coagulation cascade by the plate, thus ensuring an accurate measurement of thrombin formation due to the interaction of the plasma only with the test material. To each well of the plate, 0.3 mg of fiber sample is added. Frozen citrated pooled human plasma (Valley Biomedical), aliquoted to 10 ml, is thawed in a water-bath and 6 μ l of fluorogenic substrate Z-Gly-Gly-Arg-AMC (BA Chem.) is added. Just prior to starting the assay, 550 μ l of freshly prepared 2.75 wt% CaCl_2 solution is added to plasma and 100 μ l of the plasma solution is added to each well of the 96-well plate. The plate is then run in kinetic read mode in a Genios micro plate reader (Tecan) (Tissue culture lab, BME Department). All materials are run with concurrent replicates to ensure the precision of the assay and to prevent inaccuracy in measurement. The data from the tests is analyzed to determine the time point at which the fluorescence levels reach 10% of their maximum level above baseline. This point is termed as “time to initial thrombin formation” and correlates to the initial surge in thrombin formation, signaling the transition from the Initiation Phase of coagulation to the Propagation Phase.

3.2.2. Zeta Potential

Zeta potential is derived from streaming potential values using Helmholtz-Smoluchowski equation. Streaming potential is measured using a streaming potential jar, which was developed by Dr. Martin Hubbe in the Pulp and Paper Science Department at NC State (Figure 24).[99] This device allows for samples to be tested on a larger scale than with other commercially available devices. To measure the streaming potential, the material is placed between two electrodes within an electrolyte solution and the solution is forced to flow past the material using a pressure differential. The electrodes measure the charge of the solution before and after it flows past the material. While passing across the material's surface, the solution is stripped of charges and the charge difference between the electrodes is equivalent to the streaming potential. The fibers are loaded into the test jar in a packed bed configuration and a solution of 0.001 N KCl is forced through the material into an overflow beaker, using alternating high and low pressures. A vacuum is then applied to force the fluid to return to the test chamber, allowing for the cycle to be repeated. During this flow cycle, the charge differential is repeatedly measured before and after the solution passed through the material. The test is repeated in triplicate for each material at pH ranging from 3-10.

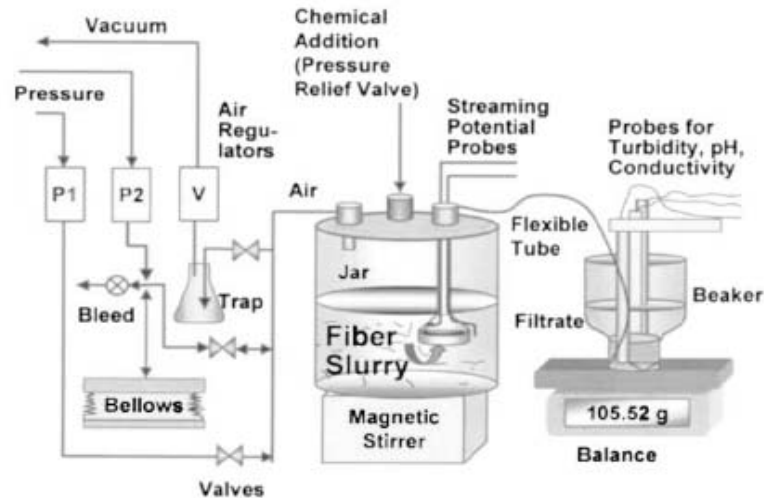


Figure 24: Streaming Potential Jar Device Setup

3.2.3. Single Fiber Contact Angle

Measuring the angle of contact between a water droplet and a material's surface is an accurate way to determine the propensity of a material to be wetted. The technique is typically performed by placing a droplet of water on a flat material surface in air and measuring the resulting angle at the interface between the material's surface and the water bead. An OCA – 20 (Dataphysics) instrument was used to measure the contact angle on our materials using the sessile drop method. The intrinsically round nature of the single fiber required that certain adaptations of the typical contact angle measurement method be made. A new suspension system had to be developed which would hold a fiber in tension over the stage of a light microscope. Using a syringe with 1.5 mm needle, a drop of water is suspended on the fiber. For precision of measurement, the droplet must be either surrounding the fiber in its entirety or suspended from the most lateral aspect of the fiber.[101], [102] A camera connected to the instrument captures the image of the droplet-fiber interface. The

image is analyzed using image editing software and the contact angle is measured. 10 readings are taken at different places along the fiber length and the average value is taken as the contact angle.

3.2.4. X-ray Photoelectron Spectroscopy (XPS)

Riber X-Ray Proton Spectroscopy (XPS) is used to characterize the surface of the materials and to confirm the TEOS coating on the materials.

3.2.5. Scanning Electron Microscopy (SEM)

Scanning electron microscopy is performed on the fibers in order to visualize the surface morphology of the fiber samples. In order to characterize the elemental composition of the surface of the materials, Energy Dispersive Spectroscopy (EDS) is being carried out using an Oxford Isis EDS system attached to Hitachi S3200 SEM.

CHAPTER 4: Results and Discussion

4.1. Results

4.1.1. X-ray Photoelectron Spectroscopy (XPS)

The XPS analysis results for control (untreated) and TEOS treated ‘yarn samples’ that were studied earlier[103] are shown in Table 3. The data revealed fluorine contamination in the treated samples. Subsequently, new batch of samples (this time fibers) were treated with TEOS and analyzed using XPS to confirm that the samples are not contaminated (Table 4). Additionally, fiberglass was treated with different chemicals to form specific functional end-groups on the surface (XPS analysis in Table 5). Deconvolution of these XPS plots confirmed the presence of specific functional end-groups (Table 6 and Figures 25 - 28)

Table 3: XPS Analysis for Control and TEOS treated Yarns studied earlier

XPS Analysis					
Sample ID	Components (At. %)				
	Carbon	Oxygen	Silicon	Fluorine	Others
Cotton	80.03	19.97	-	-	-
Cotton TEOS	47.75	46.65	2.26	3.34	-
Rayon	69.84	30.16	-	-	-
Rayon TEOS	47.7	43.69	-	8.61	-
Glass	35.66	53.56	8.87	-	Ca: 1.91
Glass TEOS	31.51	36.05	9.34	21.54	Ca: 1.56
Nylon	78	14.82	-	-	N: 7.19
Nylon TEOS	40.38	39.14	6.62	13.85	-
PET	65.84	34.16	-	-	-
PET TEOS	38.34	47.6	7.98	6.07	-
PP	92.45	7.55	-	-	-
PP TEOS	89.63	8.1	0.24	2.03	-

Table 4: XPS Analysis for TEOS treated Fibers used in this study

XPS Analysis					
Sample ID	Components (At. %)				
	Carbon	Oxygen	Silicon	Fluorine	Other
Cotton TEOS	54.66	45.34	-	-	-
Rayon TEOS	55.86	42.3	1.07	0.76	-
Glass TEOS	38.21	50.23	8.82	-	Ca: 2.74
Nylon TEOS	76.16	19.87	-	-	Na: 3.96
PET TEOS	66.73	33.27	-	-	-
PP TEOS	86.71	11.25	2.04	-	-

Table 5: XPS Analysis for Fiberglass with Specific End-Groups

XPS Analysis				
Sample ID	Components (At. %)			
	Carbon	Oxygen	Silicon	Other
Glass	35.66	53.56	8.87	Ca: 1.91
Glass + TEOS	31.51	36.05	9.34	Ca: 1.56, F: 21.54
Glass + TEOS + Aspartic Acid (Acid Catalyzed)	39.88	41.69	6.18	N: 3.15, Cl: 4.54, Ca: 1.59, F: 2.98
Glass + TEOS + Aspartic Acid (Base Catalyzed)	32.15	41.83	9.53	N: 2.79, Cl: 3.6, F: 10.1
Glass + Glycidoxypropyl trimethoxysilane	50.87	34.62	8.3	F: 6.22
Glass + Methyl triethoxysilane	49.07	36.59	12.04	F: 2.29
Glass + 1% Phosphatidylcholine	54.77	23.37	4.17	F: 17.69
Glass + 2.5% Phosphatidylcholine	42.42	14.49	3.38	F: 39.71
Glass + 1% Phosphatidylserine	53.79	30.96	6.97	F: 8.28
Glass + 2.5% Phosphatidylserine	65.29	27.23	4.31	F: 3.17

Table 6: XPS Deconvolution Data for Fiberglass with Specific End-Groups

Interpretation of Carbon Bonds from the Deconvolution Plots

	C-Si		C-C/C-H		C-NH ₂		C=O/COOH		C-OH		C-O-Si	
	Binding Energy	% Conc	Binding Energy	% Conc	Binding Energy	% Conc	Binding Energy	% Conc	Binding Energy	% Conc	Binding Energy	% Conc
Glass	284.3	63.9	285.09	36.1								
Aspartic Acid + TEOS	284.338	67.81			285.8	13.9	288.123	18.29				
Aspartic Acid + TEOS + Base	284.205	74.97			285.814	14.91	288.28	10.11				
Glycidoxypropyl Trimethoxysilane	284.05	26.85	285.08	51.26					286.66	21.89		
Methyl Triethoxysilane	284.329	70.12	285.011	9.16							286.425	20.72

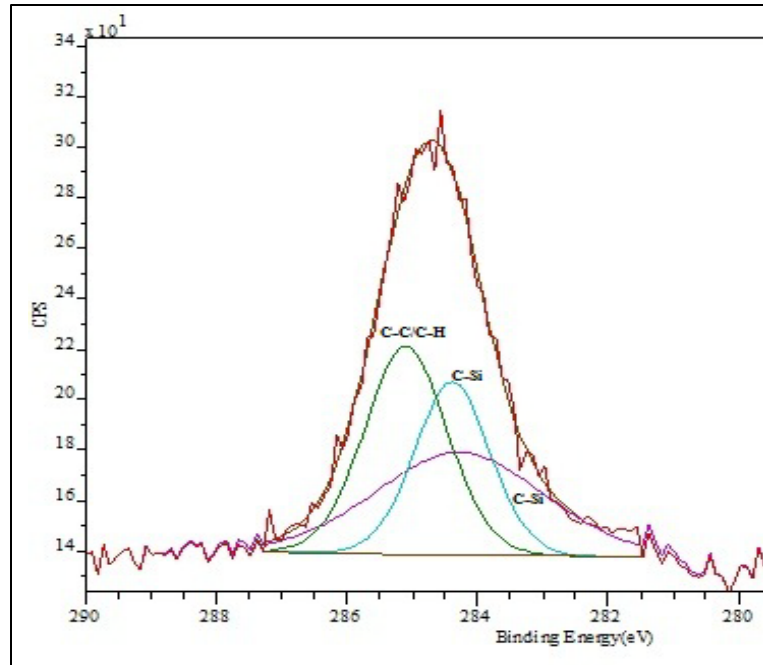


Figure 25: Deconvolution of Carbon Bonds for Untreated Fiberglass

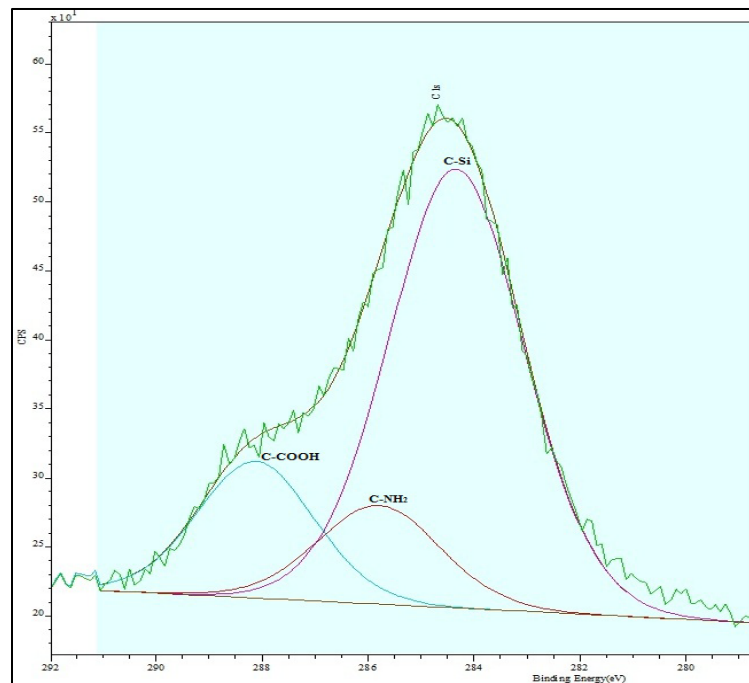


Figure 26: Deconvolution of Carbon Bonds for Fiberglass treated with Aspartic Acid

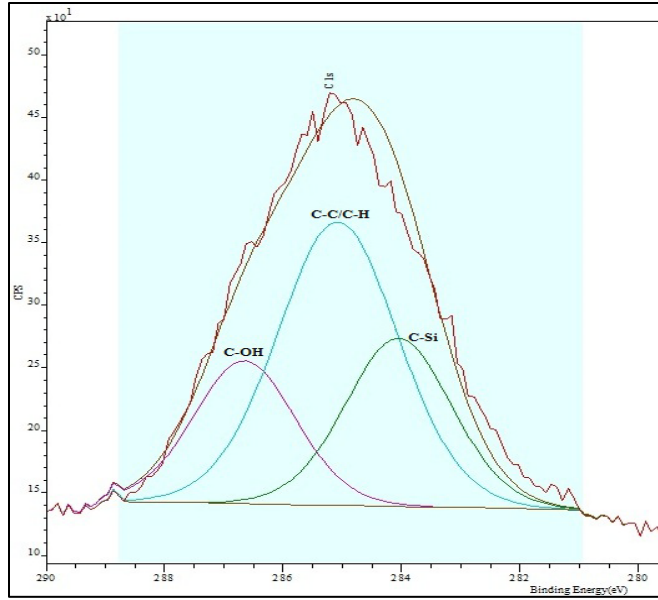


Figure 27: Deconvolution of Carbon Bonds for Fiberglass treated with Glycidoxypropyl trimethoxysilane

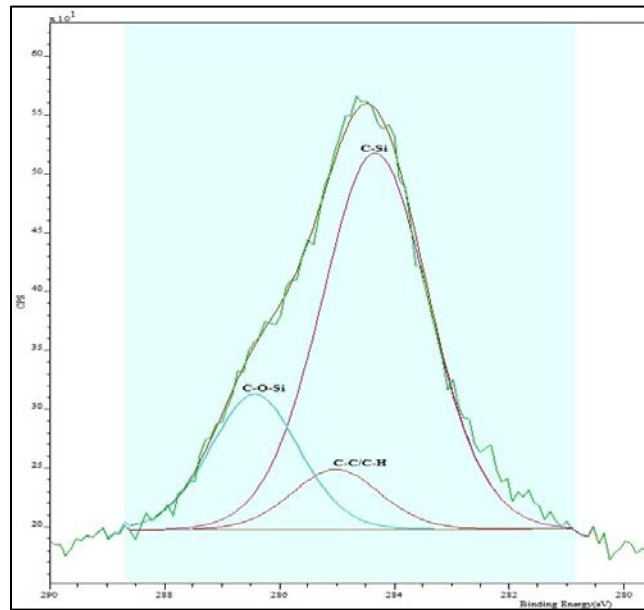


Figure 28: Deconvolution of Carbon Bonds for Fiberglass treated with Methyl triethoxysilan

4.1.2. Scanning Electron Microscopy (SEM)

Though the XPS data reflected the changes in the chemical composition of treated substrates, the technique is restricted by the depth of probe and largely affected by the surface impurities. The efficiency of TEOS treatment is characterized by the amount of Silicon on the surface, which is not really reflected by XPS analysis. For this reason, Energy-dispersive X-ray spectroscopy (EDS) was carried out using SEM. Table 7 shows the elemental composition for untreated and TEOS treated fiber samples and the data is graphically represented in Figure 29. EDS data for Fiberglass with specific end-groups is shown in Table 8 and Figure 30. Presence of Silicon on the treated samples confirms the TEOS treatment.

Table 7: EDS Analysis for Untreated and TEOS Treated Fibers

SEM Analysis										
Sample ID	Components									Other Components At. %
	Carbon			Oxygen			Silicon			
	At. %	Weight %	SD	At. %	Weight %	SD	At. %	Weight %	SD	
Cotton	83.65	79.34	2.08	16.35	20.66	1.08	-	-	-	
Cotton TEOS (Oct. 2010)	78.84	72.76	1.74	19.84	24.38	1.03	1.33	2.86	0.82	
Cotton TEOS (Dec. 2010)	78.57	70.3	1.95	16.8	20.02	1.07	4.63	9.68	0.8	
Rayon	83.05	78.63	1.99	16.95	21.37	1.05	-	-	-	
Rayon TEOS (Oct. 2010)	80.75	75.26	1.79	18.34	22.77	1.01	0.9	1.97	0.63	
Rayon TEOS (Dec. 2010)	82.16	76.7	2.08	16.66	20.71	1.1	1.18	2.58	0.83	
Nylon	89.01	85.87	2.29	10.99	14.13	0.9	-	-	-	
Nylon TEOS (Oct. 2010)	89.59	86.27	2.04	10.01	12.84	0.73	0.4	0.89	0.33	
Nylon TEOS (Dec. 2010)	85.32	79.68	2.66	12.49	15.54	1.16	2.19	4.78	1.3	
PP	93.25	90.78	2.36	6.22	8.07	1.04	-	-	-	Al: 0.53
PP TEOS (Oct. 2010)	92.97	90.85	2.13	7.03	9.15	0.8				
PET	79.04	73.9	1.89	20.96	26.1	1.13	-	-	-	
PET TEOS (Oct. 2010)	78.58	72.97	1.91	20.85	25.79	1.15	0.57	1.24	0.46	
PET TEOS (Dec. 2010)	95.5	93.56	2.21	3.92	5.11	1.09	0.58	1.33	0.46	
Glass	10.76	6.01	1.08	42.28	31.42	1.01	22.45	29.29	1.02	B: 4.81, F: 0.65, Na: 0.63, Mg: 0.21, Al: 7.42, Ca: 10.8
Glass TEOS (Oct. 2010)	9.13	4.73	1.05	41.71	28.79	1.03	26.81	32.48	1.06	Na: 0.45, Mg: 0.17, Al: 7.45, Ca: 14.28
Glass TEOS (Dec. 2010)	9.32	5.1	1.08	41.51	30.23	1.05	23.43	29.96	1.07	B: 5.29, F: 0.41, Na: 0.39, Mg: 0.16, Al: 7.35, Ca: 12.14

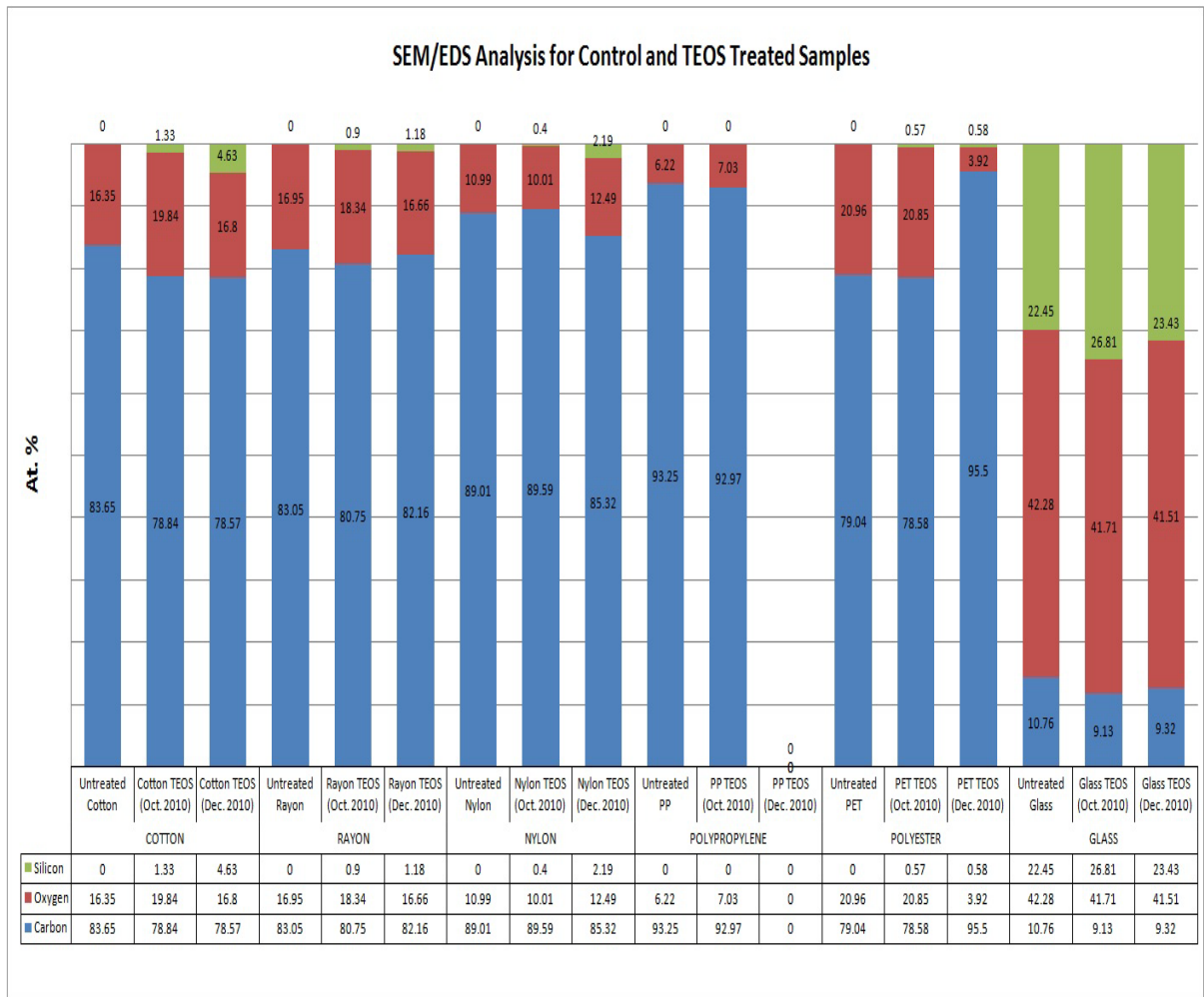


Figure 29: Graphical Representation of EDS Analysis for Untreated and TEOS Treated Fibers

Table 8: EDS Analysis for Fiberglass with Specific End-Groups

SEM Analysis										
Sample ID	Components									Other Components At. %
	Carbon			Oxygen			Silicon			
	At. %	Weight %	SD	At. %	Weight %	SD	At. %	Weight %	SD	
Untreated Glass	10.76	6.01	1.08	42.28	31.42	1.01	22.45	29.29	1.02	B: 4.81, F: 0.65, Na: 0.63, Mg: 0.21, Al: 7.42, Ca: 10.8
Glass TEOS	9.32	5.1	1.08	41.51	30.23	1.05	23.43	29.96	1.07	B: 5.29, F: 0.41, Na: 0.39, Mg: 0.16, Al: 7.35, Ca: 12.14
Glass Diamine	55.63	41.75	1	24.24	24.23	0.97	12.4	21.76	0.95	N: 3.26, F: 0.21, Na: 0.21, Mg: 0.05, Al: 1.33, Cl: 0.55, Ca: 2.13
Glass Glycidoxypropyl trimethoxysilane	44.06	28.52	1.14	26.04	22.46	1.02	18.05	27.32	1.11	F: 0.21, Na: 0.12, Mg: 0.14, Al: 4.76, Cl: 0.37, Ca: 6.25
Glass Methyl triethoxysilane	72.15	57.71	1.37	15.48	16.5	0.83	6.42	12	0.68	Na: 0.11, Al: 2.25, Ca: 3.59
Glass TEOS + Aspartic Acid	14.63	8.48	0.88	45.76	35.31	0.98	24.98	33.84	1.01	N: 1.06, F: 0.47, Na: 0.33, Mg: 0.04, Al: 4.98, Cl: 3.02, Ca: 4.75
Glass TEOS + Aspartic Acid + Base	16.38	8.74	0.85	35.17	25.01	1	25.33	31.61	1.05	N: 1.17, F: 0.38, Na: 0.05, Mg: 0.02, Al: 5.9, Cl: 6.54, Ca: 9.06
Glass Serine 2.5%	14.48	8.04	0.95	43.78	32.36	1.01	23.06	29.93	1.02	Na: 0.67, Mg: 0.08, Al: 7.14, Cl: 0.37, Ca: 10.79
Glass Choline 2.5%	16.26	9.35	0.73	45.13	34.59	0.99	20.92	28.15	1.02	F: 0.58, Na: 0.66, Mg: 0.14, Al: 7.55, Ca: 8.57, P: 0.19

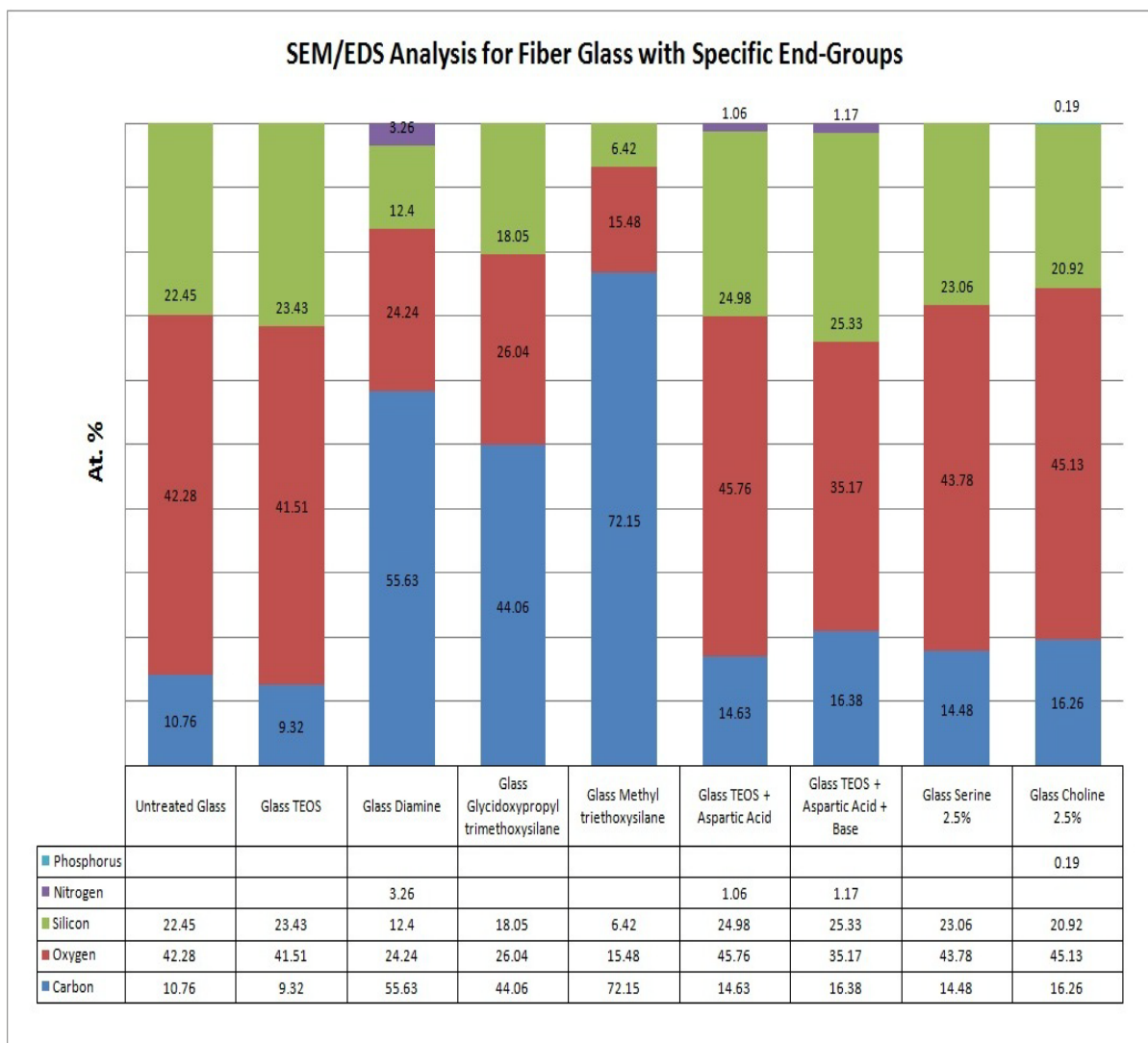


Figure 30: Graphical Representation of EDS Analysis for Fiberglass with Specific End-Groups

4.1.3. Streaming Potential

Streaming potential data obtained using Streaming Potential Jar is converted to Zeta potential (ζ) values using Helmholtz-Smoluchowski equation. Average zeta potential values of 10 measurements are then plotted against pH ranging from 3 to 10 for all control samples (Figure 31) and for all TEOS treated samples (Figure 32). Figures 33 - 38 show zeta potential values for individual fibers in comparison to their TEOS treated counterparts.

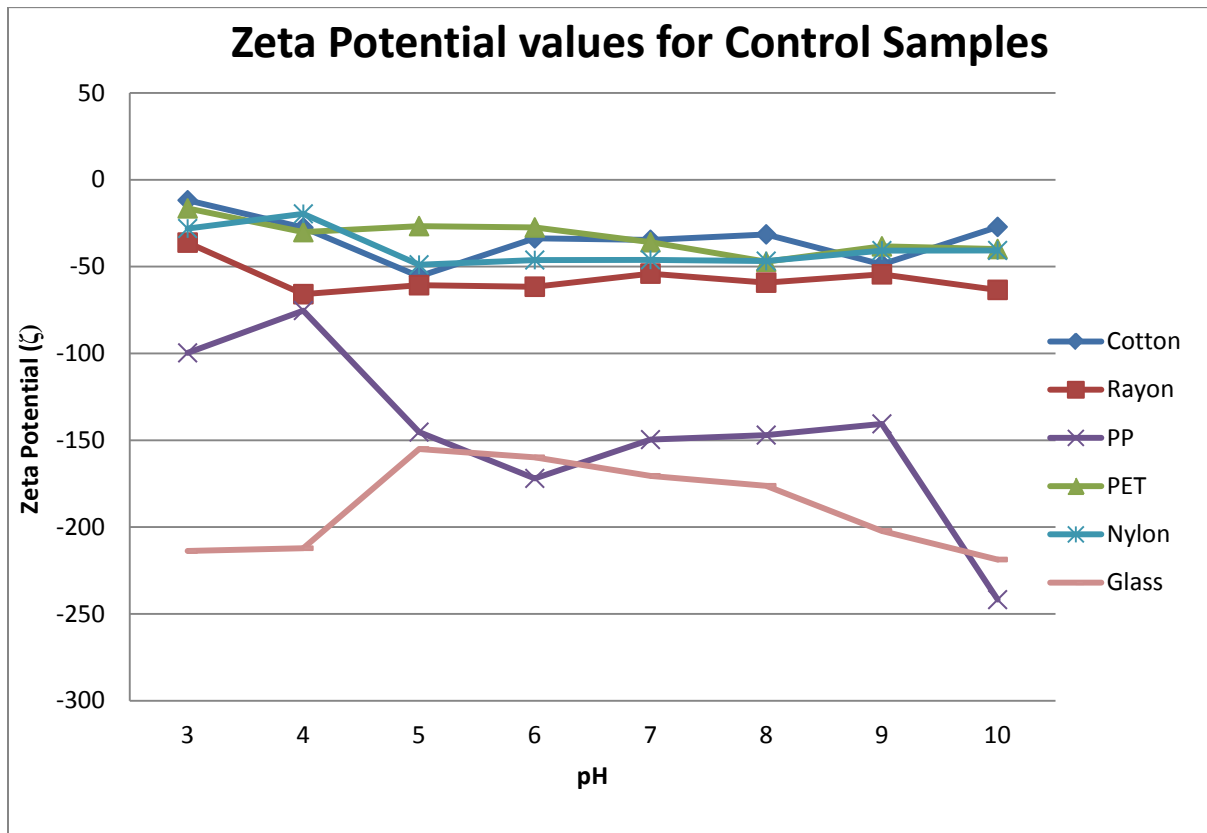


Figure 31: Zeta Potential values for Control Fibers

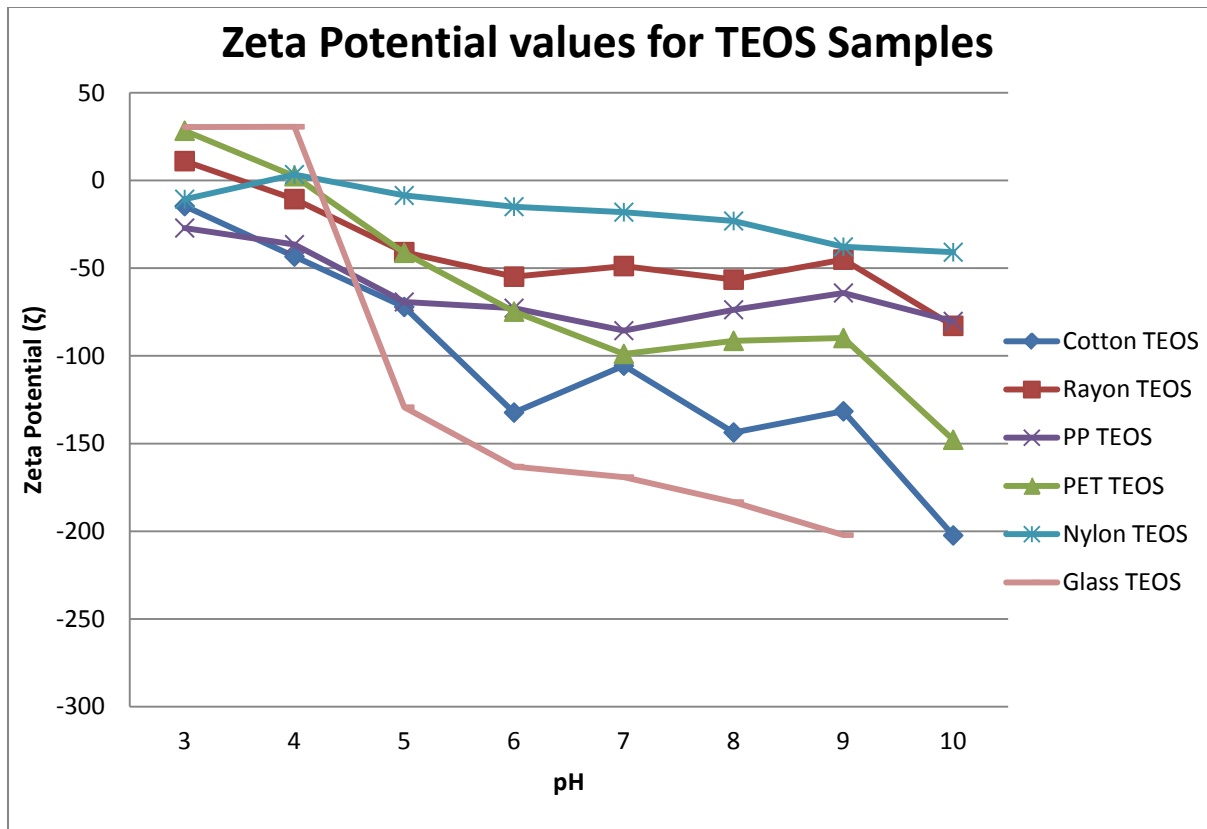


Figure 32: Zeta Potential values for TEOS Fibers

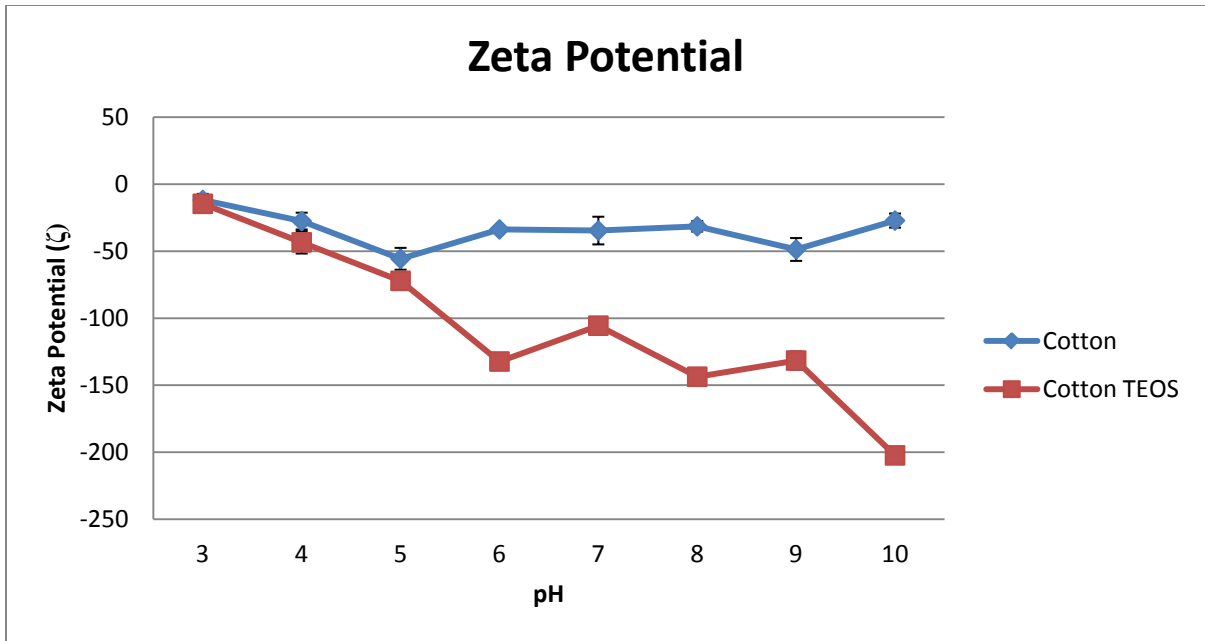


Figure 33: Zeta Potential values for Cotton

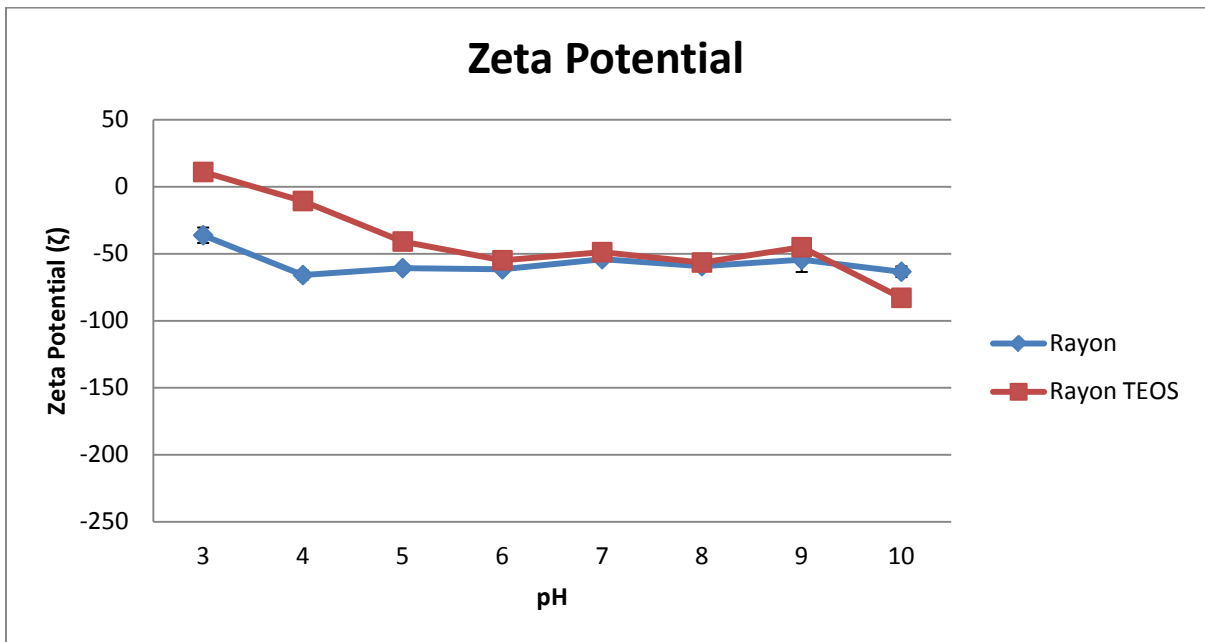


Figure 34: Zeta Potential values for Rayon

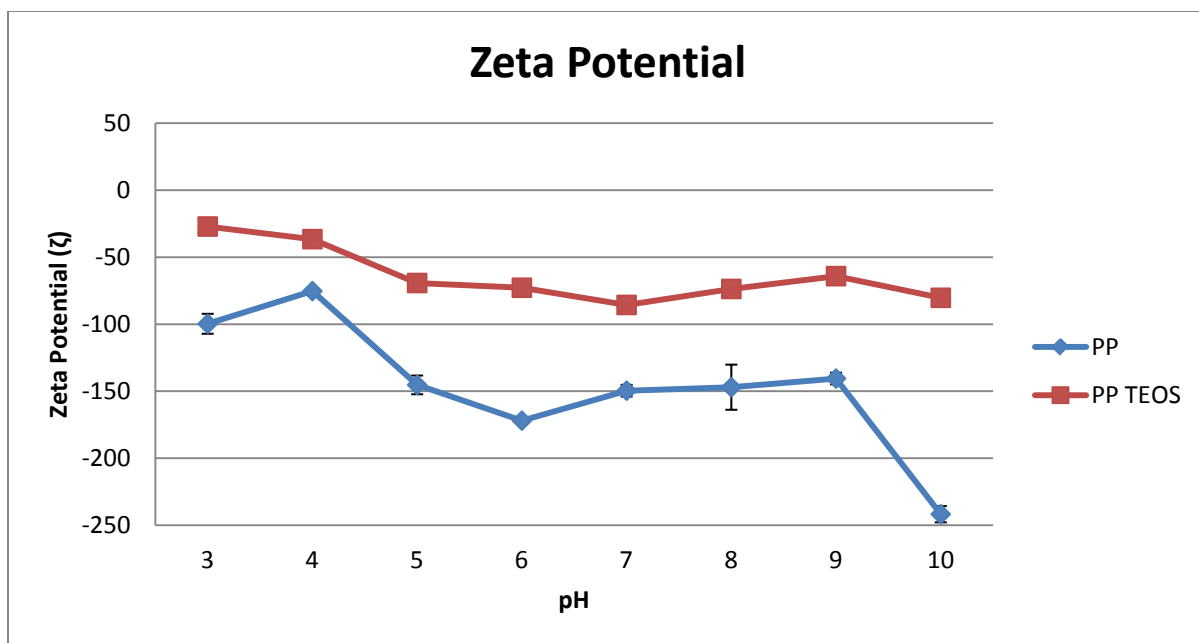


Figure 35: Zeta Potential values for PP

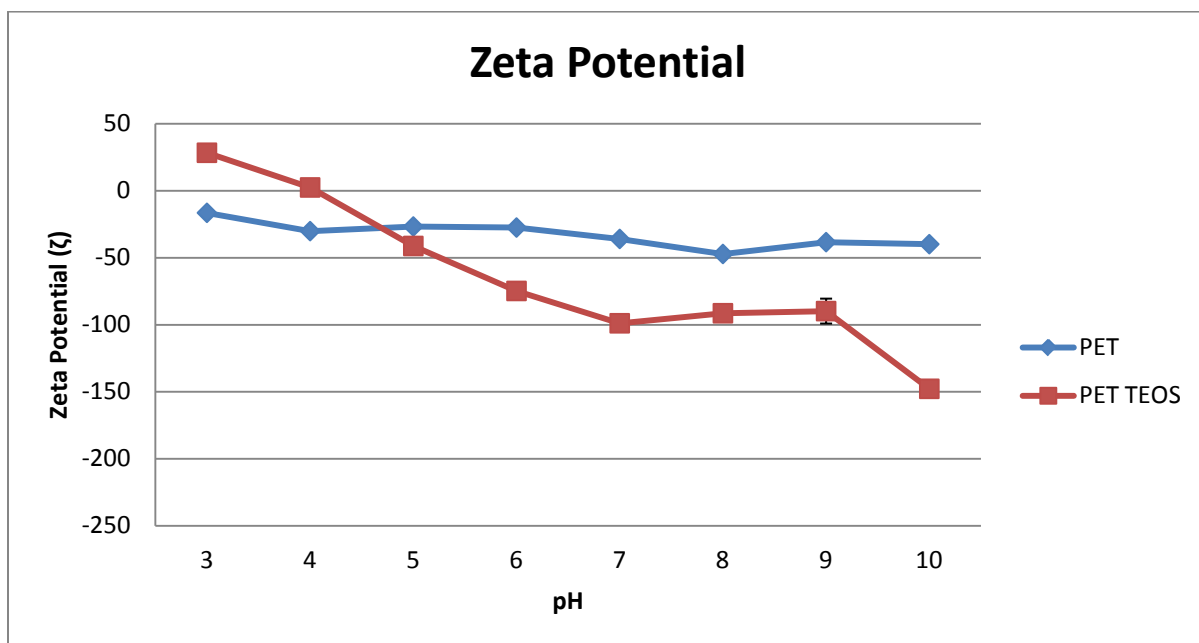


Figure 36: Zeta Potential values for PET

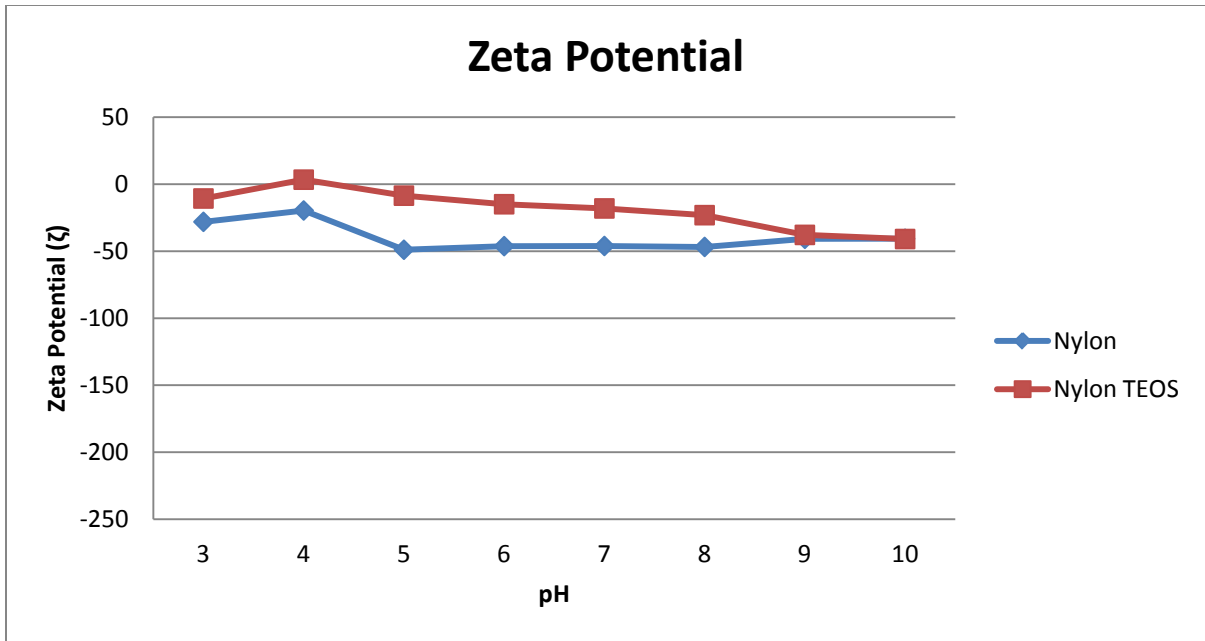


Figure 37: Zeta Potential values for Nylon

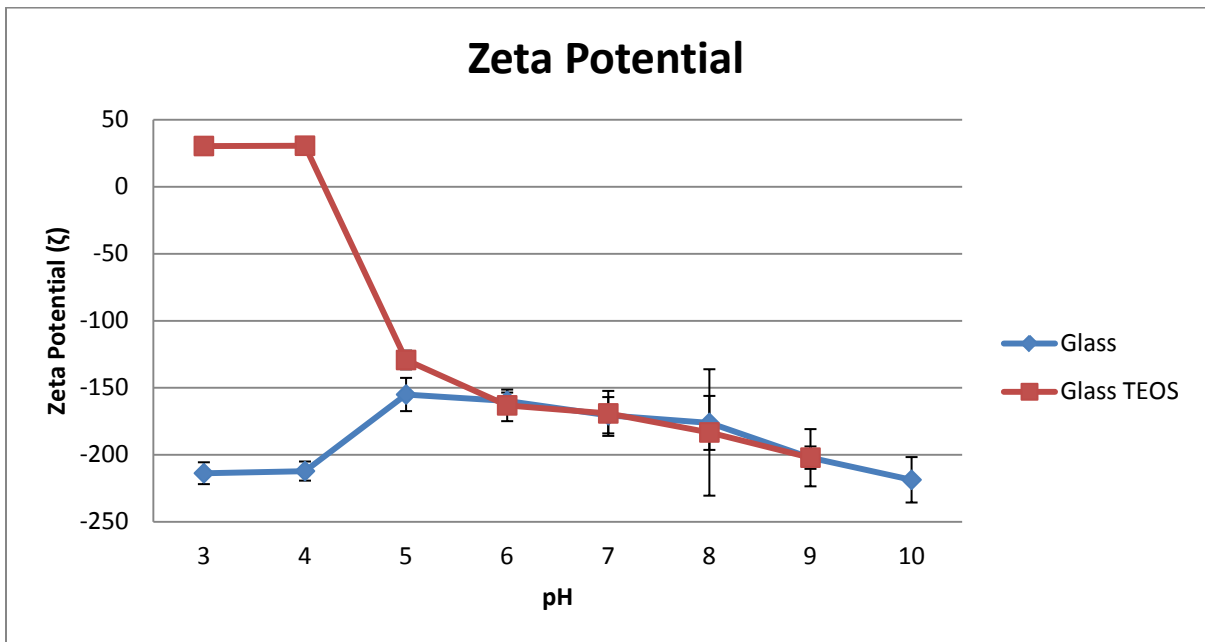


Figure 38: Zeta Potential values for Glass

4.1.4. Single Fiber Contact Angle

Table 9 shows values of 10 readings and the average value for single fiber contact angle measurement for each of the untreated and TEOS treated fibers. Figure 39 is the graphical representation for the same. Table 10 and Figure 40 show the contact angle values for Fiberglass with specific end-groups. In all cases, except Fiberglass, TEOS treatment reduced the contact angle compared to the untreated counterparts i.e. TEOS treatment made the materials more hydrophilic. In case of Fiberglass, TEOS treatment increased the contact angle, making it more hydrophobic.

Table 9: Single Fiber Contact Angle Measurements for Control and TEOS Fibers

Reading No.	Glass	Glass TEOS	PET	PET TEOS	PP	PP TEOS	Nylon	Nylon TEOS	Cotton	Cotton TEOS	Rayon	Rayon TEOS
1	38.3	55.3	54	25	78.6	68	56.8	36.5	17.3	10.4	14	8.4
2	39.9	58.8	56.2	26.7	81.6	70.2	59.4	38.9	17.51	10.7	15.2	8.5
3	40.8	64.6	58.7	27.3	82.2	70	60.1	43.3	18.3	11.2	17.5	9.1
4	41.2	65.7	59.3	28	84.6	71.6	63.5	44.5	18.81	12.1	18.8	9.11
5	41.7	65.8	60.9	30.6	86.7	72.6	64	46.5	20.7	12.2	20	12.6
6	42.2	66.8	62.2	31.2	87.7	72.8	65.6	49.9	21.4	14.4	20.2	14.8
7	43.4	66.9	65.2	32.9	89.6	72.82	67.6	51.4	22.5	19.4	21.9	14.9
8	43.5	68.5	67.5	36	90.6	74.5	69	53.5	23.1	19.6	23.3	15
9	45.4	68.9	69.8	42.2	94.2	75.2	70.2	57.6	25.7	19.8	23.7	16.6
10	48.1	69.1	70.1	43.6	95.9	76.8	73.5	60.7	26.2	19.9	24	17.1
AVG.	42.45	65.04	62.39	32.35	87.17	72.45	64.97	48.28	21.15	14.97	19.86	12.61
SD	2.81	4.53	5.60	6.43	5.57	2.64	5.25	7.82	3.23	4.19	3.51	3.51

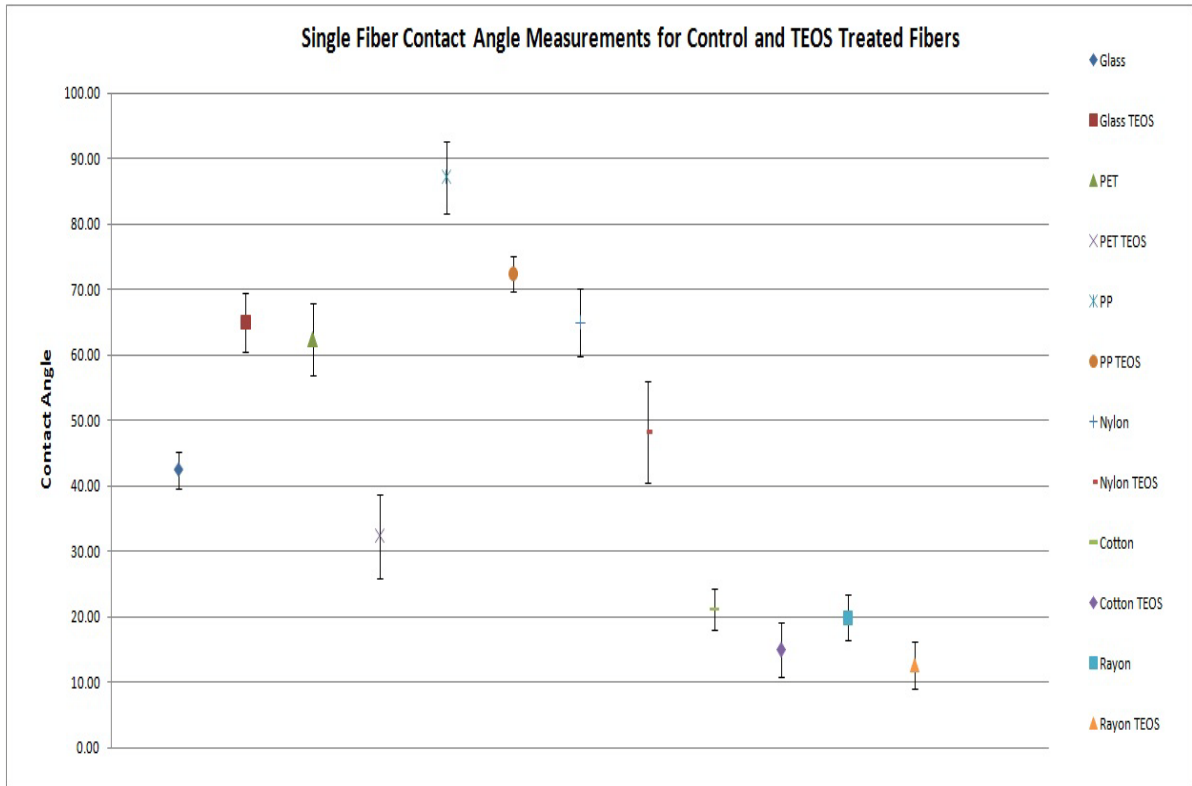


Figure 39: Single Fiber Contact Angle Measurement for Control and TEOS Fibers

Table 10: Contact Angle Measurements for Fiberglass with Specific End-Groups

Reading No.	Glass	Glass TEOS	Glass Aspartic Acid	Glass Methyl	Glass Serine	Glass Choline	Glass Diamine	Glass Glycidoxypropyl trimethoxysilane
1	38.3	55.3	34.1	73.1	47.3	54.3	67	22
2	39.9	58.8	34.2	74.4	51.5	55.4	68.3	24.6
3	40.8	64.6	35.8	75.3	53.1	56.2	72.9	25.2
4	41.2	65.7	38.2	78	54	60.1	77.3	28.8
5	41.7	65.8	40.2	80.1	54.6	61.9	79.2	29.6
6	42.2	66.8	41.1	80.4	55.2	61.9	80.8	30.8
7	43.4	66.9	42.6	82	55.5	62.7	81.7	32.8
8	43.5	68.5	43.5	82.3	56.2	63.3	82.8	33.9
9	45.4	68.9	44.6	83.2	57.7	66.8	83.8	35.6
10	48.1	69.1	44.7	84	59.6	68.8	86.2	39.7
AVG.	42.45	65.04	39.9	79.28	54.47	61.14	78	30.3
SD	2.81	4.53	4.12	3.88	3.39	4.76	6.57	5.44

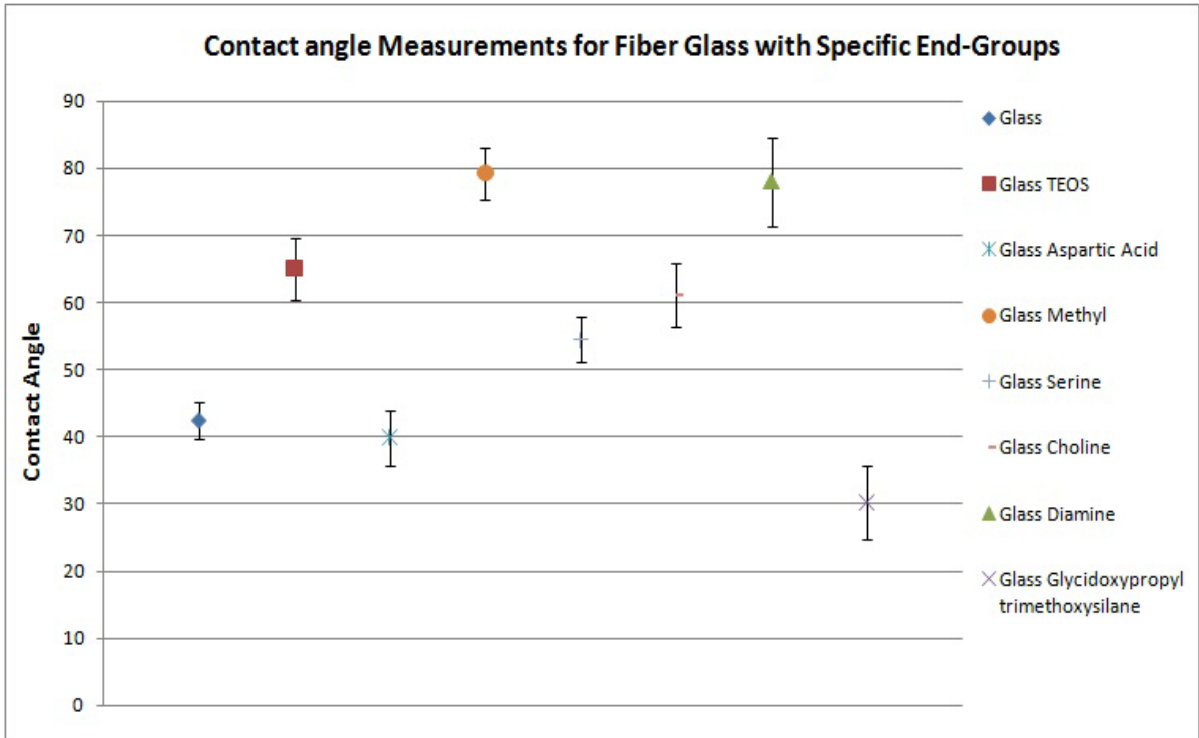


Figure 40: Contact Angle Measurement for Fiberglass with Specific End-Groups

4.1.5. Thrombin Assay

Time to thrombin formation (in minutes) is given by the thrombin assay. The thrombin assay for control fibers is shown in Figure 41. Figure 42 shows the comparison for the thrombin time for control and TEOS treated samples. For all samples, except Fiberglass, TEOS treatment reduced the time to thrombin formation i.e. it made the substrate more thrombogenic. Effect of various end-groups on thrombogenicity has been shown by the thrombin assay for Fiberglass with specific end-groups (Figure 43).

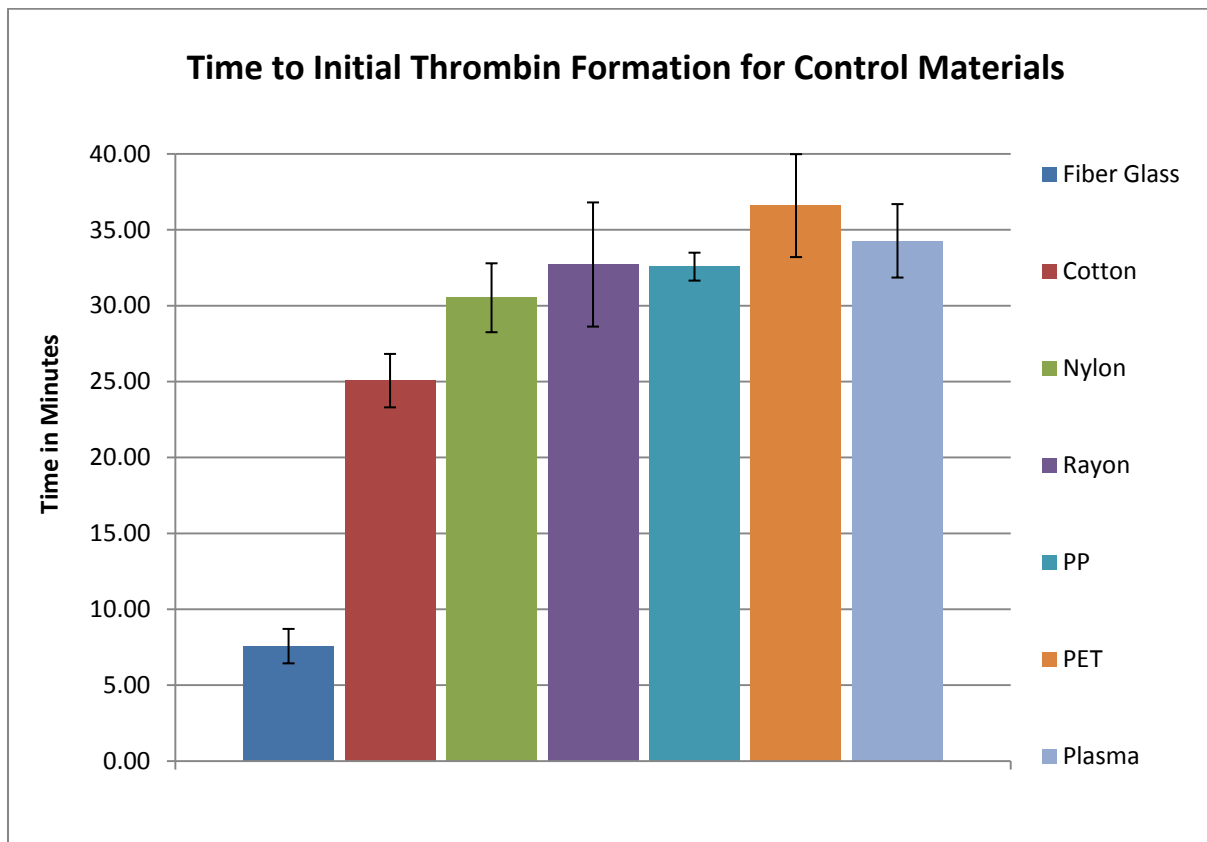


Figure 41: Thrombin Assay for Control Fibers

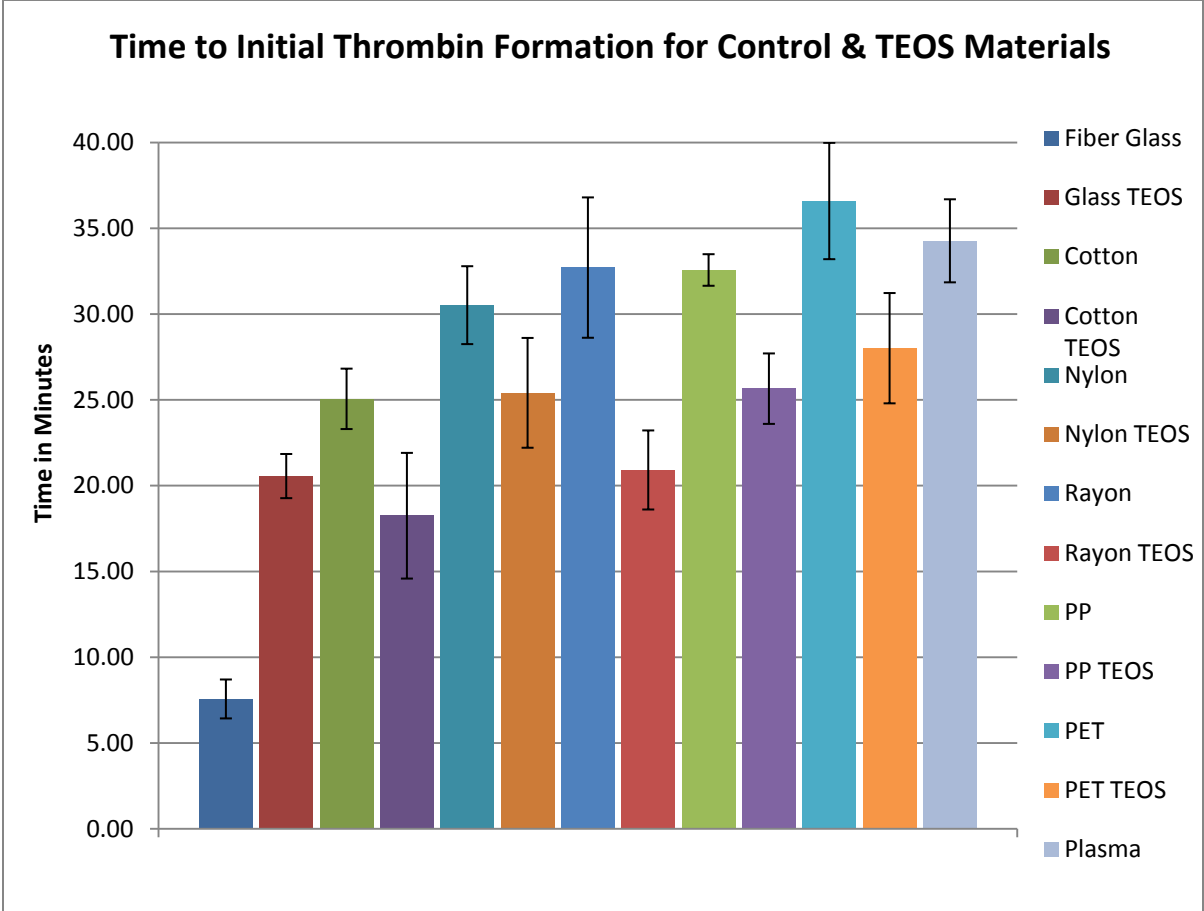


Figure 42: Thrombin Assay Comparison for Control and TEOS Fibers

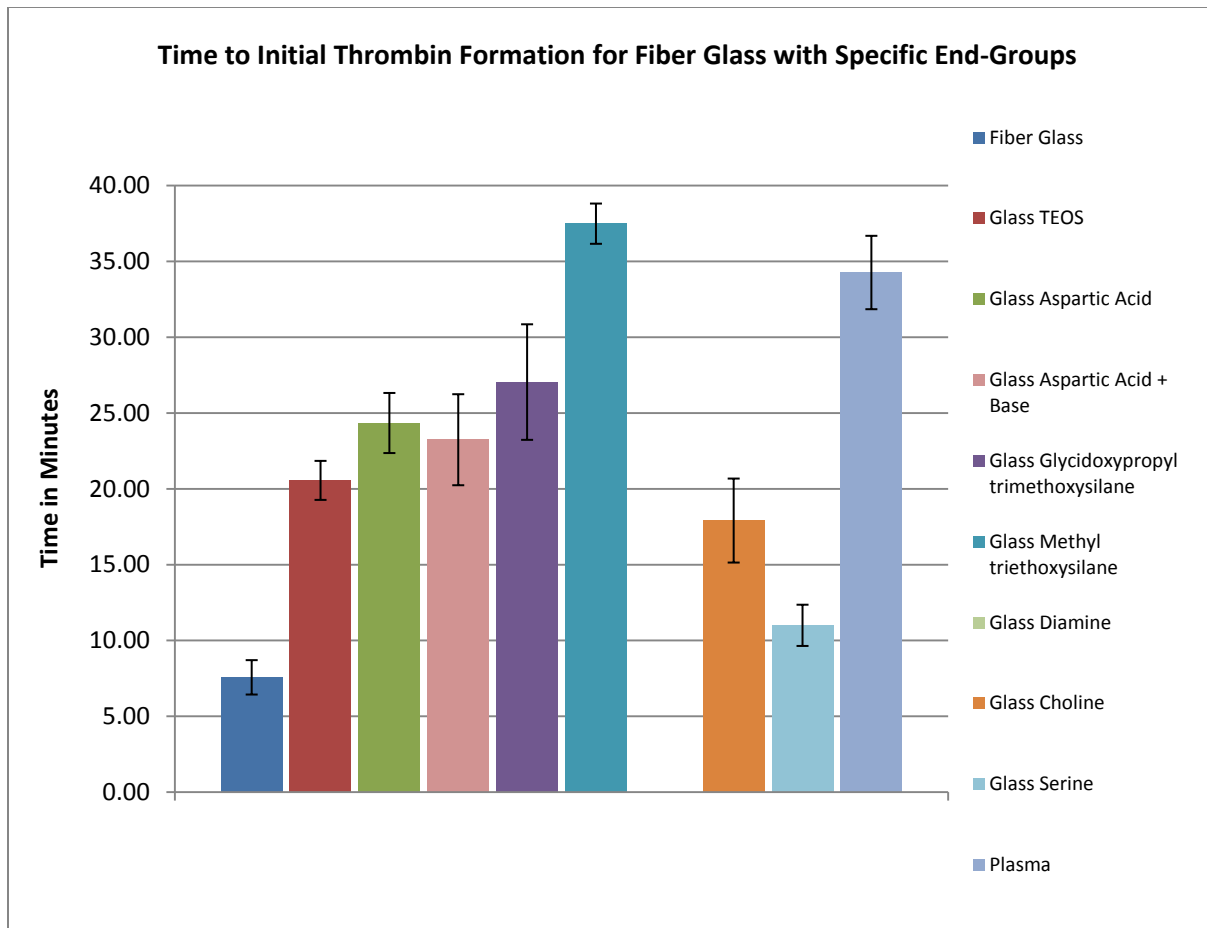


Figure 43: Thrombin Assay for Fiberglass with Specific End-Groups

4.1.6. SEM Images

Apart from quantitative elemental analysis, Scanning Electron Microscopy is also used to obtain high magnification images of control and treated fibers. Change in the surface morphology is clearly seen with the treatment which confirms the surface modification (Figures 44 – 55)

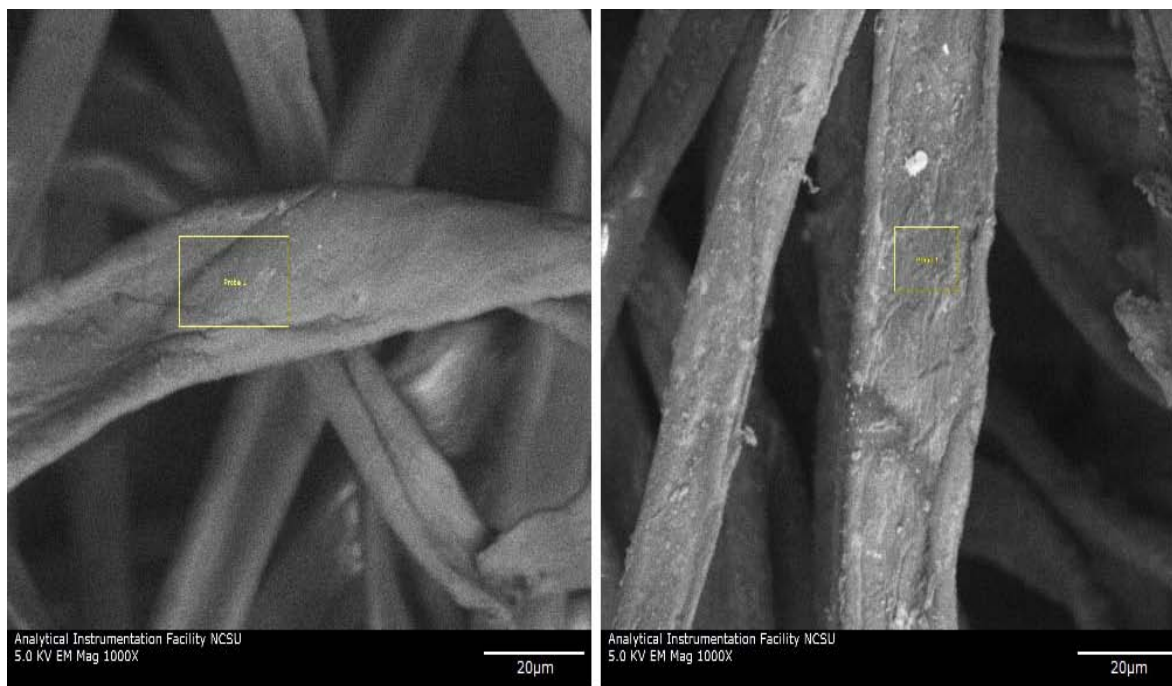


Figure 44: SEM Image of Untreated Cotton (left) and Cotton TEOS (right)

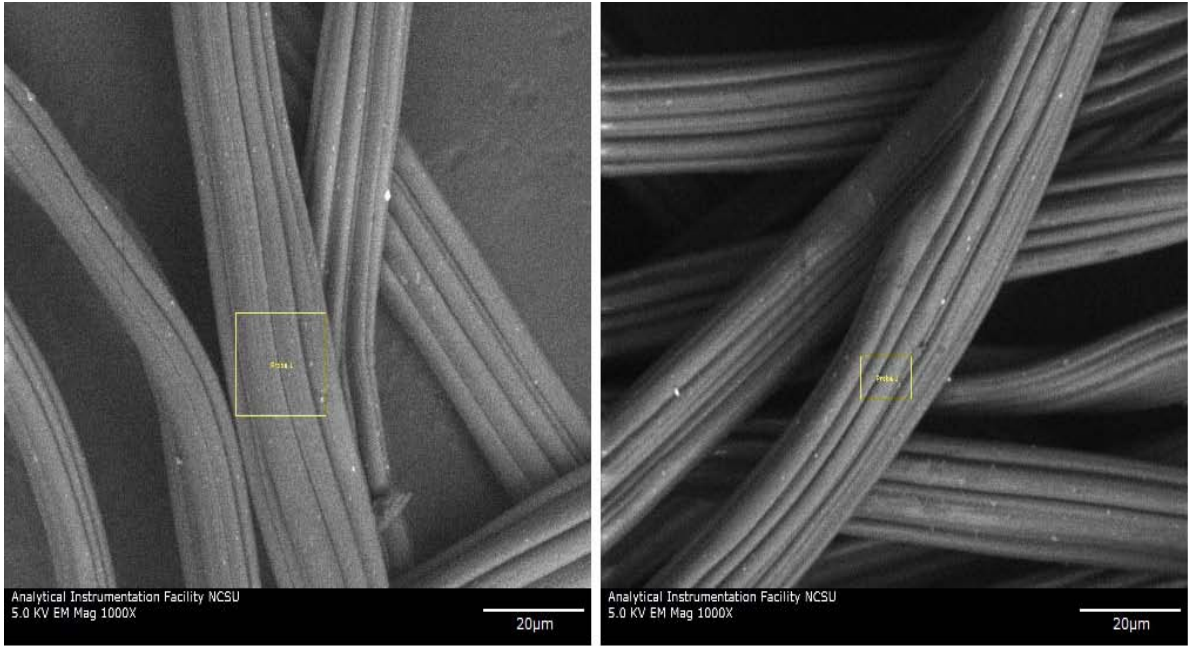


Figure 45: SEM Image of Untreated Rayon (left) and Rayon TEOS (right)

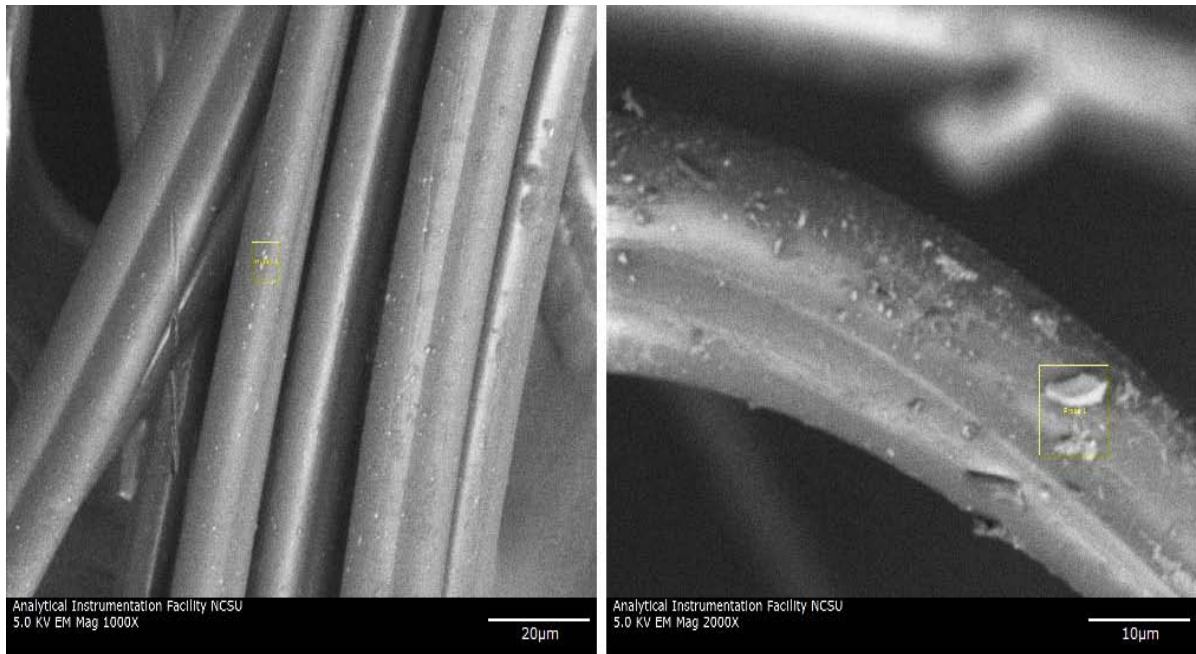


Figure 46: SEM Image of Untreated Nylon (left) and Nylon TEOS (right)

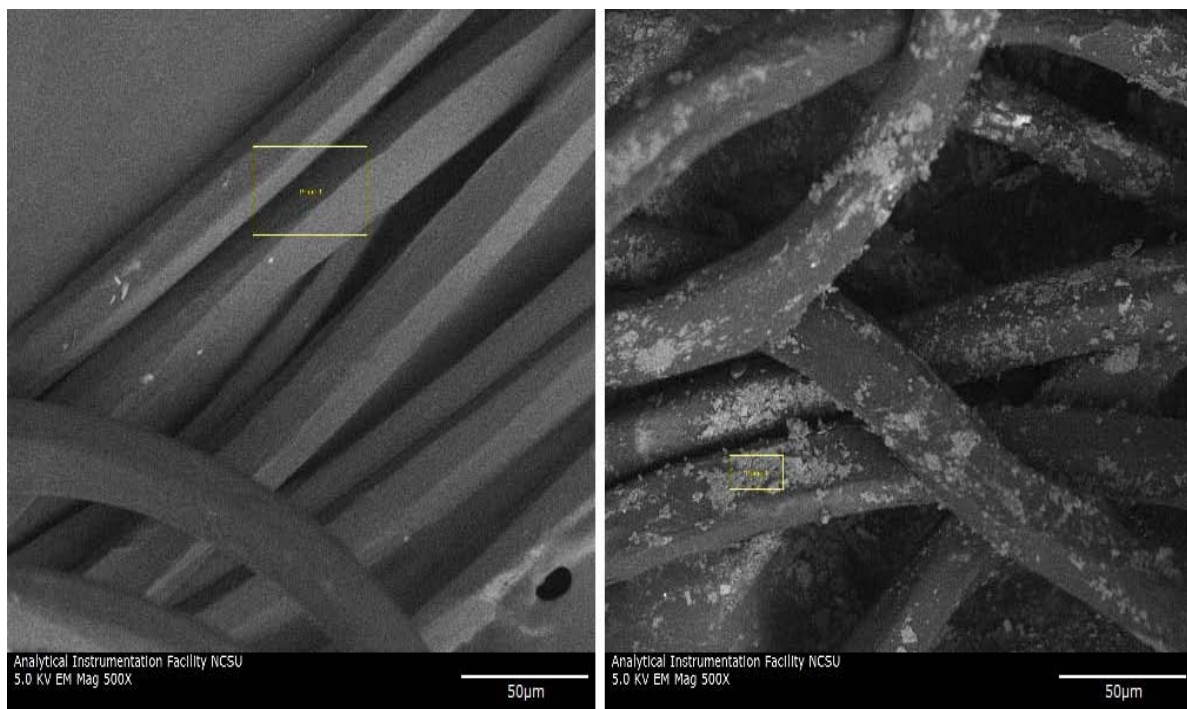


Figure 47: SEM Image of Untreated PP (left) and PP TEOS (right)

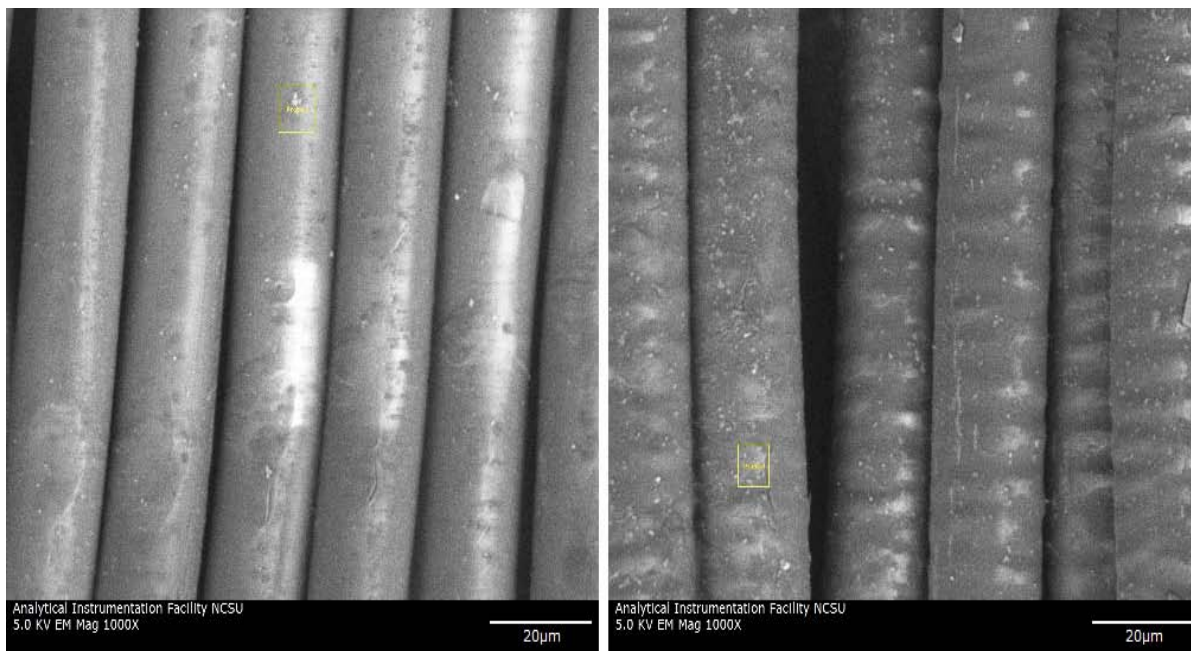


Figure 48: SEM Image of Untreated PET (left) and PET TEOS (right)

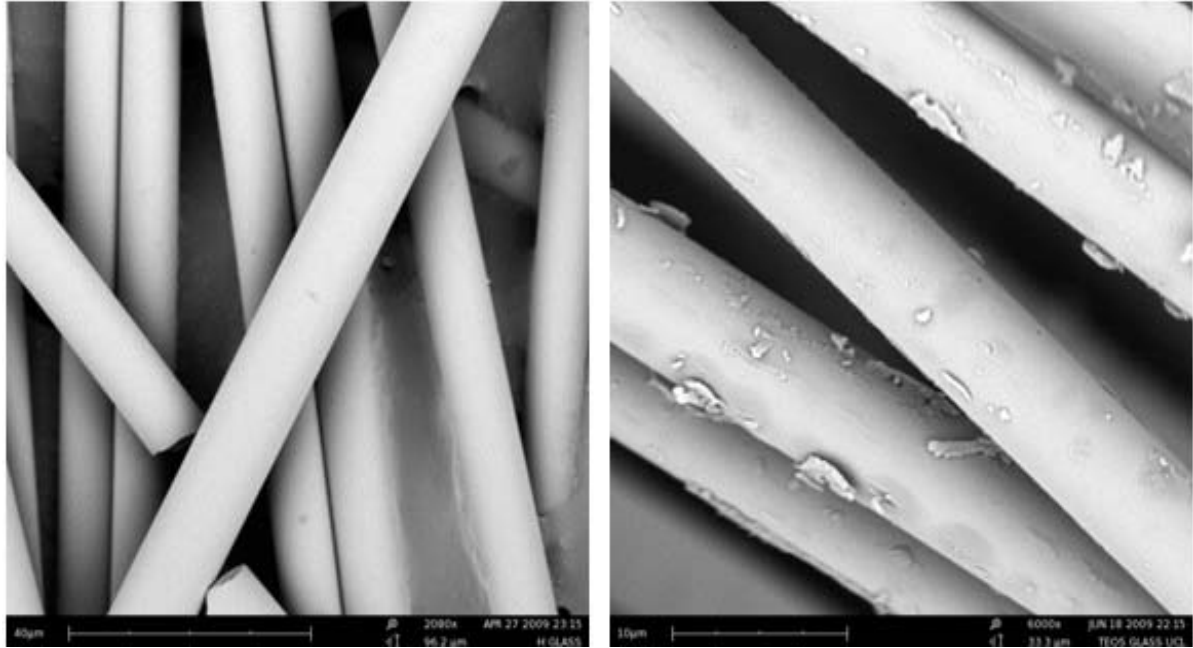


Figure 49: SEM Image of Untreated Fiberglass (left) and Fiberglass TEOS (right)

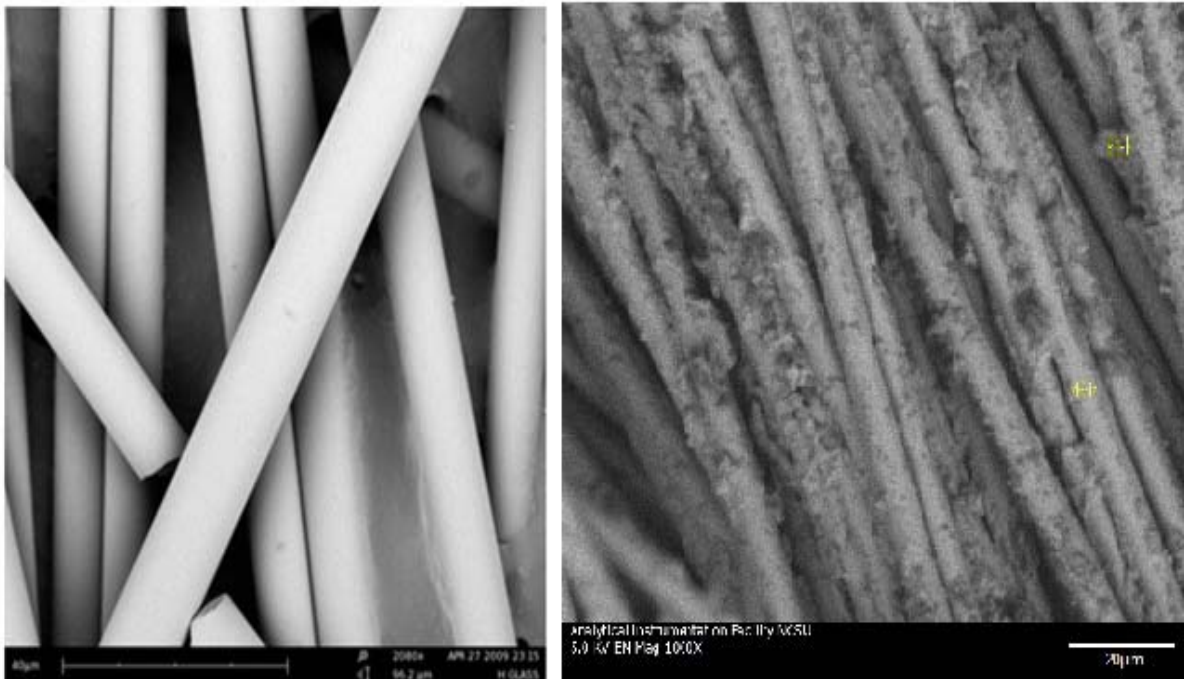


Figure 50: SEM Image of Untreated Fiberglass (left) and Glass Aspartic Acid (right)

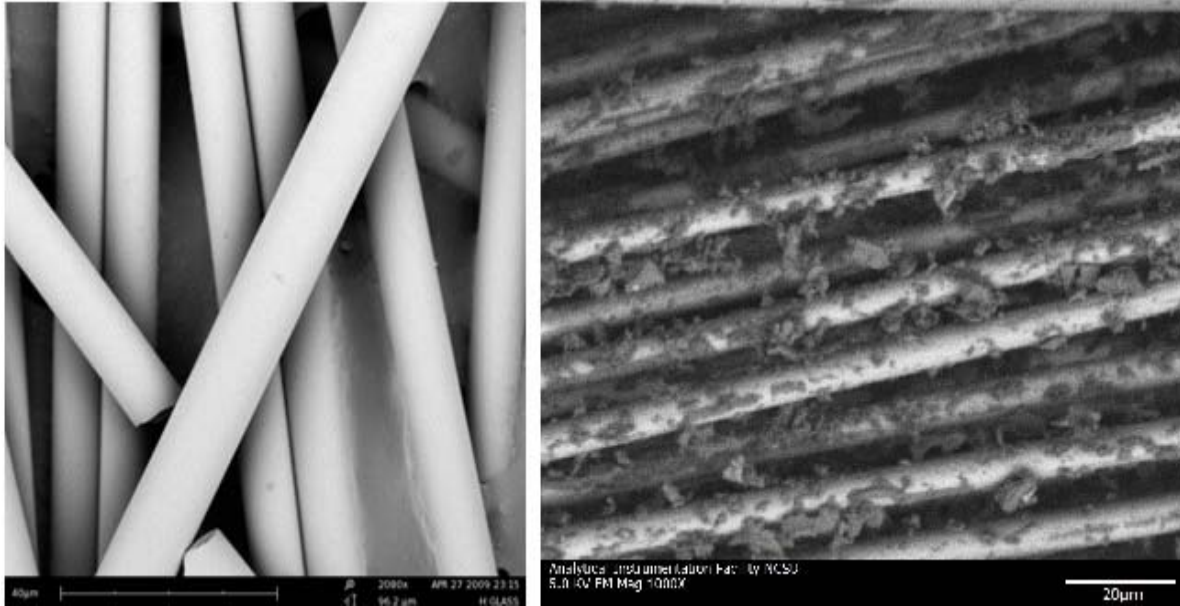


Figure 51: SEM Image of Untreated Fiberglass (left) and Glass Glycidoxypopyl trimethoxysilane (right)

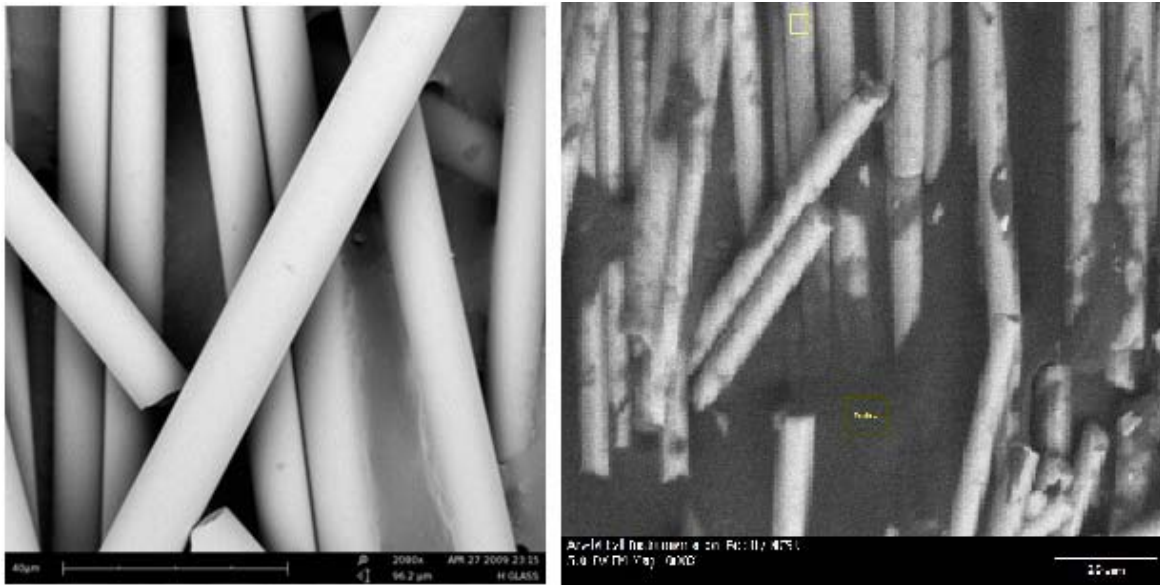


Figure 52: SEM Image of Untreated Fiberglass (left) and Glass Methyl triethoxysilane (right)

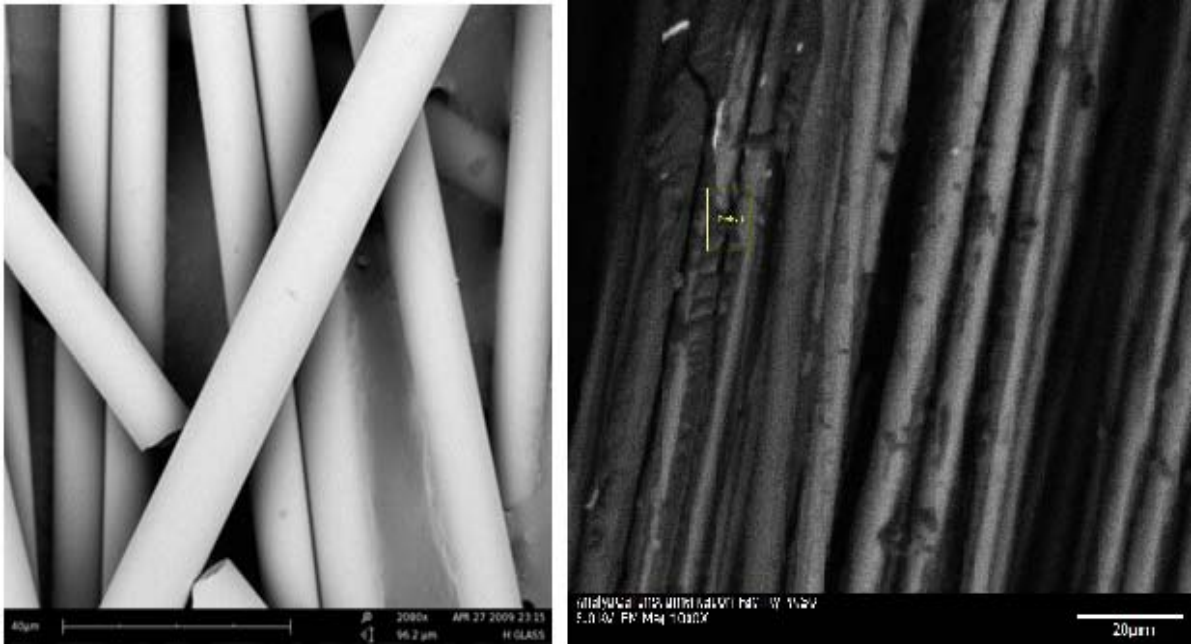


Figure 53: SEM Image of Untreated Fiberglass (left) and Glass Diamine (right)

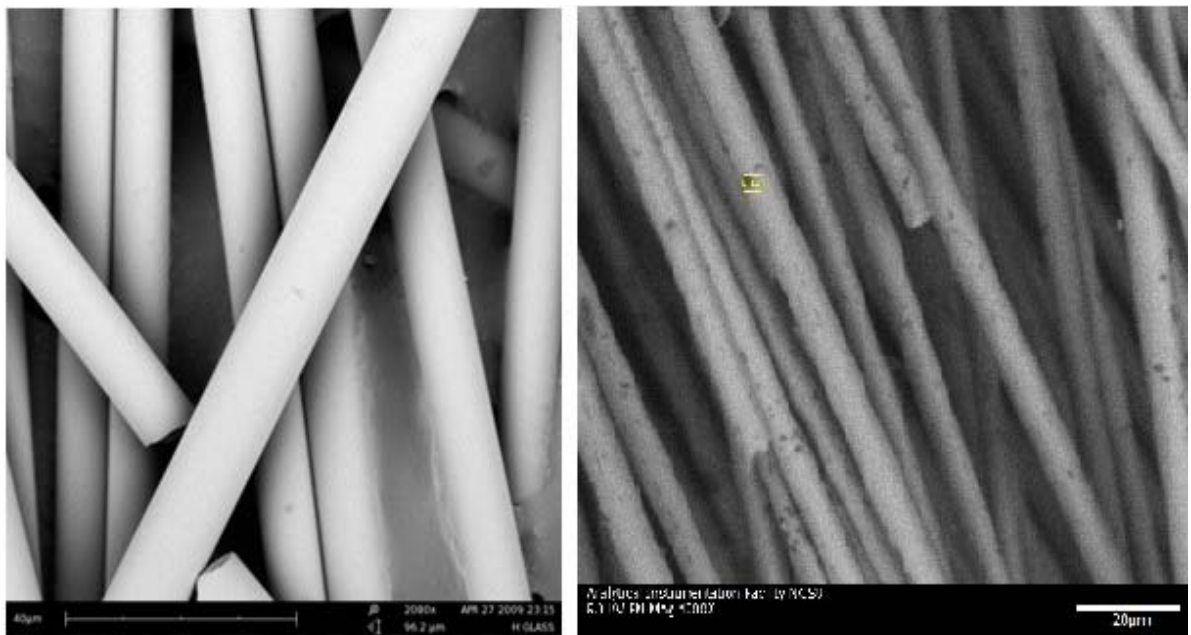


Figure 54: SEM Image of Untreated Fiberglass (left) and Glass Serine (right)

4.2. Discussion

The goal of this study is to understand the correlation between fiber properties and its hemostatic characteristic and thus improve the hemostatic property for common textile fibers for the use in wound dressings. Fiberglass has been shown in previous work as well as this research to be a highly potent hemostatic material. The surface structure of glass is believed to enhance the coagulation process through contact activation. If this is true, a similar surface structure on a different material may be expected to perform in a similar manner. Hence, different fibers are coated with TEOS, which imparts a glass-like surface. Figure 56 shows chemical structure of glass surface and Figure 57 shows glass-like chemical structure formed by TEOS on different fiber surfaces. Table 11 shows the chemical composition of E-glass.[104]

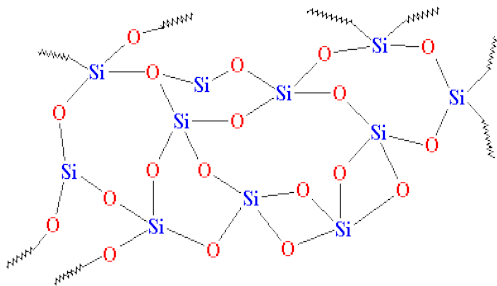


Figure 56: Glass Surface[105]

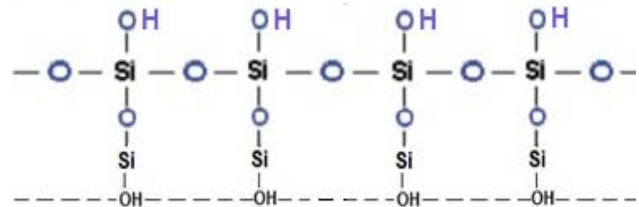


Figure 57: TEOS Coated Surface

Table 11: Chemical Composition of E-Glass

Chemical Constituents	Weight %
SiO ₂	55
Al ₂ O ₃ + Fe ₂ O ₃	14.5
CaO + MgO	22
B ₂ O ₃	7.5
Na ₂ O + K ₂ O	< 1

Moreover, various articles also mention the effect of different functional groups on coagulation process through contact activation. Hence, to study these effects, Fiberglass is treated with different chemicals that impart specific end-groups on the surface.

XPS and SEM techniques are used for characterization and confirmation of these finishes on fibers. XPS data of the TEOS treated samples used for earlier study showed Fluorine contamination (Table 3). A new batch of TEOS treated fibers was obtained and the XPS data confirmed that the new samples are free from Fluorine contamination (Table 4). XPS technique is limited only to the upper surface (up to the depth of 10 nm) and therefore, sensitive to surface impurities. XPS studies did not show the presence of much Silicon on the TEOS treated surfaces. However, in case of fiberglass treated with different chemicals, the deconvolution of the XPS carbon peak confirmed the presence of carboxyl (-COOH) and amino (-NH₂) end-groups for aspartic acid, hydroxyl groups (-OH) for

glycidoxypropyltrimethoxysilane and methyl groups (-CH₃) for methyltriethoxysilane treated samples (Table 6).

EDS analysis using SEM confirmed the TEOS coating on the fibers, which is reflected through the detection of Silicon (Table 7). For Fiberglass samples treated with different chemicals, the atomic percentage of Carbon and Oxygen correlate with the chemical constituent of the treatments which again confirm the treatment with specific end-groups (Table 8). SEM images of treated samples clearly show changes in the surface morphology (Figure 44 – 55).

The zeta potential values depend not only on the surface charges and finishes on the material but also on the pH and concentration of electrolyte solution. Zeta potentials for the control samples and TEOS treated samples are measured over the pH range of 3 to 10 and using 0.001 M KCl solution (Figure 31 and 32). However, for the purpose of wound dressing, physiological pH at the wound site (6 to 8) is of importance. In case of cellulosic fibers (Cotton and Rayon), dissociation of acidic groups at higher pH explains the Zeta Potential vs. pH curve. At lower pH, the acidic groups attract proton from the electrolyte solution and the charge on the fiber is close to zero or less negative. As pH increases (around 5), most of the acidic groups are dissociated and the surface negativity increases and hence the zeta potential becomes more negative. As pH approaches 7, all the acidic groups are ionized and a plateau is seen in the alkaline range. For synthetic fibers, adsorption of electrolyte ions is responsible for surface charge and highly negative zeta potential. In case of Nylon, the zeta potential may

show a sign reversal (i.e. zeta potential is positive or very close to zero, if negative) at low pH. This is due to the protonization of amino end-groups.[96] Large number of highly dissociable silanol groups (-Si-OH) on the surface of Fiberglass gives them the most negative zeta potential of all fibers. In theory, the zeta potential curve also denotes the hydrophilicity or hydrophobicity of the material. In case of hydrophilic material, the adsorption of ions that determine the zeta potential occurs in competition with the adsorption of water. The higher the adsorption energy of water, i.e. the higher the hydrophilicity, the lower is the adsorption of ions from the electrolyte and lesser is the negativity of zeta potential. Moreover, adsorption of water causes swelling of the fibers thereby shifting the shear plane of Electric Double Layer into the bulk solution. Thus, the hydrophilic fibers like cotton and rayon show less negative zeta potential while nylon, polyester and polypropylene with increasing order of hydrophobicity, show increasing order of negativity in zeta potential. However, fiberglass shows exceptionally high negativity in zeta potential despite it being comparatively hydrophilic. Thus, for fiberglass the dependence of zeta potential on the hydrophilicity could not be established, which was mentioned in another study as well.[106]

For TEOS treated materials, the plateau in zeta potential is less pronounced due to the coverage of original surface groups with silane molecules. The mechanism for surface charge changes from dissociation of acidic groups to adsorption of electrolyte anions. Moreover, presence of silanol end-groups (-Si-OH) on the surface of TEOS treated materials makes the surface more hydrophilic compared to the untreated samples. Hence, TEOS treatment resulted in lower negativity of zeta potential compared to the untreated samples in case of

rayon, polypropylene and nylon. However, for cotton and polyester, TEOS treatment increased the negativity of zeta potential. Fiberglass showed no difference in zeta potential values compared to the treated samples over the pH range of 6 to 9.

Zeta potential values are sensitive to a large number of parameters like sample size, fluid volumes, pressure, flow rates, fiber orientation and fiber density (porosity).[97] Hence, comparison with the values mentioned in different literatures is impractical. Though quantitative analysis might not be accurate using zeta potential, it can be used for qualitative analysis and comparison of treated samples with untreated ones.

Single fiber contact angle measurements correlate with the changes in the surface chemistry of the materials. TEOS treatment introduces silanol groups (-Si-OH) on the surface, making it more hydrophilic. This is seen by the reduction in contact angle for all the TEOS treated samples, except fiberglass (Table 9). For fiberglass, TEOS treatment increases the contact angle, making the surface more hydrophobic, which might be attributed to the surface morphology (roughness) caused by the TEOS treatment (Figure 49). For fiberglass samples treated with different chemicals for specific end-groups, the contact angle data relates to the specific end-groups for each treatment. For example, treatment with glycidoxypropyltrimethoxysilane shows lowest contact angle of all the treatments because of water-loving hydroxyl (-OH) end-groups (Table 10).

The thrombin assay is the most important aspect of this study which actually shows the extent to which a material would act as hemostatic agent and whether any treatment influenced the thrombogenicity of the substrate. Comparison of the thrombogenic potential of untreated samples is shown in Figure 41. Fiberglass is clearly the most powerful hemostatic agent with the time to thrombin formation less than 8 minutes. Three findings explain the highly hemostatic activity of fiberglass. First, the glass surface is conducive to platelet adherence and activation. Second, plasma proteins (factor XII and fibrinogen) undergo chemical and physical adsorption process on foreign surfaces. Third, factor XII plays an important role in initiating coagulation through contact activation at glass-blood interface.[4] The surface structure of glass helps in binding platelets and other plasma proteins, bringing them together. Adhered proteins have been shown to be 500 times more active. However, protein adhesion alone is not sufficient and conformational transformation is required as well for the proteins to activate platelets and initiate the coagulation process.[32] Glass surface is believed to assist in the conformational distortion of plasma proteins and facilitating platelet activation. For Cotton, time to thrombin formation was 25 minutes while for all other fibers it was more than 30 minutes. Hydrophilic surface and specific surface groups might be the reason for lower thrombin time for cotton as compared to other fibers. The time to thrombin formation for control plasma was close to 35 minutes.

TEOS treatment reduced the time to thrombin formation significantly for all samples except fiberglass, for which, the treatment increased the time to thrombin formation. Reduction in the contact angle, i.e. increase in the hydrophilicity due to silanol (-Si-OH) end-groups and

glass-like surface chemistry imparted by TEOS, are thought to be the reason for reduction in time to thrombin formation. Increase in the time to thrombin formation for fiberglass after TEOS treatment is believed to be caused by the increase in the hydrophobicity and change in the surface chemistry and morphology (i.e. roughness). This might be interfering with the adhesion and activation of plasma proteins and platelets, which are critical for coagulation via contact activation. Although TEOS treatment reduces the time to thrombin formation for all fibers, it does not induce a level of thrombogenicity as high as that of fiberglass. This means that the TEOS treatment does not replicate fully the surface properties of glass. Moreover, the time to thrombin formation after TEOS treatment is not same for all fibers. This implies that either the TEOS coating is not uniform on all the surfaces or the original substrate still plays a role in the coagulation process thereby giving different times for different fibers.

In contrast to the popular belief, we did not see a direct correlation between thrombogenicity and hydrophilicity or negativity of the zeta potential of a surface. Fiberglass, the most thrombogenic material of all, showed the most negative zeta potential but the contact angle is not the least. It is a moderately hydrophilic surface. Polypropylene showed relatively more negative zeta potential but its thrombogenicity is not better. Cotton treated with TEOS showed the most hydrophilic surface and relatively less time to thrombin formation but it has the least negative zeta potential. These observations raise concern over the belief that the hemostatic agent should be a hydrophilic substrate with a highly negative surface charge. We propose that a surface with a moderate contact angle, i.e. neither too hydrophilic nor too

hydrophobic, and with a specific surface chemistry (with end-groups and surface charge similar to glass) would provide an ideal solution.

All the fiberglass samples with specific end-groups showed increased time to thrombin formation as compared to the untreated fiberglass, which shows a change in the optimum surface characteristics (Figure 43). With all the treatments, except phosphatidylserine and phosphatidylcholine, time to thrombin formation increased to more than 20 minutes. Phosphatidylserine showed promising results, with time to thrombin formation close to fiberglass. Again, no correlation was seen between thrombogenicity and hydrophilicity of the surface. Fiberglass treated with glycidoxypropyltrimethoxysilane with hydroxyl (-OH) end-groups showed the least contact angle i.e. the most hydrophilic surface of all but its time to thrombin formation is more than 25 minutes. Consistent with our previous finding[103], samples with amine end-groups showed no visible fluorescence in thrombin assay. Amine groups might be making the surface non-reactive to plasma proteins and hence no contact activation occurs. As expected, samples with methyl end-groups showed significant increase in time to thrombin formation (more than 35 minutes) and they showed hydrophobic surface characteristics as well.

Another observation during the study was that the fiber orientation in the thrombin assay affected the time to thrombin formation. Randomly oriented fibers showed higher time to thrombin formation as compared to fibers that were twisted together to align in parallel orientation. This corroborates the findings of Fischer et al. that parallel orientation (β

structure) of poly-N-acetyl glucosamine fibers is more thrombogenic than the random orientation (α Structure) of those fibers.[62] More work to explore this observation would be planned in future.

All these findings point out that thrombogenic potential of a surface is function more of surface chemistry and specific end-groups rather than surface hydrophilicity or negativity of zeta potential. A glass surface provides optimum surface properties for contact activation and in future we would work to more closely replicate this surface on other materials so that they are also as thrombogenic as fiberglass.

CHAPTER 5: Future Work

The results of this study are encouraging enough to continue further research on hemostatic textiles. In future, we plan to investigate other chemicals, preferably natural and low-cost, that could give more glass-like hemostatic properties to wound dressing materials. Additional treatments with a wider range of functional groups would be studied.

Moreover, the existing test methods would be modified to better resemble the in-vivo conditions. For example, the thrombin assay can be run using whole blood or phospholipids that are analogous to platelet rich plasma (PRP) which allows a more accurate in-vitro model of the in-vivo interactions between a material and blood constituents. The streaming potential study would be done using more physiologically relevant solutions such as NaCl or CaCl₂. In addition to static contact angle measurements, advancing and receding contact angle measurements would provide a better understanding of surface hydrophilicity.

Thus, the future work would involve exploring more material treatments and wider variety of functional groups with improvised test methods that would characterize the coagulation property in more realistic physiological conditions with the aim of achieving an ideal hemostatic wound dressing material!

REFERENCES

- [1] H. B. Alam, D. Burris, J. A. DaCorta, and P. Rhee, "Hemorrhage Control in the Battlefield: Role of New Hemostatic Agents.," *Military Medicine*, vol. 170, no. 1, pp. 63 - 69, 2005.
- [2] H. R. Champion, R. F. Bellamy, C. P. Roberts, and A. Leppaniemi, "A Profile of Combat Injury," *The Journal of Trauma*, vol. 54, no. 5, 2003.
- [3] J. F. Kelly et al., "Injury Severity and Causes of Death From Operation Iraqi Freedom and Operation Enduring Freedom: 2003-2004 Versus 2006," *The Journal of Trauma: Injury, Infection, and Critical Care*, vol. 64, no. Supplement, p. S21-S27, Feb. 2008.
- [4] T. H. Fischer et al., "The design and testing of a dual fiber textile matrix for accelerating surface hemostasis," *Journal of Biomedical Materials Research Part B: Applied Biomaterials*, vol. 91, no. 1, pp. 381-389, Oct. 2009.
- [5] J. A. Evans, K. J. P. Wessem, D. McDougall, K. A. Lee, T. Lyons, and Z. J. Balogh, "Epidemiology of Traumatic Deaths: Comprehensive Population-Based Assessment," *World Journal of Surgery*, vol. 34, no. 1, pp. 158-163, Oct. 2009.
- [6] S. Samudrala, "Topical Hemostatic Agents in Surgery: A Surgeon's Perspective," *AORN*, vol. 88, no. 3, p. S2-S11, Sep. 2008.
- [7] Y. Oyelese, W. E. Scorza, R. Mastroia, and J. C. Smulian, "Postpartum Hemorrhage," *Obstetrics and Gynecology Clinics of North America*, vol. 34, no. 3, pp. 421-441, Sep. 2007.
- [8] I. Marcovici, "Postpartum Hemorrhage - A Review," *jurnalul de chirurgie (Journal of Surgery)*, vol. 1, no. 4, pp. 383 - 389, Oct. 2005.

- [9] “Thigh tourniquet, Roman, 199 BCE-500 CE.” [Online]. Available:
<http://www.sciencemuseum.org.uk/broughttolife/objects/display.aspx?id=4304>.
[Accessed: 11-Mar-2011].
- [10] E. Bell, A. Malik, B. Nahlovsky, and M. Young, “Field dressing for control of exsanguination,” U.S. Patent 5800372, Sep-1998.
- [11] L. J. Unger, “Human Blood Plasma and Plasma Substances,” *The American Journal of Nursing*, vol. 54, no. 1, pp. 50-52, Jan. 1954.
- [12] I. Wedmore, J. G. McManus, A. E. Pusateri, and J. B. Holcomb, “A Special Report on the Chitosan-based Hemostatic Dressing: Experience in Current Combat Operations,” *The Journal of Trauma: Injury, Infection, and Critical Care*, vol. 60, no. 3, pp. 655-658, Mar. 2006.
- [13] C. T. Esmon, “Cell mediated events that control blood coagulation and vascular injury,” *Annual review of cell biology*, vol. 9, no. 1, pp. 1–26, 1993.
- [14] S. Butenas, K. G. Mann, and Butenas, “Blood Coagulation,” *Biochemistry (Moscow)*, vol. 67, no. 1, pp. 3-12-12, Jan. 2002.
- [15] G. Casey, “Haemostasis, anticoagulants and fibrinolysis,” *Nursing standard*, vol. 18, no. 7, pp. 45–51, 2003.
- [16] R. L. Lundblad, R. A. Bradshaw, D. Gabriel, T. L. Ortel, J. Lawson, and K. G. Mann, “A review of the therapeutic uses of thrombin,” *Thrombosis and haemostasis*, vol. 91, no. 5, pp. 851–860, 2004.

- [17] "Introduction: Hemostasis: Merck Manual Professional." [Online]. Available: <http://www.merckmanuals.com/professional/sec11/ch134/ch134a.html>. [Accessed: 16-Mar-2011].
- [18] T. G. DeLoughery, *Hemostasis and thrombosis*, 2nd ed. Texas: Landes Bioscience, 2004.
- [19] J. B. Lefkowitz, "Coagulation Pathway and Physiology." [Online]. Available: http://www.cap.org/apps/docs/cap_press/hemostasis_testing/coagulation_pathway.pdf.
- [20] H. M. H. Spronk, J. W. P. Govers-Riemslog, and H. ten Cate, "The blood coagulation system as a molecular machine," *BioEssays*, vol. 25, no. 12, pp. 1220-1228, 2003.
- [21] B. Dahlbäck, "Blood coagulation," *The Lancet*, vol. 355, no. 9215, pp. 1627-1632, May. 2000.
- [22] D. Basmadjian, M. V. Sefton, and S. A. Baldwin, "Coagulation on biomaterials in flowing blood: some theoretical considerations," *Biomaterials*, vol. 18, no. 23, pp. 1511-1522, Dec. 1997.
- [23] R. Zhuo, C. A. Siedlecki, and E. A. Vogler, "Competitive-protein adsorption in contact activation of blood factor XII," *Biomaterials*, vol. 28, no. 30, pp. 4355-4369, Oct. 2007.
- [24] N. Mackman, "Role of Tissue Factor in Hemostasis, Thrombosis, and Vascular Development," *Arterioscler Thromb Vasc Biol*, vol. 24, no. 6, pp. 1015-1022, Jun. 2004.
- [25] M. B. Gorbet and M. V. M. V. Sefton, "Biomaterial-associated thrombosis: roles of coagulation factors, complement, platelets and leukocytes," *Biomaterials*, vol. 25, no. 26, pp. 5681-5703, Nov. 2004.

- [26] V. Kumar, R. Cotran, and S. Robbins, *Robbins basic pathology*, 7th ed. Philadelphia, PA: Saunders, 2002.
- [27] L. B. Jaques, E. Fidler, E. T. Feldsted, and A. G. Macdonald, "SILICONES AND BLOOD COAGULATION," *Canadian Medical Association Journal*, vol. 55, no. 1, pp. 26-31, Jul. 1946.
- [28] E. A. Vogler, J. C. Graper, G. R. Harper, H. W. Sugg, L. M. Lander, and W. J. Brittain, "Contact activation of the plasma coagulation cascade. I. Procoagulant surface chemistry and energy," *Journal of Biomedical Materials Research*, vol. 29, no. 8, pp. 1005-1016, Aug. 1995.
- [29] T. A. Ostomel, Q. Shi, P. K. Stoimenov, and G. D. Stucky, "Metal oxide surface charge mediated hemostasis," *Langmuir: The ACS Journal of Surfaces and Colloids*, vol. 23, no. 22, pp. 11233-11238, Oct. 2007.
- [30] T. H. Fischer, C. J. Smith, and J. N. Vournakis, "Mechanisms for the interaction of hemostatic systems with foreign materials," in *Biomaterials research advances*, J. B. Kendall, Ed. New York: Nova Science Publishers, 2007, pp. 1 - 19.
- [31] R. W. COLMAN, C. F. SCOTT, A. H. SCHMAIER, Y. T. WACHTFOGEL, R. A. PIXLEY, and L. H. EDMUNDS, "Initiation of Blood Coagulation at Artificial Surfaces," *Annals of the New York Academy of Sciences*, vol. 516, no. 1, pp. 253-267, 1987.
- [32] J. H. Griffin, "Role of surface in surface-dependent activation of Hageman factor (blood coagulation Factor XII)," *Proceedings of the National Academy of Sciences*, vol. 75, no. 4, pp. 1998 -2002, Apr. 1978.

- [33] E. A. Vogler and C. A. Siedlecki, "Contact activation of blood-plasma coagulation," *Biomaterials*, vol. 30, no. 10, pp. 1857-1869, Apr. 2009.
- [34] R. Røjkjær and I. Schousboe, "The Surface-Dependent Autoactivation Mechanism of Factor XII," *European Journal of Biochemistry*, vol. 243, no. 1-2, pp. 160-166, 1997.
- [35] T. Groth et al., "Contact activation of plasmatic coagulation on polymeric membranes measured by the activity of kallikrein in heparinized plasma," *Journal of Biomaterials Science. Polymer Edition*, vol. 8, no. 10, pp. 797-807, 1997.
- [36] R. Zhuo, C. A. Siedlecki, and E. A. Vogler, "Autoactivation of blood factor XII at hydrophilic and hydrophobic surfaces," *Biomaterials*, vol. 27, no. 24, pp. 4325-4332, Aug. 2006.
- [37] A. Golas, P. Parhi, Z. O. Dimachkie, C. A. Siedlecki, and E. A. Vogler, "Surface-energy dependent contact activation of blood factor XII," *Biomaterials*, vol. 31, no. 6, pp. 1068-1079, Feb. 2010.
- [38] C. Sperling, M. Fischer, M. F. Maitz, and C. Werner, "Blood coagulation on biomaterials requires the combination of distinct activation processes," *Biomaterials*, vol. 30, no. 27, pp. 4447-4456, Sep. 2009.
- [39] M. A. Griep, K. Fujikawa, and G. L. Nelsestuen, "Possible basis for the apparent surface selectivity of the contact activation of human blood coagulation factor XII," *Biochemistry*, vol. 25, no. 21, pp. 6688-6694, Oct. 1986.
- [40] C. Schonauer, E. Tessitore, G. Barbagallo, V. Albanese, and A. Moraci, "The use of local agents: bone wax, gelatin, collagen, oxidized cellulose," *European Spine Journal*, vol. 13, no. 1, p. S89-S96, Jun. 2004.

- [41] H. Seyednejad, M. Imani, T. Jamieson, and A. M. Seifalian, "Topical haemostatic agents," *British Journal of Surgery*, vol. 95, no. 10, pp. 1197-1225, Oct. 2008.
- [42] "Surgicel PMA - Premarket Approval," *U.S. Food and Drug Administration, Center for Drug Evaluation and Research*, 14-Oct-1960. [Online]. Available: <http://www.accessdata.fda.gov/scripts/cdrh/cfdocs/cfPMA/pma.cfm?id=4550>. [Accessed: 23-Apr-2011].
- [43] "BloodStop 510(k) Summary: K071578," *U.S. Food and Drug Administration, Center for Drug Evaluation and Research*, 04-Jun-2007. [Online]. Available: http://www.accessdata.fda.gov/cdrh_docs/pdf7/K071578.pdf. [Accessed: 23-Apr-2011].
- [44] "TraumaDex 510(k) Summary: K013225," *U.S. Food and Drug Administration, Center for Drug Evaluation and Research*, 26-Sep-2001. [Online]. Available: http://www.accessdata.fda.gov/cdrh_docs/pdf/K013225.pdf. [Accessed: 23-Apr-2011].
- [45] M. C. Neuffer, J. McDivitt, D. Rose, K. King, C. C. Cloonan, and J. S. Vayer, "Hemostatic dressings for the first responder: a review," *Military Medicine*, vol. 169, no. 9, pp. 716-720, Sep. 2004.
- [46] H. E. Achneck, B. Sileshi, R. M. Jamiolkowski, D. M. Albala, M. L. Shapiro, and J. H. Lawson, "A Comprehensive Review of Topical Hemostatic Agents," *Annals of Surgery*, vol. 251, no. 2, pp. 217-228, Feb. 2010.
- [47] W. Lew and F. Weaver, "Clinical use of topical thrombin as a surgical hemostat," *Biologics: Targets & Therapy*, vol. 2, no. 4, pp. 593-599, Aug. 2008.
- [48] Y. Tomizawa, "Clinical benefits and risk analysis of topical hemostats: a review," *Journal of Artificial Organs*, vol. 8, no. 3, pp. 137-142, Oct. 2005.

- [49] W. R. Wagner, J. M. Pachence, J. Ristich, and P. C. Johnson, "Comparative In Vitro Analysis of Topical Hemostatic Agents," *Journal of Surgical Research*, vol. 66, no. 2, pp. 100-108, Dec. 1996.
- [50] M. R. Jackson, "Fibrin sealants in surgical practice: An overview," *The American Journal of Surgery*, vol. 182, no. 2, Supplement 1, p. S1-S7, Aug. 2001.
- [51] D. H. Sierra, "Fibrin Sealant Adhesive Systems: A Review of Their Chemistry, Material Properties and Clinical Applications," *Journal of Biomaterials Applications*, vol. 7, no. 4, pp. 309 -352, Apr. 1993.
- [52] C. Doria and S. Vaccino, "Topical hemostasis: a valuable adjunct to control bleeding in the operating room, with a special focus on thrombin and fibrin sealants," *Expert Opinion on Biological Therapy*, vol. 9, no. 2, pp. 243-247, Feb. 2009.
- [53] B. S. Kheirabadi et al., "Development of Hemostatic Dressings for Use in Military Operations," presented at the RTO HFM Symposium on "Combat Casualty Care in Ground Based Tactical Situations: Trauma Technology and Emergency Medical Procedures," St. Pete Beach, USA, 2004.
- [54] J. Jesty, M. Wieland, and J. Niemiec, "Assessment in vitro of the active hemostatic properties of wound dressings," *Journal of Biomedical Materials Research Part B: Applied Biomaterials*, vol. 89, no. 2, pp. 536-542, May. 2009.
- [55] "Thrombin JMI," *Pfizer Product Information*. [Online]. Available: http://www.pfizer.com/files/products/uspi_thrombinjmi.pdf. [Accessed: 01-May-2011].
- [56] M. C. Oz, J. F. Rondinone, and N. S. Shargill, "FloSeal Matrix: New generation topical hemostatic sealant," *Journal of Cardiac Surgery*, vol. 18, no. 6, pp. 486-493, 2003.

- [57] J. Barnard and R. Millner, "A Review of Topical Hemostatic Agents for Use in Cardiac Surgery," *Ann Thorac Surg*, vol. 88, no. 4, pp. 1377-1383, Oct. 2009.
- [58] H. S. Whang, W. Kirsch, Y. H. Zhu, C. Z. Yang, and S. M. Hudson, "Hemostatic Agents Derived from Chitin and Chitosan," *Journal of Macromolecular Science, Part C: Polymer Reviews*, vol. 45, no. 4, pp. 309-323, 2005.
- [59] T.-C. Chou, E. Fu, C.-J. Wu, and J.-H. Yeh, "Chitosan enhances platelet adhesion and aggregation," *Biochemical and Biophysical Research Communications*, vol. 302, no. 3, pp. 480-483, Mar. 2003.
- [60] H.-Y. Yeh and J.-C. Lin, "Surface characterization and in vitro platelet compatibility study of surface sulfonated chitosan membrane with amino group protection-deprotection strategy," *Journal of Biomaterials Science. Polymer Edition*, vol. 19, no. 3, pp. 291-310, 2008.
- [61] M. A. Brown, M. R. Daya, and J. A. Worley, "Experience with Chitosan Dressings in a Civilian EMS System," *Journal of Emergency Medicine*, vol. 37, no. 1, pp. 1-7, Jul. 2009.
- [62] T. H. Fischer, A. P. Bode, M. Demcheva, and J. N. Vournakis, "Hemostatic properties of glucosamine-based materials," *Journal of Biomedical Materials Research Part A*, vol. 80, no. 1, pp. 167-174, Jan. 2007.
- [63] S.-Y. Ong, J. Wu, S. M. Moochhala, M.-H. Tan, and J. Lu, "Development of a chitosan-based wound dressing with improved hemostatic and antimicrobial properties," *Biomaterials*, vol. 29, no. 32, pp. 4323-4332, Nov. 2008.

- [64] C. Marcus, "Bio-Hemostat-Acute Treatment Modality for High Pressure Hemorrhage," *DTIC Online*, Apr-2002. [Online]. Available: <http://handle.dtic.mil/100.2/ADA405035>. [Accessed: 04-May-2011].
- [65] "QuikClot 510(k) Summary: K013390," *U.S. Food and Drug Administration, Center for Drug Evaluation and Research*, 29-May-2002. [Online]. Available: http://www.accessdata.fda.gov/cdrh_docs/pdf/K013390.pdf. [Accessed: 23-Apr-2011].
- [66] H. B. Alam et al., "Application of a zeolite hemostatic agent achieves 100% survival in a lethal model of complex groin injury in Swine," *The Journal of Trauma*, vol. 56, no. 5, pp. 974-983, May. 2004.
- [67] B. S. Kheirabadi et al., "Safety evaluation of new hemostatic agents, smectite granules, and kaolin-coated gauze in a vascular injury wound model in swine," *The Journal of Trauma*, vol. 68, no. 2, pp. 269-278, Feb. 2010.
- [68] "QuikClot eX 510(k) Summary: K072474," *U.S. Food and Drug Administration, Center for Drug Evaluation and Research*, 04-Oct-2007. [Online]. Available: http://www.accessdata.fda.gov/cdrh_docs/pdf7/K072474.pdf. [Accessed: 23-Apr-2011].
- [69] "Stasilon 510(k) Summary: K072890," *U.S. Food and Drug Administration, Center for Drug Evaluation and Research*, 09-Oct-2007. [Online]. Available: http://www.accessdata.fda.gov/cdrh_docs/pdf7/K072890.pdf. [Accessed: 23-Apr-2011].
- [70] B. G. Keselowsky, D. M. Collard, and A. J. García, "Surface chemistry modulates fibronectin conformation and directs integrin binding and specificity to control cell adhesion," *Journal of Biomedical Materials Research Part A*, vol. 66, no. 2, pp. 247-259, 2003.

- [71] J. M. Nigretto, E. Corretge, and M. Jozefowicz, "Contributions of negatively charged chemical groups to the surface-dependent activation of human plasma by soluble dextran derivatives," *Biomaterials*, vol. 10, no. 7, pp. 449-454, Sep. 1989.
- [72] E. W. SALZMAN, J. LINDON, G. McMANAMA, and J. A. WARE, "Role of Fibrinogen in Activation of Platelets by Artificial Surfaces," *Annals of the New York Academy of Sciences*, vol. 516, no. 1, pp. 184-195, 1987.
- [73] "TEOS/O₂ Thermal CVD of SiO₂," *TimeDomain CVD, Inc.* [Online]. Available: http://www.timedomaincvd.com/CVD_Fundamentals/films/TEOS_O2_thermal.html. [Accessed: 14-May-2011].
- [74] B. ARKLES, "TAILORING SURFACES WITH SILANES," *CHEMTECH*, vol. 7, no. 12, pp. 766-778, 1977.
- [75] S. Chen, A. Osaka, S. Hayakawa, K. Tsuru, E. Fujii, and K. Kawabata, "Novel One-pot Sol-Gel Preparation of Amino-functionalized Silica Nanoparticles," *Chemistry Letters*, vol. 37, no. 11, pp. 1170-1171, 2008.
- [76] B. R. Lentz, "Exposure of platelet membrane phosphatidylserine regulates blood coagulation," *Progress in Lipid Research*, vol. 42, no. 5, pp. 423-438, Sep. 2003.
- [77] T. Tsuda, H. Yoshimura, and N. Hamasaki, "Effect of phosphatidylcholine, phosphatidylethanolamine and lysophosphatidylcholine on the protein C/protein S anticoagulation system," *Blood Coagulation & Fibrinolysis*, vol. 17, no. 6, pp. 453-458, Sep. 2006.

- [78] M. K. Ramjee, "The Use of Fluorogenic Substrates to Monitor Thrombin Generation for the Analysis of Plasma and Whole Blood Coagulation," *Analytical Biochemistry*, vol. 277, no. 1, pp. 11-18, Jan. 2000.
- [79] J. J. Van Veen, A. Gatt, and M. Makris, "Thrombin generation testing in routine clinical practice: are we there yet?," *British Journal of Haematology*, vol. 142, no. 6, pp. 889-903, Sep. 2008.
- [80] T. Baglin, "The measurement and application of thrombin generation," *British Journal of Haematology*, vol. 130, no. 5, pp. 653-661, Sep. 2005.
- [81] H. C. Hemker, R. Al Dieri, and S. Béguin, "Thrombin generation assays: accruing clinical relevance," *Current Opinion in Hematology*, vol. 11, no. 3, pp. 170-175, May. 2004.
- [82] H. C. Hemker, R. Al Dieri, E. De Smedt, and S. Béguin, "Thrombin generation, a function test of the haemostatic-thrombotic system," *Thrombosis and Haemostasis*, vol. 96, no. 5, pp. 553-561, Nov. 2006.
- [83] H. C. Hemker et al., "The calibrated automated thrombogram (CAT): a universal routine test for hyper- and hypocoagulability," *Pathophysiology of Haemostasis and Thrombosis*, vol. 32, no. 5-6, pp. 249-253, Dec. 2002.
- [84] H. C. Hemker et al., "Calibrated automated thrombin generation measurement in clotting plasma," *Pathophysiology of Haemostasis and Thrombosis*, vol. 33, no. 1, pp. 4-15, 2003.

- [85] H. C. Hemker, P. L. Giesen, M. Ramjee, R. Wagenvoord, and S. Béguin, "The thrombogram: monitoring thrombin generation in platelet-rich plasma," *Thrombosis and Haemostasis*, vol. 83, no. 4, pp. 589-591, Apr. 2000.
- [86] M. Adams, "Assessment of thrombin generation: useful or hype?," *Seminars in Thrombosis and Hemostasis*, vol. 35, no. 1, pp. 104-110, Feb. 2009.
- [87] A. S. Wolberg, "Thrombin generation assays: understanding how the method influences the results," *Thrombosis Research*, vol. 119, no. 6, pp. 663-665, 2007.
- [88] K. A. Tappenden, M. J. Gallimore, G. Evans, I. J. Mackie, and D. W. Jones, "Thrombin generation: a comparison of assays using platelet-poor and -rich plasma and whole blood samples from healthy controls and patients with a history of venous thromboembolism," *British Journal of Haematology*, vol. 139, no. 1, pp. 106-112, Oct. 2007.
- [89] R. Al Dieri and C. H. Hemker, "Thrombin generation in whole blood," *British Journal of Haematology*, vol. 141, no. 6, pp. 895-895, Jun. 2008.
- [90] A. V. Delgado, F. González-Caballero, R. J. Hunter, L. K. Koopal, and J. Lyklema, "Measurement and Interpretation of Electrokinetic Phenomena (IUPAC Technical Report)," *Pure and Applied Chemistry*, vol. 77, no. 10, pp. 1753-1805, 2005.
- [91] M. Hubbe, "Sensing the electrokinetic potential of cellulosic fiber surfaces," *BioResources*, vol. 1, no. 1, pp. 116-149, 2006.
- [92] V. Ribitsch and K. Stana-Kleinscheck, "Characterizing Textile Fiber Surfaces with Streaming Potential Measurements," *Textile Research Journal*, vol. 68, no. 10, pp. 701 - 707, Oct. 1998.

- [93] C. Bellmann et al., "Electrokinetic properties of natural fibres," *Colloids and Surfaces A: Physicochemical and Engineering Aspects*, vol. 267, no. 1-3, pp. 19-23, Oct. 2005.
- [94] B. J. Kirby and E. F. Hasselbrink Jr, "Zeta potential of microfluidic substrates: 1. Theory, experimental techniques, and effects on separations," *Electrophoresis*, vol. 25, no. 2, pp. 187-202, Jan. 2004.
- [95] B. J. Kirby and E. F. Hasselbrink Jr, "Zeta potential of microfluidic substrates: 2. Data for polymers," *Electrophoresis*, vol. 25, no. 2, pp. 203-213, Jan. 2004.
- [96] H.-J. Jacobasch, G. Baubock, and J. Schurz, "Problems and results of zeta-potential measurements on fibers," *Colloid & Polymer Science*, vol. 263, no. 1, pp. 3-24, Jan. 1985.
- [97] J. Ciriacks, "An Investigation of the Streaming Current Method for Determining the Zeta Potential of Fibers," Dissertation, Institute of Paper Chemistry, Lawrence University, 1967.
- [98] M. Hubbe and F. Wang, "Charge-Related Measurements –A Reappraisal. Part 2: Fibre-Pad Streaming Potential," *Paper Technology*, vol. 45, no. 9, pp. 27-34, Nov. 2004.
- [99] F. Wang and M. A. Hubbe, "Development and evaluation of an automated streaming potential measurement device," *Colloids and Surfaces A: Physicochemical and Engineering Aspects*, vol. 194, no. 1-3, pp. 221-232, Dec. 2001.
- [100] N. Guzelsu, C. Wienstien, and S. P. Kotha, "A new streaming potential chamber for zeta potential measurements of particulates," *Review of Scientific Instruments*, vol. 81, no. 1, 2010.

- [101] “Part III: The Behavior of Liquids on Single Textile Fibers,” *Textile Research Journal*, vol. 29, no. 12, pp. 940 -949, Dec. 1959.
- [102] B. J. Carroll, “The accurate measurement of contact angle, phase contact areas, drop volume, and Laplace excess pressure in drop-on-fiber systems,” *Journal of Colloid and Interface Science*, vol. 57, no. 3, pp. 488-495, Dec. 1976.
- [103] T. Rush, “Hemostatic Mechanisms of Common Textile Wound Dressing Materials,” MS Thesis, North Carolina State University, 2010.
- [104] H. Watson, A. Norström, Å. Torrkulla Å, and J. Rosenholm, “Aqueous Amino Silane Modification of E-glass Surfaces,” *Journal of Colloid and Interface Science*, vol. 238, no. 1, pp. 136-146, Jun. 2001.
- [105] “Is Glass a Polymer?,” *The Macrogalleria*. [Online]. Available: <http://pslc.ws/macrogcss/glass.html>. [Accessed: 24-May-2011].
- [106] A. Bismarck, A. R. Boccaccini, E. Egiá-Ajuriagojeaskoa, D. Hülsenberg, and T. Leutbecher, “Surface characterization of glass fibers made from silicate waste: Zeta-potential and contact angle measurements,” *Journal of Materials Science*, vol. 39, no. 2, pp. 401-412, Jan. 2004.

APPENDICES

Appendix A: Protocols

TEOS Modification

TEOS treatment of fibers was carried out as under:

- 1) The fibers received are already scoured/bleached. However, they are washed with hot water and non-ionic detergent prior to the treatment.
- 2) The solution (by volume) is prepared and used immediately –
 - a. 75% Isopropyl Alcohol
 - b. 20% TEOS
 - c. 5% 1M NH_4OH
- 3) Fibers are dipped into the solution to wet.
- 4) Fibers are squeezed slightly to remove excess solution and placed in microwave for 30 seconds.
- 5) This process is repeated 3 times.
- 6) After the treatment, fibers are washed and rinsed thoroughly with water.
- 7) Fibers are then dried overnight in a vacuum oven.

Thrombin Assay

Costar 96-well plates are blocked using a solution of 1:4 25% Human Serum Albumin and Citrated Saline. 150 μ L of the blocking solution is pipetted into each well plate. The plate is then sealed by stretching the Para film over the plate and incubated overnight at 37 °C. Para film is then removed and the solution is emptied. Plate lid is replaced and the edges of the plates sealed with Para film. Sealed plates are placed in refrigerator for storage until later use.

Running the plate in Tecan® Genios Plate Reader:

- 1) Click on Megellan icon.
- 2) Check for correct filters (Excitation – 360 nm and Emission – 465 nm)
- 3) Click ‘Start Measurement’
- 4) Select the method for thrombin assay
- 5) Place 96-well plate in the plate holder with A1 in top left corner
- 6) Click the start button
- 7) After the test is finished, click next and then save button
- 8) Click back button and then data view button
- 9) Click Excel export to get the data in Excel file
- 10) Copy the data from Excel file into the Excel template to measure lag-time and max-slope of the substrate fluorescence curve

Streaming Potential Jar

1. Turn on air valves. The bottom left blue valve, then the left most valve on the middle row, then the rightmost valve on the middle row, then the leftmost valve on the top row
2. Double click “Shortcut to !SPJ run.vi”
3. Fill plastic jar (with rim) with 750ml of KCl solution
4. Adjust solution to correct pH level using 0.1N and 1N HCl and NaOH
5. Place small amount of material in packed bed chamber (fill to bottom of threading), then screw on bottom of chamber (making sure electrode wire points towards the top of the chamber)
6. Connect packed bed chamber to device by inserting the white translucent plastic tubing on the top of the packed bed chamber into the flexible air hose inside the vacuum chamber tighten the clamp to secure using flat head screw driver
7. Place packed bed chamber into the solution so it is in the vertical orientation so the bottom of the packed bed chamber touches the bottom of the plastic tub of KCl and electrodes are facing the top of the vacuum chamber for attachment
8. Connect the electrodes of the packed bed chamber to the wires in the vacuum chamber (black to black, plain to green)
9. Position lid on vacuum chamber and secure closed
10. On computer click “Manual Mode” Button in SPJ program. This opens a screen that allows you to manually cycle through the high pressure-> low pressure-> vacuum cycle the device does automatically when running a sample

11. Click on high pressure button, count ten seconds, then click the low pressure button, count 15 seconds, then click the vacuum button, count until the overflow beaker is empty, make note of the total time vacuum was running. The goal of this step is to verify that the total volume in the overflow beaker during the high and low pressure parts of the cycle is at least 300ml and does NOT exceed 700ml. If the volume in the overflow beaker is greater than 700ml at the end of the overflow cycle you will likely get bubbling (this will look like a “rolling boil” in the overflow beaker). **AS SOON AS YOU SEE BUBBLING LIKE THIS OR THE VOLUME GOES OVER 700ML PRESS THE VACUUM BUTTON!!!** After the overflow beaker has been emptied by the vacuum cycle, click vacuum off. You will then need to open the vacuum chamber disconnect the packed bed chamber and add more material. Then repeat the manual mode steps to ensure the correct amount of material is in the packed bed chamber. If the volume of the overflow beaker never reaches 300ml then after the vacuum cycle, remove the packed bed chamber form the device and remove some material from the packed bed, then repeat the manual mode step to ensure the correct amount of material is in the packed bed chamber.
12. Click Exit to return to the main screen, and then click the “Configure Test” button. Click the “Import” button to load a preset protocol to the program. The program we use is called: Tabitha_Stasilon_KCl_11-4-08
13. Click OK to close the file window. In the white box along the left side of the screen there is a list of the four parts of the automated cycle. Click on each to see the Time duration of each part of the cycle. The high pressure should have 10 seconds, the low

pressure should have 15 seconds, the vacuum should have 50 seconds and the rest should have 10 seconds. The vacuum time should be the only time you change in this screen; the other times are preset to allow for adequate signal measurement and clarity. NOTE: If, when running the manual mode, the time during the vacuum portion took longer than 50 seconds to completely empty the beaker then change the vacuum time duration to the amount of time it took to COMPLETELY empty the beaker (i.e. until you hear a sucking sound). If the vacuum you counted in the manual mode is less than 50 seconds, leave the preset value.

14. Once the correct protocol has been chosen and the time durations verified click on the green Use Changes button to return to the main screen.
15. Click the “Run Test” button and assign a file name using the following naming system:

Date-> Project-> Solution-> Material->pH

Example: For the stasilon project rayon run on Oct. 9, 2009 in 0.01N KCl solution at pH 4 would be named as: Y91009_Stasilon_KClx10_rayon pH 4
16. Click OK after you have entered the filename to start the automated protocol
17. When the red “Abort Test” button turns back to a blue “Run Test” button the automated protocol is complete. Click on the “View Saved Data” button
18. Adjust the pre/post T2 data collection/delay times so that the plateau areas of each cycle are encompassed by pre/post data collection (see graph for further explanation).

Graph showing how the Pre/Post T2 delay/collection times should be assigned

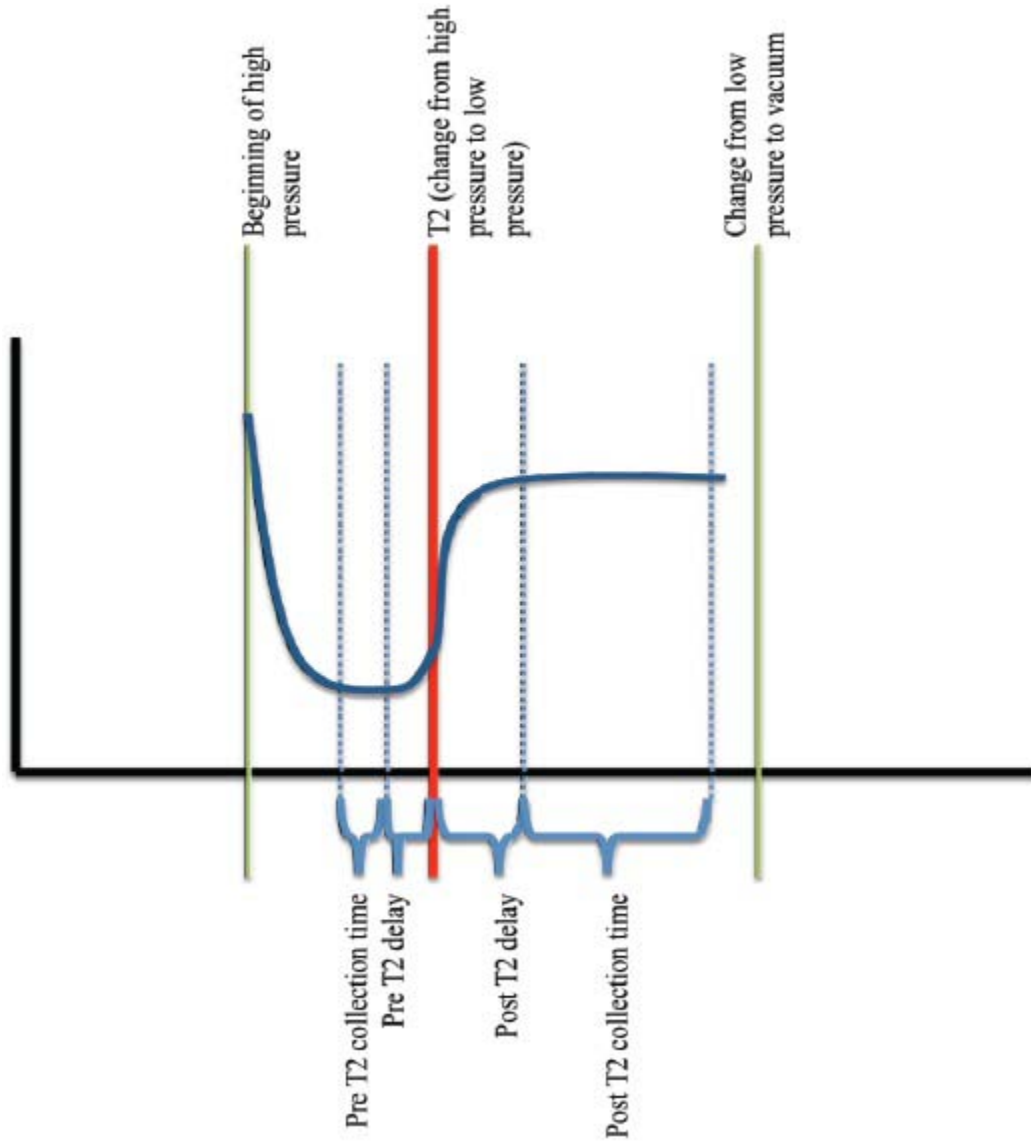


Figure: Pre/Post T2 delay/collection time assignments

- The pre T2 collection time and pre T2 delay should always be less than the total high pressure time (10 sec)

- The post T2 collection time and post T2 delay should always be less than the total low pressure time (15 sec).
 - NOTE: In general some good numbers to start with are:
 - Pre T2 delay: 0.5 sec
 - Pre T2 collection time: 1-2 sec
 - Post T2 delay: 8-11 sec
 - Post T2 collection time: 4-7 sec
 - Begin with the suggested numbers and adjust them as necessary. A good fit to the data will show an E1 SD and E2 SD values of 1.0 or smaller. An ideal fit to the data will show an E1 SD and E2 SD value of 0.5 or smaller.
19. After adjusting the pre/post T2 delay and collection times so that the E1 and E2 SD values are within the acceptable range click “ Save Analysis Data” button. Enter the same file name used in the “Run Test” step and append .csv to the end of the filename. NOTE: .CSV MUST BE ADDED TO THE END OF THE FILE NAME OR THE DATA WILL NOT SAVE!!!
20. Click exit to return to the main screen.
21. Remove the packed bed chamber from the vacuum chamber by disconnecting it from the wires and the air hose. Remove the plastic beaker with rim from the vacuum chamber. Empty the material from the packed bed chamber into a trashcan and rinse both the plastic beaker and packed bed chamber briefly in DI water (from the DI water tap)

22. Repeat the above steps for each material for pH 3-11. A total of 3 trials need to be run for each material (3x pH 3-11). NOTE: For subsequent tests for the same material (even at different pHs) it is not necessary to perform the Manual Mode and Configure Test steps so long as you use the same amount of material. However, keep a close eye on the total amount of fluid in the overflow beaker to ensure that adjustments aren't needed. If you find that during a test adjustments to the amount of material or duration of the vacuum cycle need to be made, click "Abort test" button then click the radio button beside Vacuum on the main screen, once the overflow beaker is completely empty, click the radio button beside all off on the main screen and make the necessary changes (i.e add/remove material, go into manual mode to check timing, and/or go into configure test to adjust vacuum duration
23. Exit the SPJ control program.
24. Turn off air flow control valves

Recipe for 0.001N KCL solution

Fill 23L carboy, then add 1.72g of KCl powder. Agitate gently to ensure complete dissolution.

Appendix B: Raw Data for Thrombin Assay

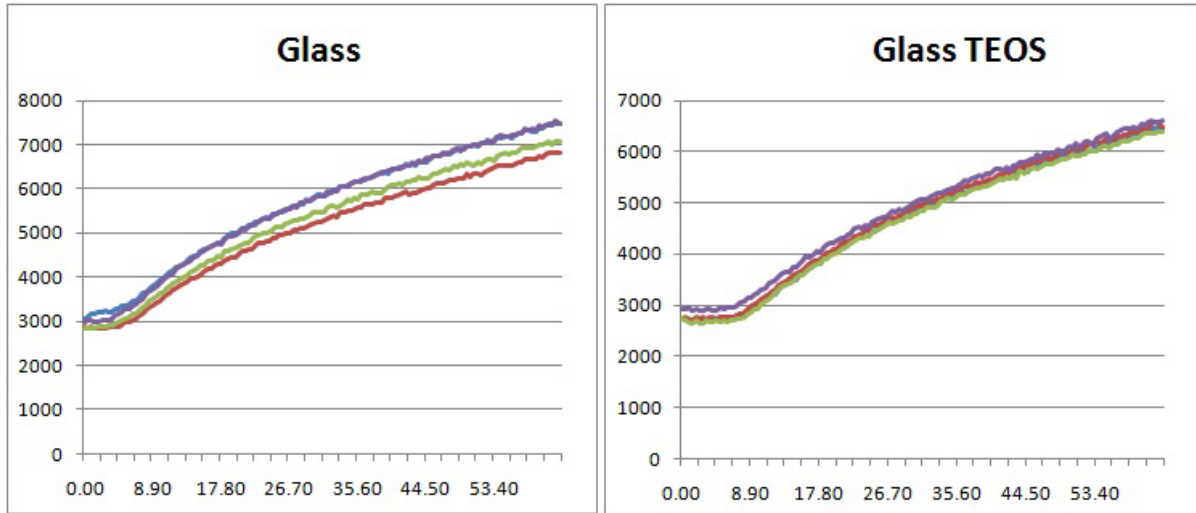


Figure: Thrombin Assay Data for Glass

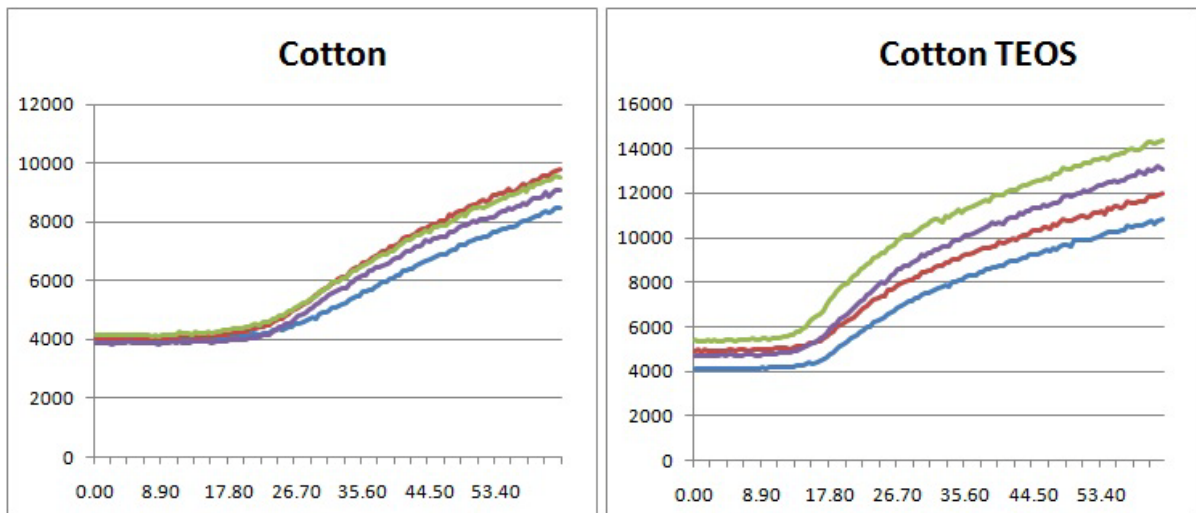


Figure: Thrombin Assay Data for Cotton

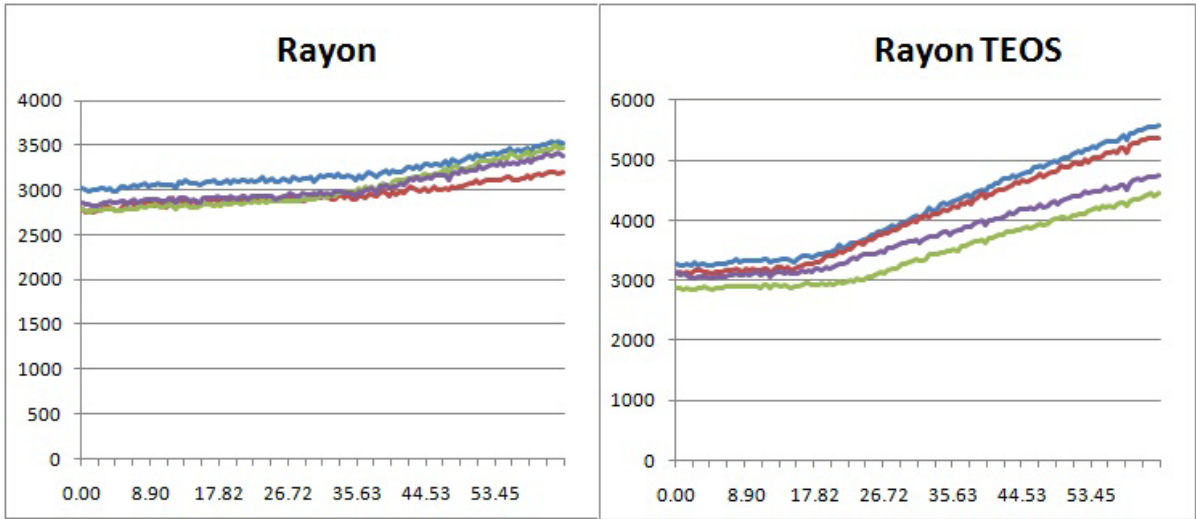


Figure: Thrombin Assay Data for Rayon

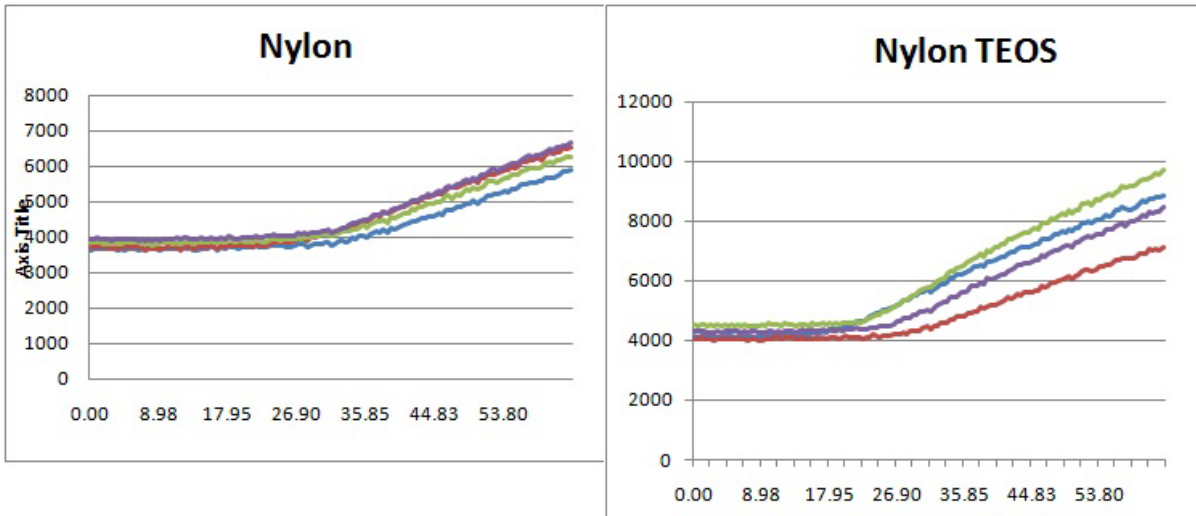


Figure: Thrombin Assay Data for Nylon

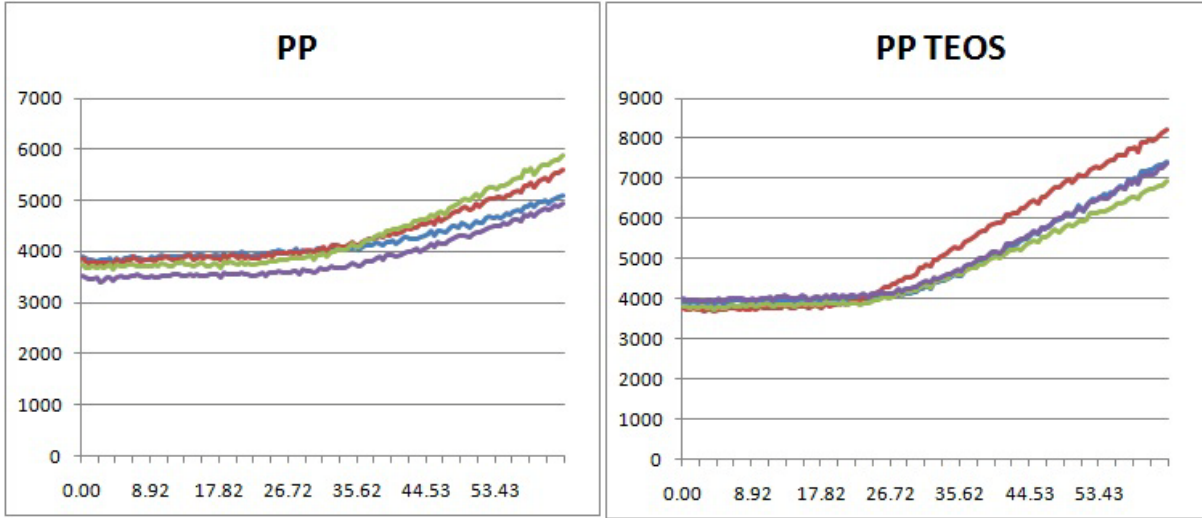


Figure: Thrombin Assay Data for PP